4. Properties of 2D Semiconductors
Part 1

서 울 대 학 교
SEOUL NATIONAL UNIVERSITY

Family of 2D Semiconductors

Graphene family	Graphene	hBN 'white graphene'	BCN	Fluorographene	Graphene oxide
2D chalcogenides	MoS_2, WS_2, $MoSe_2$, WSe_2	Semiconducting dichalcogenides: $MoTe_2$, WTe_2, ZrS_2, $ZrSe_2$ and so on		Metallic dichalcogenides: $NbSe_2$, NbS_2, TaS_2, TiS_2, $NiSe_2$ and so on Layered semiconductors: GaSe, GaTe, InSe, Bi_2Se_3 and so on	
2D oxides	Micas, BSCCO Layered Cu oxides	MoO_3, WO_3 TiO_2, MnO_2, V_2O_5, TaO_3, RuO_2 and so on	Perovskite-type: $LaNb_2O_7$, $(Ca,Sr)_2Nb_3O_{10}$, $Bi_4Ti_3O_{12}$, $Ca_2Ta_2TiO_{10}$ and so on	Hydroxides: $Ni(OH)_2$, $Eu(OH)_2$ and so on Others	

Nature Photonics 10, 202–204 (2016)

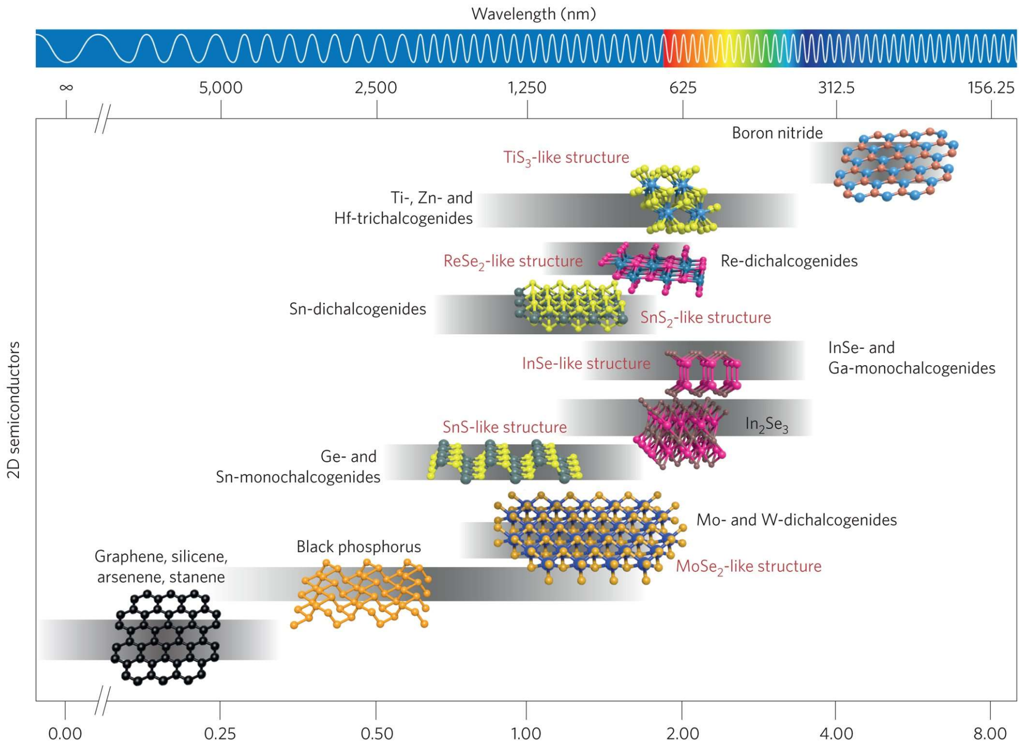

Nature Photonics 10, 202–204 (2016)

- Bandgap : 0.8 ~ 2.5eV
- Layered structure : monolayer, few-layer, bulk
- High mobility
- Transparency
- Flexibility
- Optical response
- Extra degree of freedom
- Broken symmetry

History of 2D Semiconductors

Molybdenum Disulfide (MoS_2)

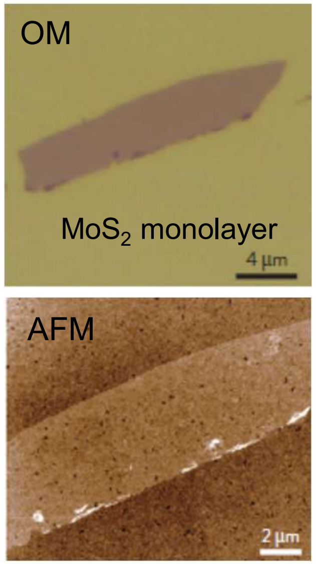

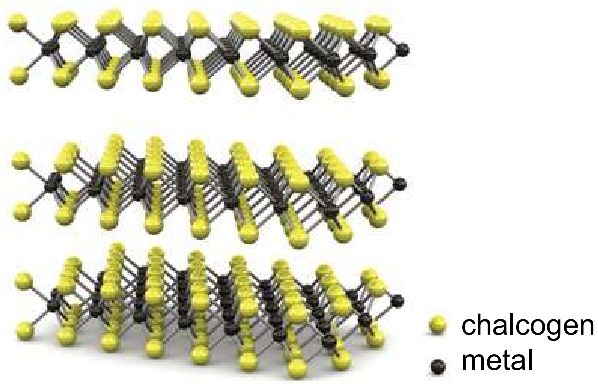

Two-dimensional atomic crystals

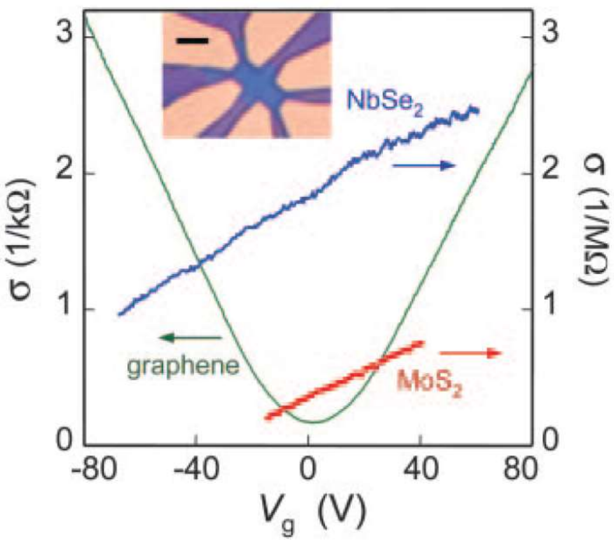

K. S. Novoselov et al. PNAS (2005)

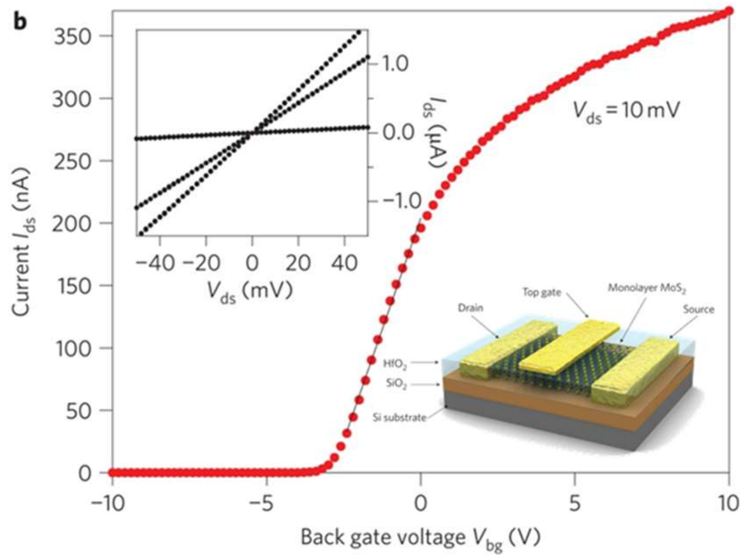

A. Kis et al. Nature Nanotechnol. (2011)

Transition Metal Chalcogenides (TMDs)

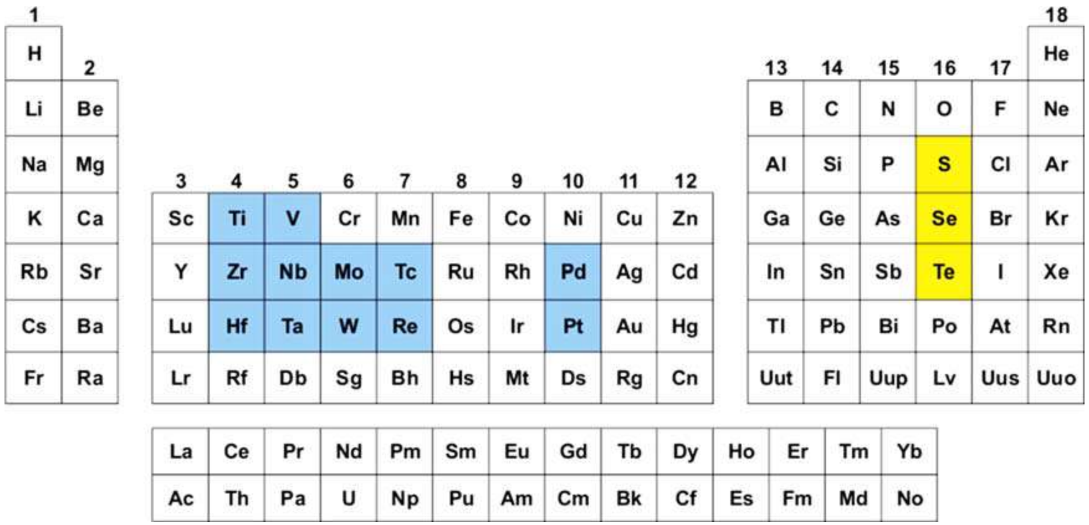

Layered structure of the form X-M-X.
Chalcogen atoms: hexagonal plane
Metal atoms: a plane between two chalcogen planes

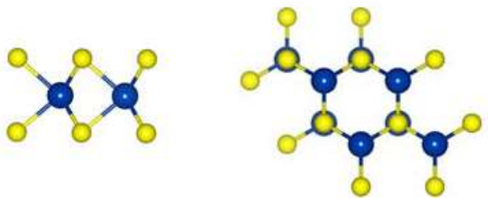

1. Good lubricant property
2. Catalyst for optoelectronics and photovoltaics

A. Kuc et al. BooK: Chemical Modeling (2014)

Table 1 | Summary of TMDC materials and properties.

	$-S_2$ Electronic characteristics	$-S_2$ References	$-Se_2$ Electronic characteristics	$-Se_2$ References	$-Te_2$ Electronic characteristics	$-Te_2$ References
Nb	Metal; superconducting; CDW	138 (E)	Metal; superconducting; CDW	138,164 (E)	Metal	83 (T)
Ta	Metal; superconducting; CDW	138,164 (E)	Metal; superconducting; CDW	138,164 (E)	Metal	83 (T)
Mo	Semiconducting 1L: 1.8 eV Bulk: 1.2 eV	31 (E) 88 (E)	Semiconducting 1L: 1.5 eV Bulk: 1.1 eV	82 (T) 88 (E)	Semiconducting 1L: 1.1 eV Bulk: 1.0 eV	82 (T) 165 (E)
W	Semiconducting 1L: 2.1 eV 1L: 1.9 eV Bulk: 1.4 eV	25 (T) 82 (T) 88 (E)	Semiconducting 1L: 1.7 eV Bulk: 1.2 eV	83 (T) 88 (E)	Semiconducting 1L: 1.1 eV	83 (T)

The electronic characteristic of each material is listed as metallic, superconducting, semiconducting or charge density wave (CDW). For the semiconducting materials, the bandgap energies for monolayer (1L) and bulk forms are listed. The cited references are indicated as experimental (E) or theoretical (T) results.

H. Q. Wang et al. Nature Nano (2012)

Crystal Structure of Transition Metal Chalcogenides

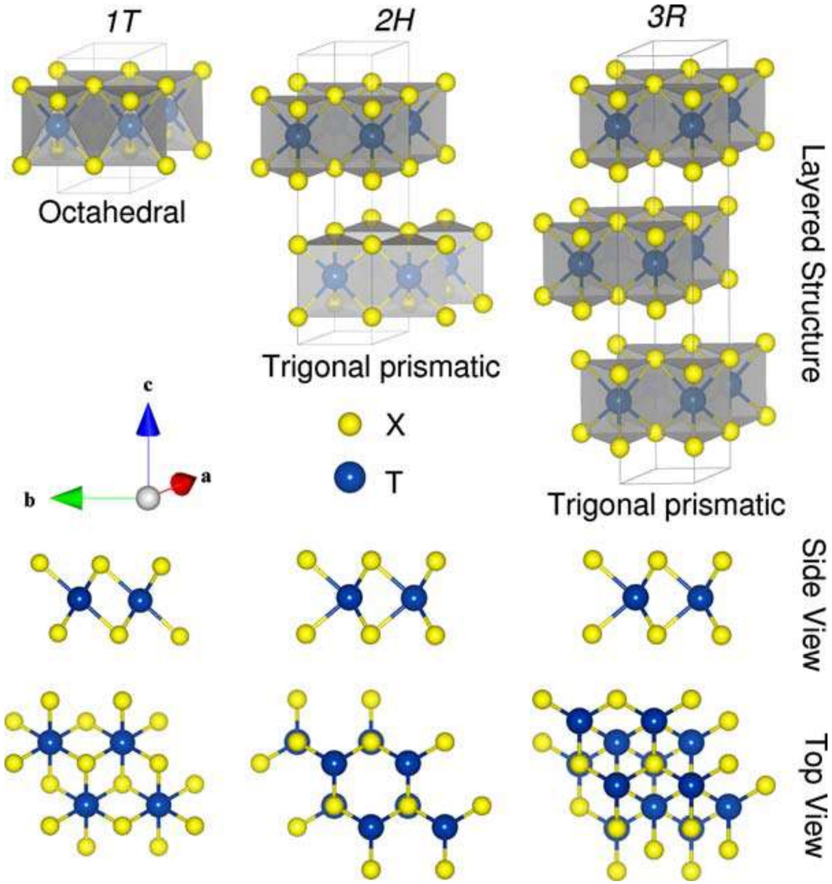

A. Kuc et al. BooK: Chemical Modeling (2014)

Monolayer TMDs

1) Broken inversion symmetry
   2H : $P6_3/mmcD_{6h}^4$ (Bulk) → 1H : $P\bar{6}m2D_{3h}^1$ (ML)

2) Quantum confinement

3) Direct bandgap for ML @ K and K'

4) Valley degree of freedom

5) Strong spin-orbit coupling

6) Large exciton binding energy (0.5-1eV)

7) Trion

8) Self-passivation

9) Strong interaction with light

F. Xia et al. Nature Photonics (2014)

2D Material Spectra

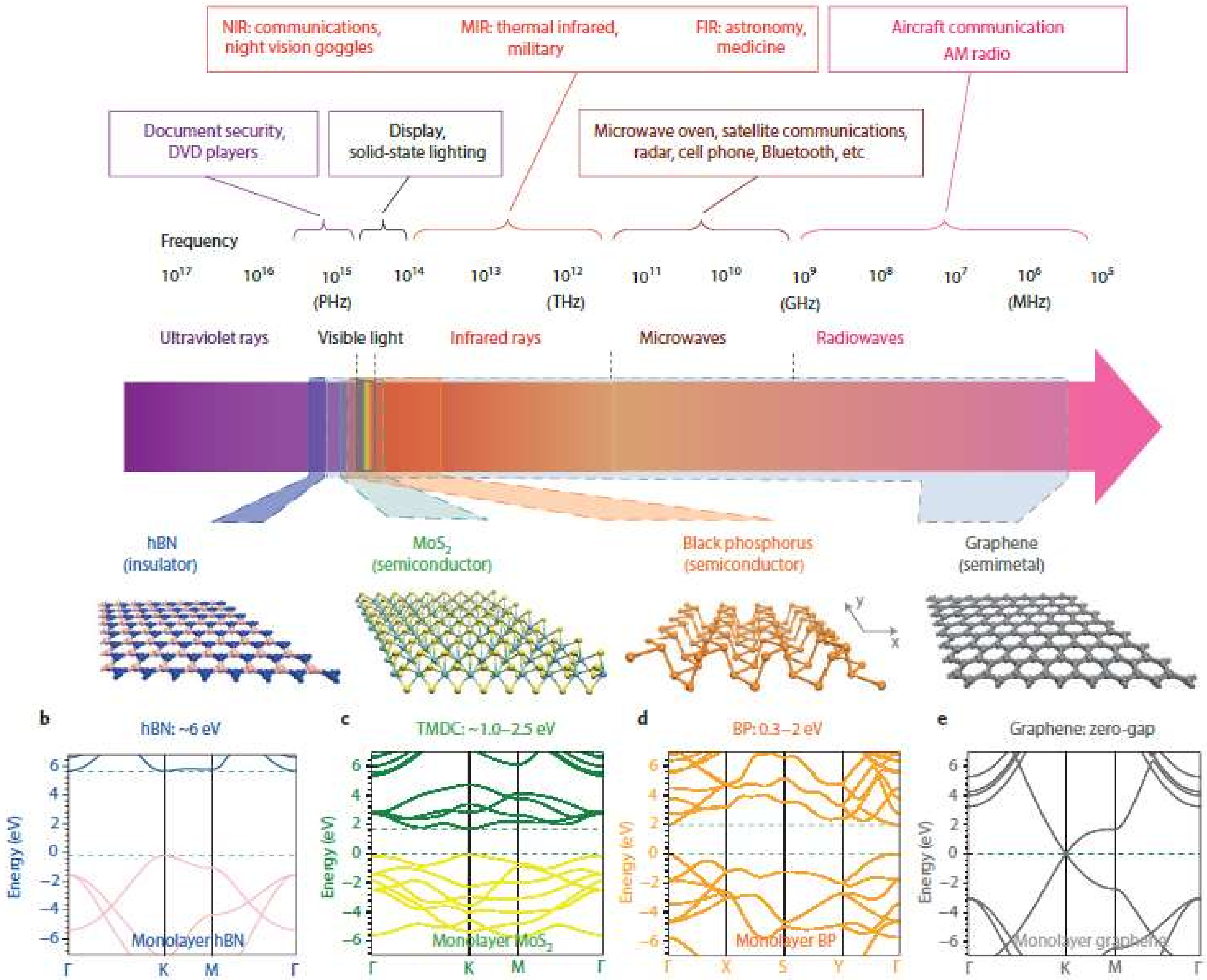

F. Xia et al. Nature Photonics (2014)

Electronic Structure of TMDs

Band gap changes with layer number due to quantum confinement & hybridization of d-orbital of metal atom and p_z orbital of chalcogen atom.

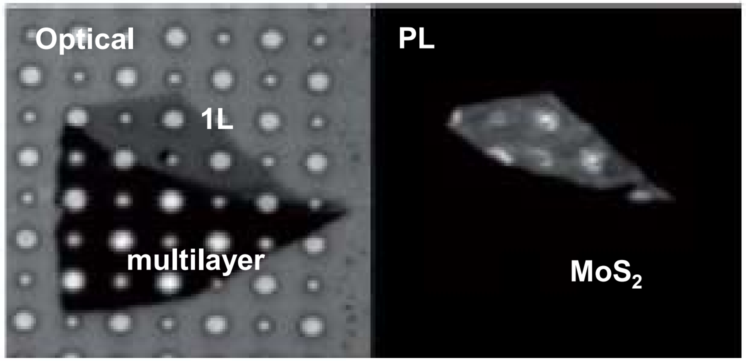

K-point : remain unchanged with layer number
Γ-point : changed with layer number

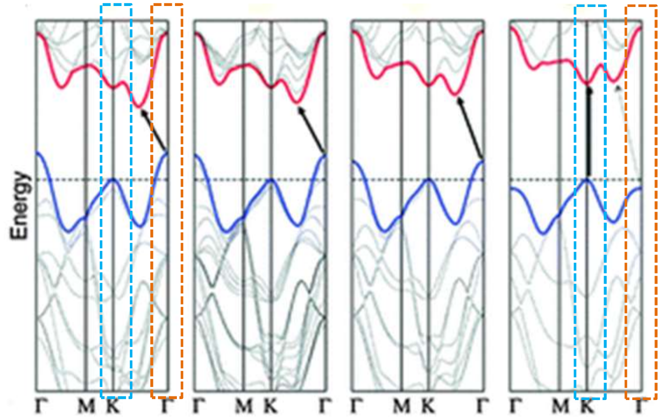

Thickness decreases. ------------►

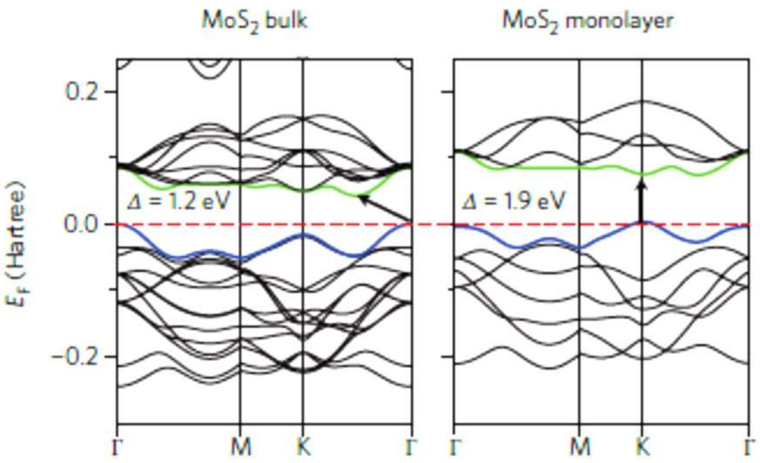

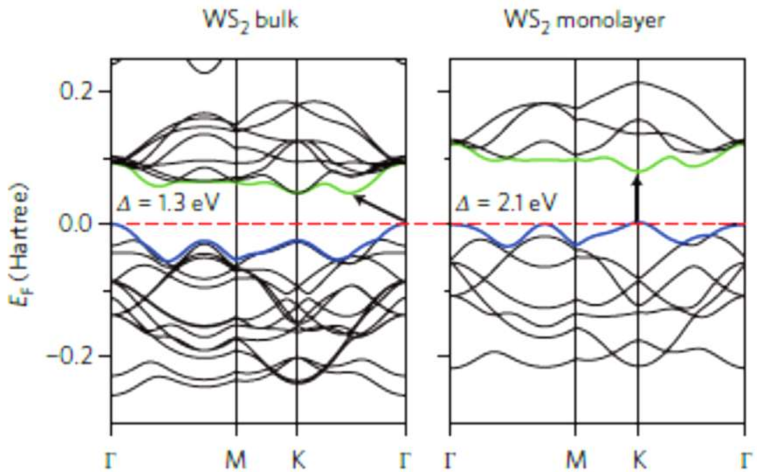

As thickness decreases, bandgap increases and band structure transforms from indirect to direct.

K. F. Mak et al. PRL (2012) & H. Q. Wang et al. Nature Nano (2012)

Electronic Structure of TMDs

Normalized PL spectra of MoS_2

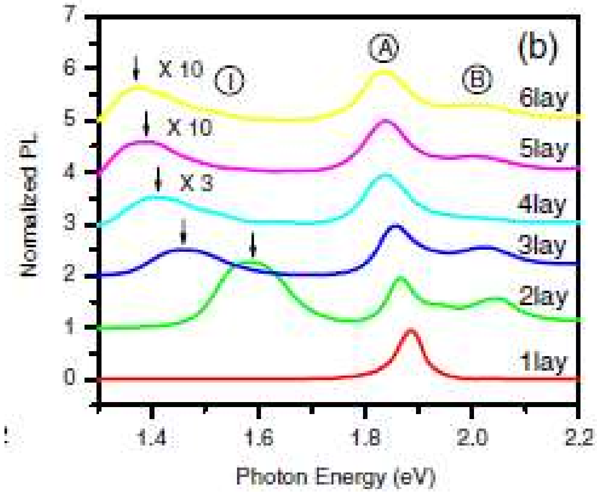

Band structure of monolayer MoS_2

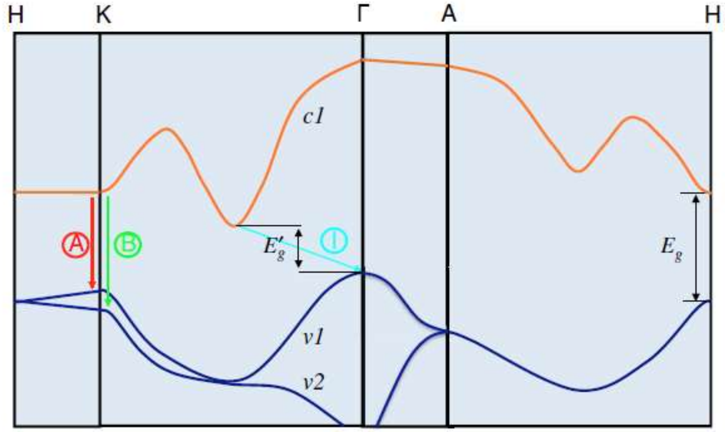

Absorption spectra

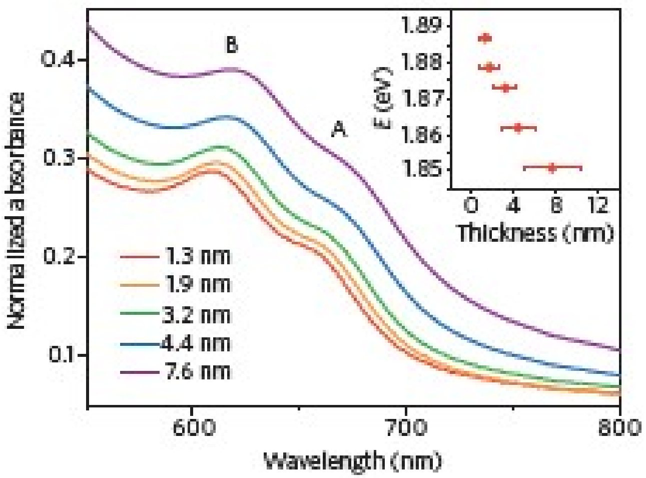

PL spectra

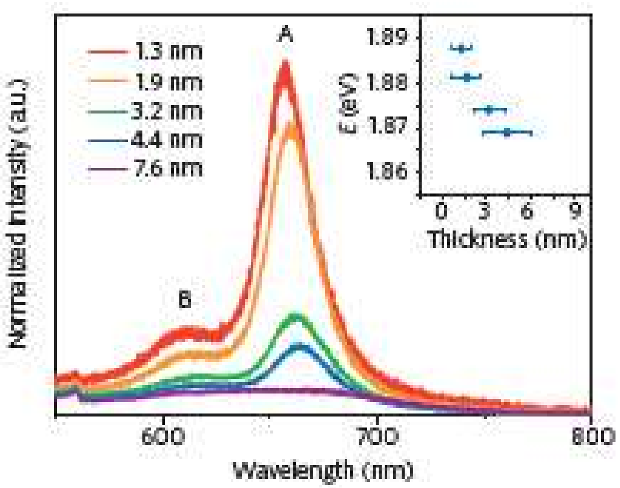

Effect of substrate on PL

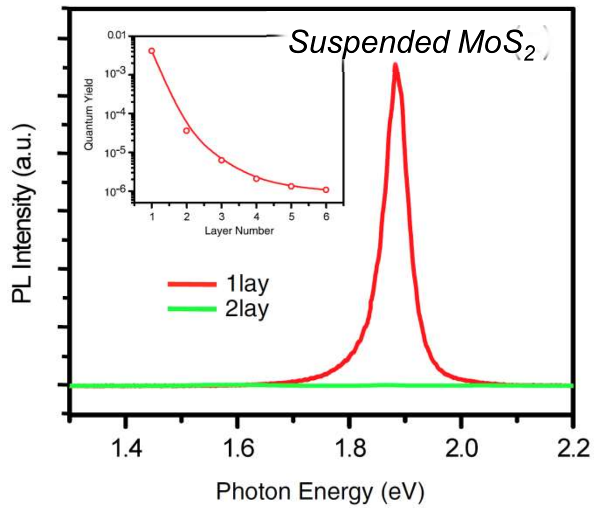

Optical properties of MoS_2 depends on the thickness and substrate.

K. F. Mak et al. PRL (2012)

Quantum yield enhancement

S-vacancies healing by PSS

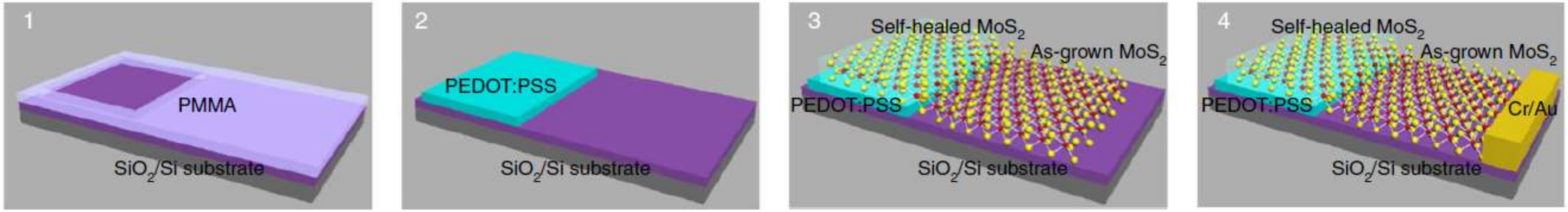

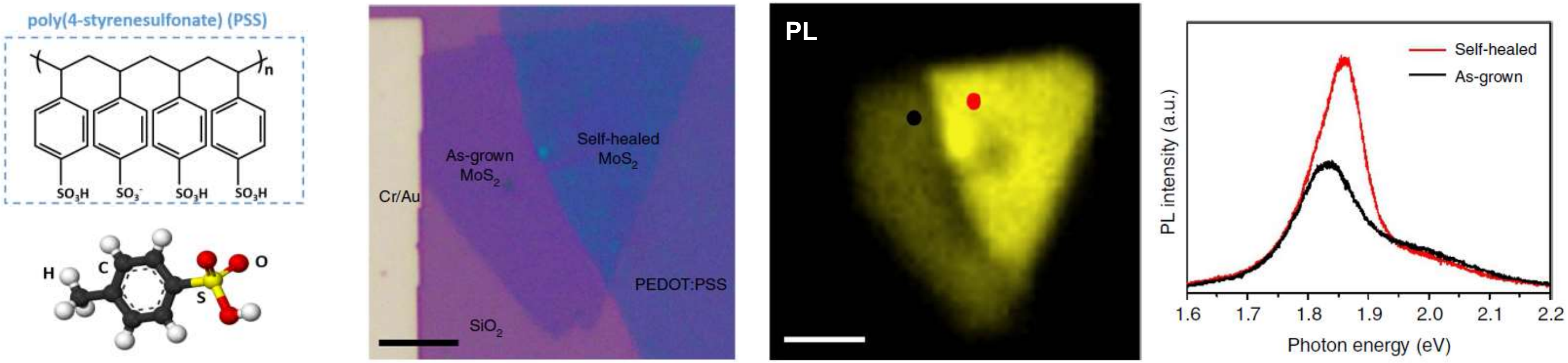

S-vacancies are self-healed by poly(4-styrenesulfonate) (PSS).

By this, not only the PL spectrum intensity of the self-healed one is drastically enhanced, but also the peak energy is obviously blue shifted.

Xiankun Zhang et al. Nature communications (2017)

Quantum yield enhancement

By solvent evaporation–mediated decoupling(SEMD) process

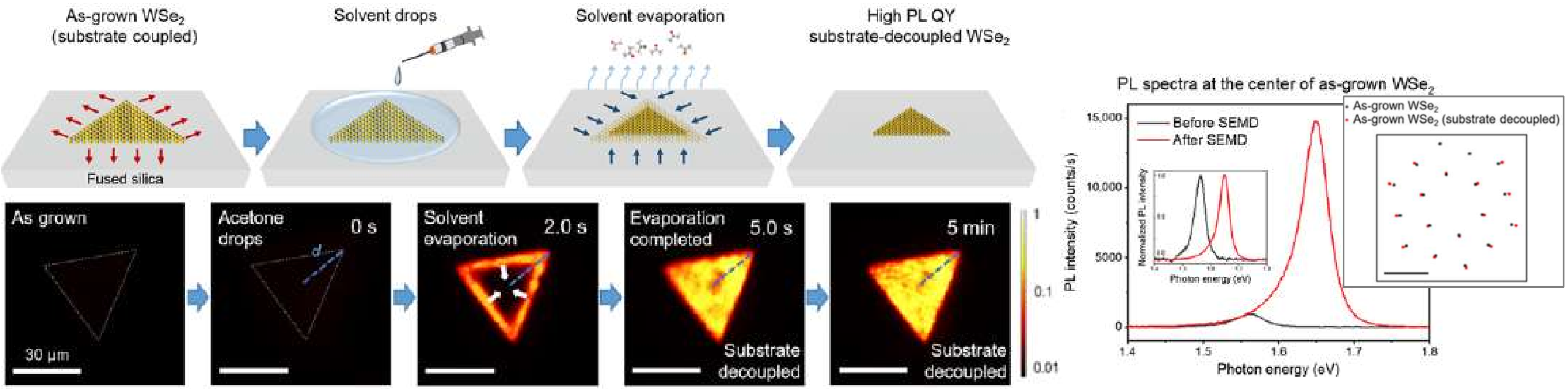

Kim et al., Sci. Adv. 5, eaau4728 (2019)

By electrostatic doping

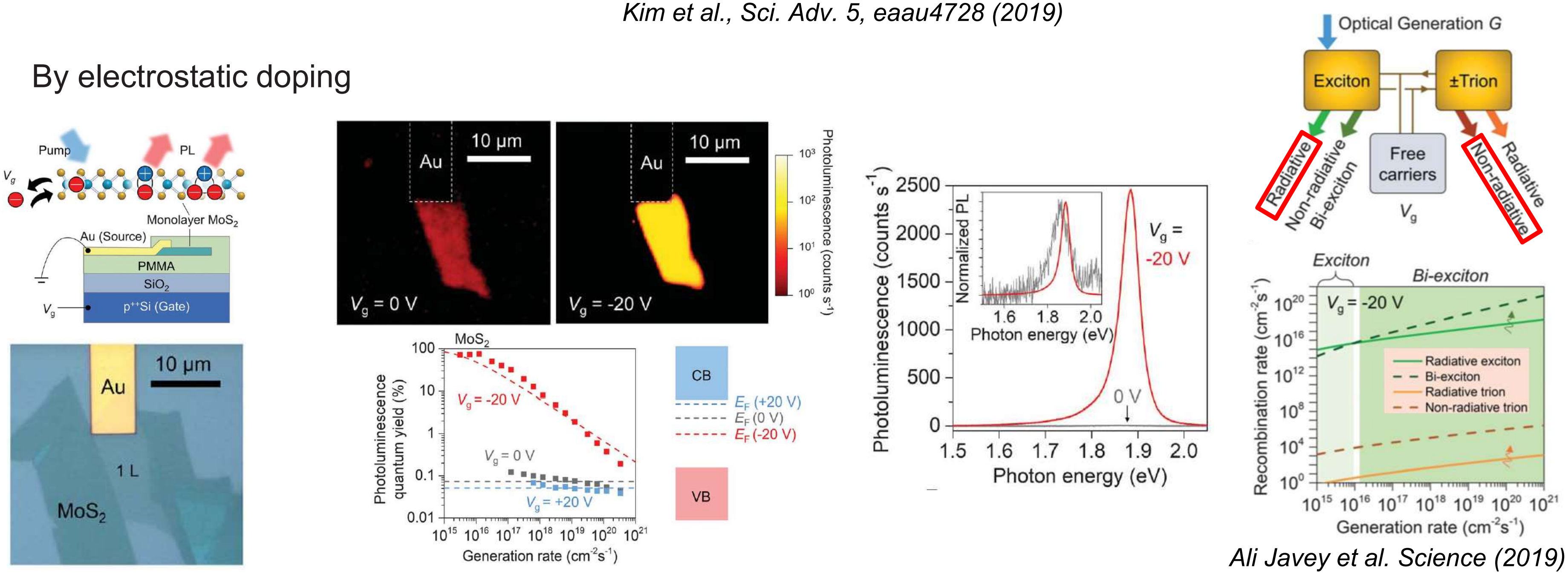

Ali Javey et al. Science (2019)

Effect of Substrate on PL

Doping by functionalized substrate

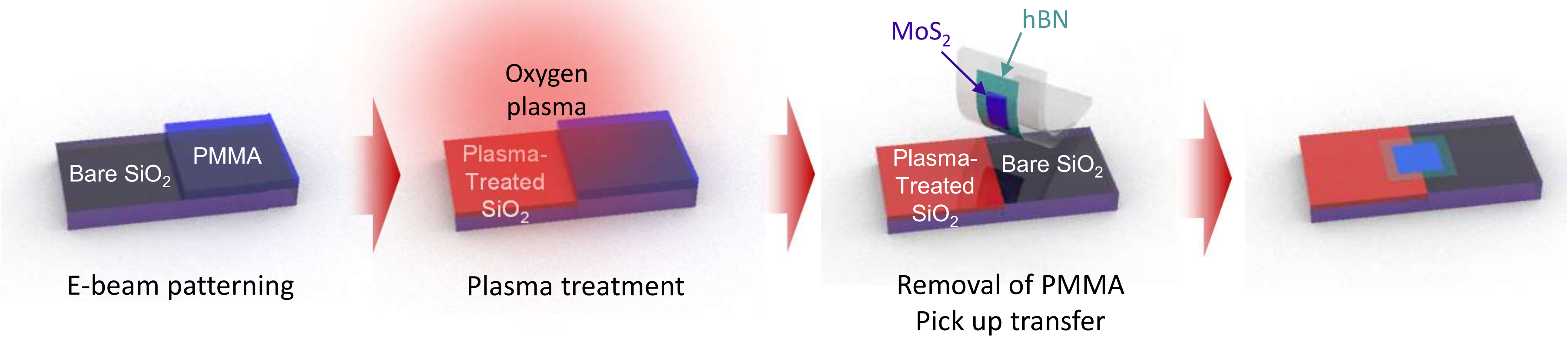

✓ It is well known that the plasma-treated SiO_2 substrate becomes hydrophilic owing to the formation of hydroxyl (–OH) functional groups on the surface.

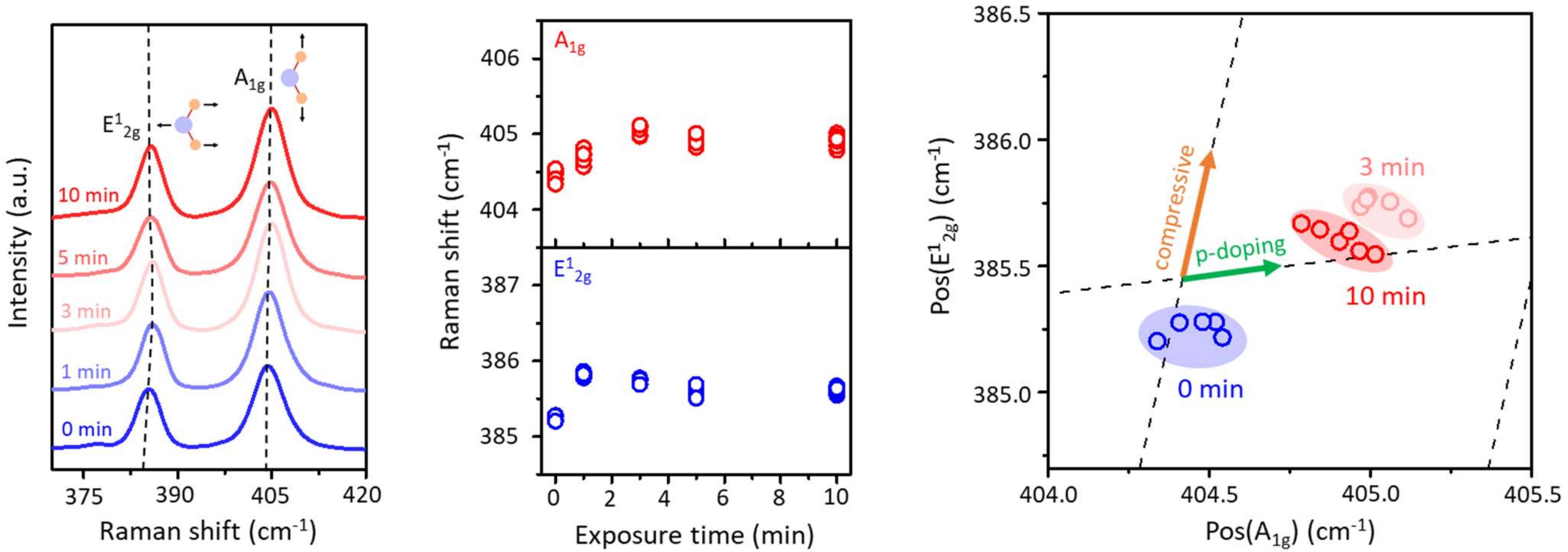

E.J. Ji, K.M. Yang, G.H. Lee, **Nanoscale** (2022)

Effect of Substrate on PL

Exciton-dominant PL of MoS_2 on plasma-treated substrate

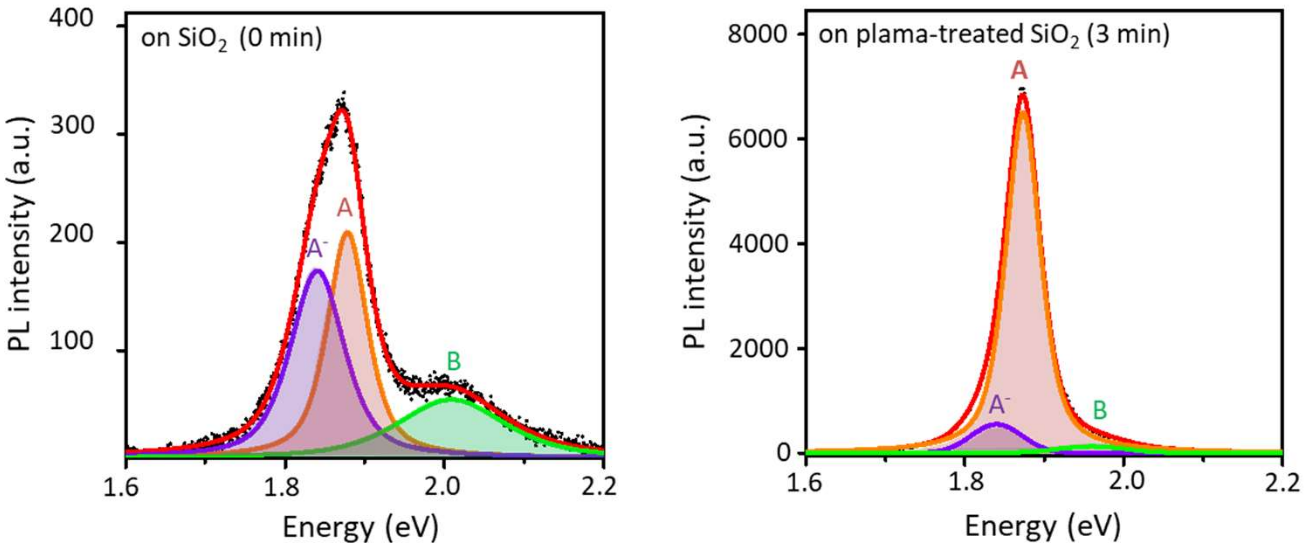

Suppression of non-radiative recombination by trion

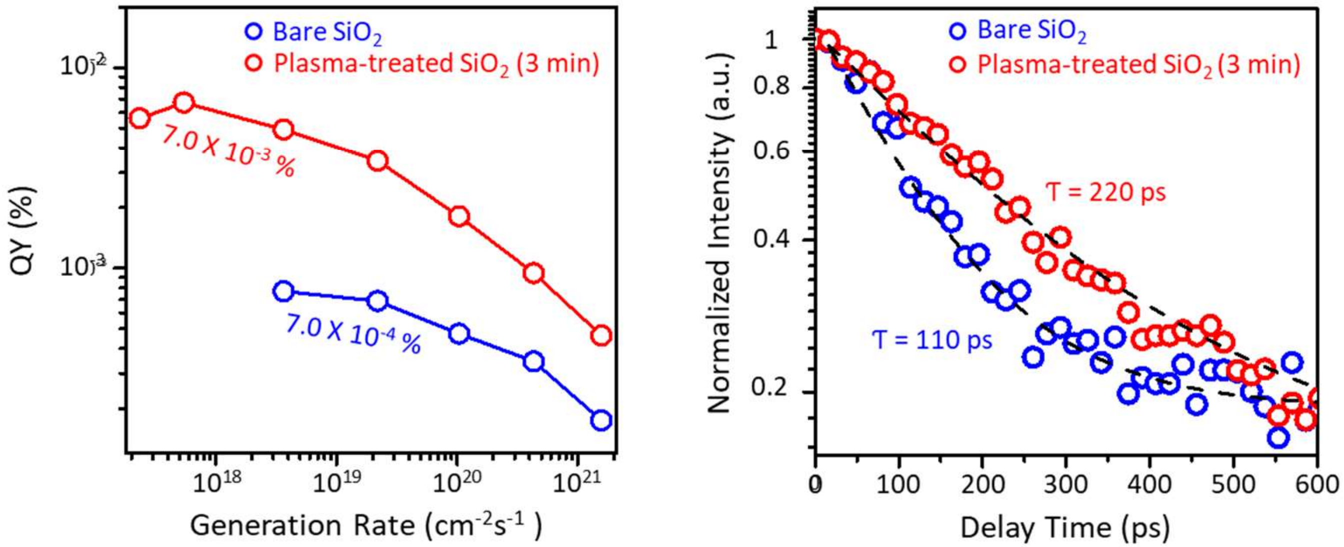

E.J. Ji, K.M. Yang, G.H. Lee, **Nanoscale** (2022)

Electronics Based on Two-dimensional Materials

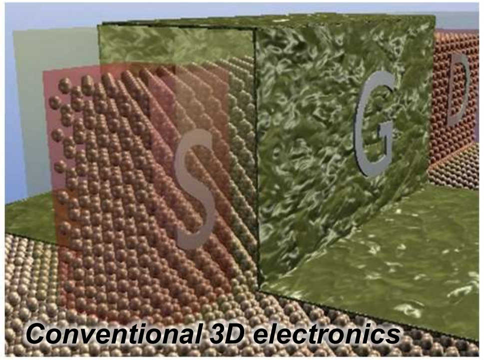

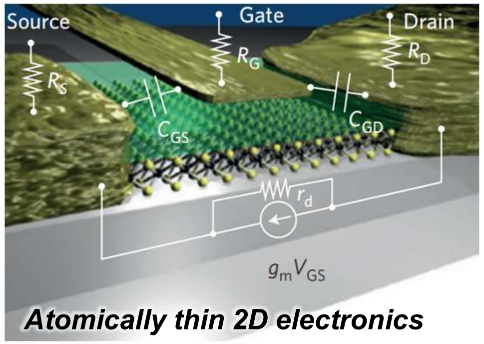

G. Fiori et al. Nat. Nanotechnol. (2014)

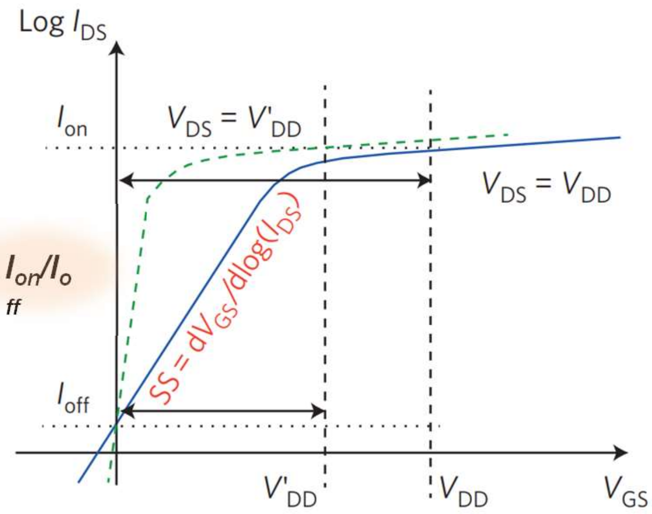

- Two terminal device: open-circuited or short-circuited at $V_{GS} > V_T$ (threshold voltage)
- Minimizing I_{off} = low standby power consumption
- Maximizing I_{on} = high switching speed
- I_{on}/I_{off} ratio needs to be larger than 10^4.
- Intrinsic limit for subthreshold swing (SS) at room T = 60 mV/dec (large I_{on}/I_{off} ratio at small supply voltage)
- For high-performance applications, large switching speed at the cost of high power dissipation
- For low-power applications, low power consumption (a key requirement in portable electronics)

Challenges for conventional electronics

- Extreme scaling down with electrostatic control of the channel
- Thin gate oxides which leads to increased leakage

Main opportunities for 2D electronics

- Ultimately thin channel transistor
- Perfect gate control over the channel barrier
- Reduced short-channel effect

Electronic Transport of TMDs

Molybdenum Disulfide (MoS_2)

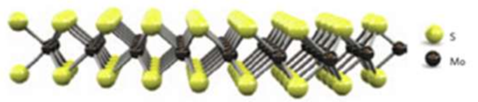

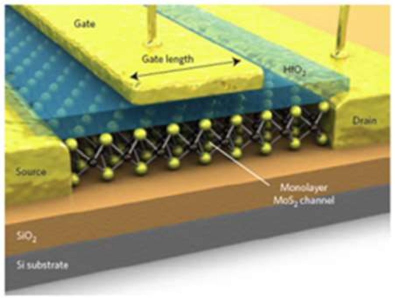

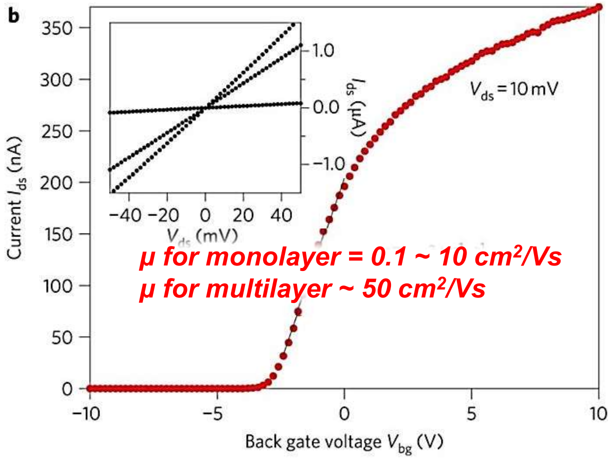

μ for monolayer = 0.1 ~ 10 cm²/Vs
μ for multilayer ~ 50 cm²/Vs

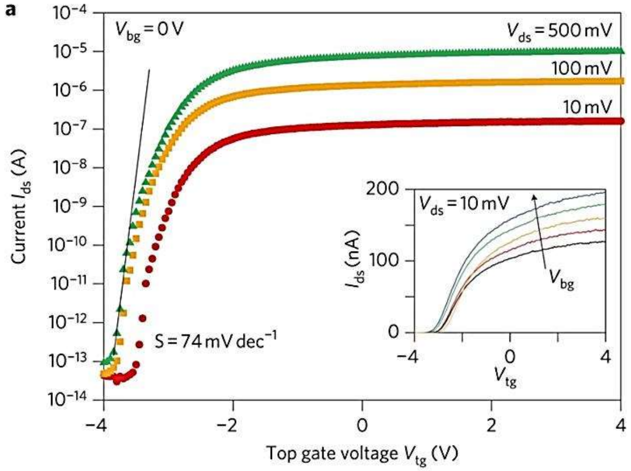

B. Radisavljevic et al. Nature Nano (2011)

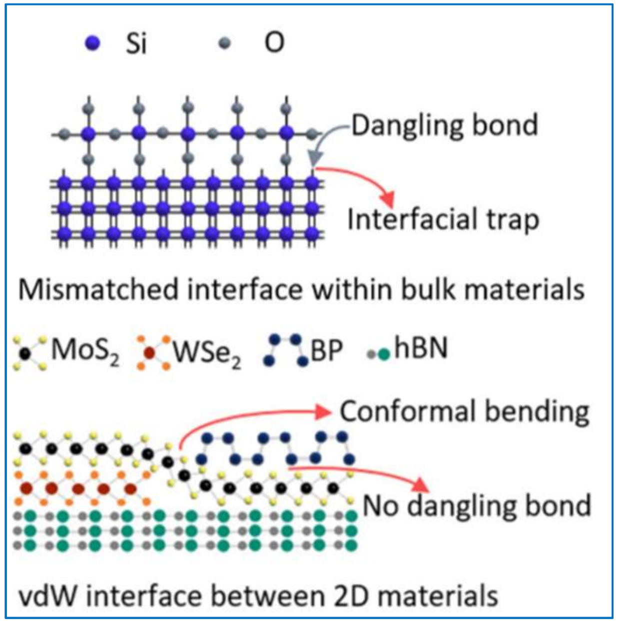

npj 2D Mater. Appl. 51 (2022)

Simulated

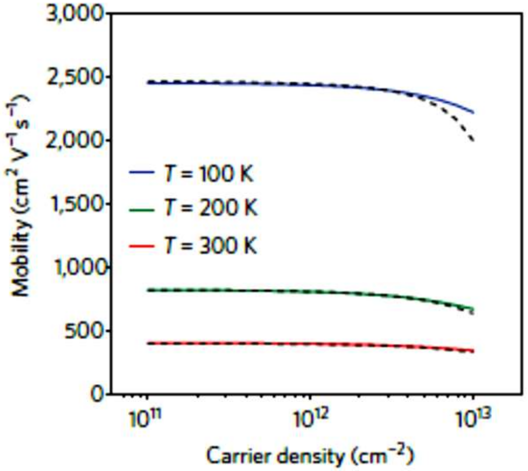

Q. H. Wang et al. Nature Nano (2012)

Experimental

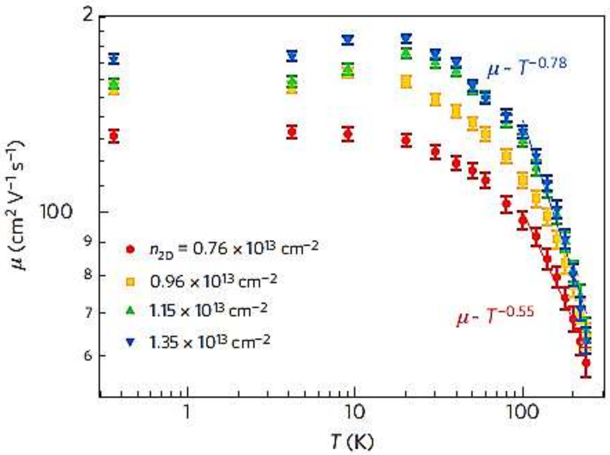

B. Radisavljevic et al. Nature Mater. (2014)

Electronic Transport of TMDs

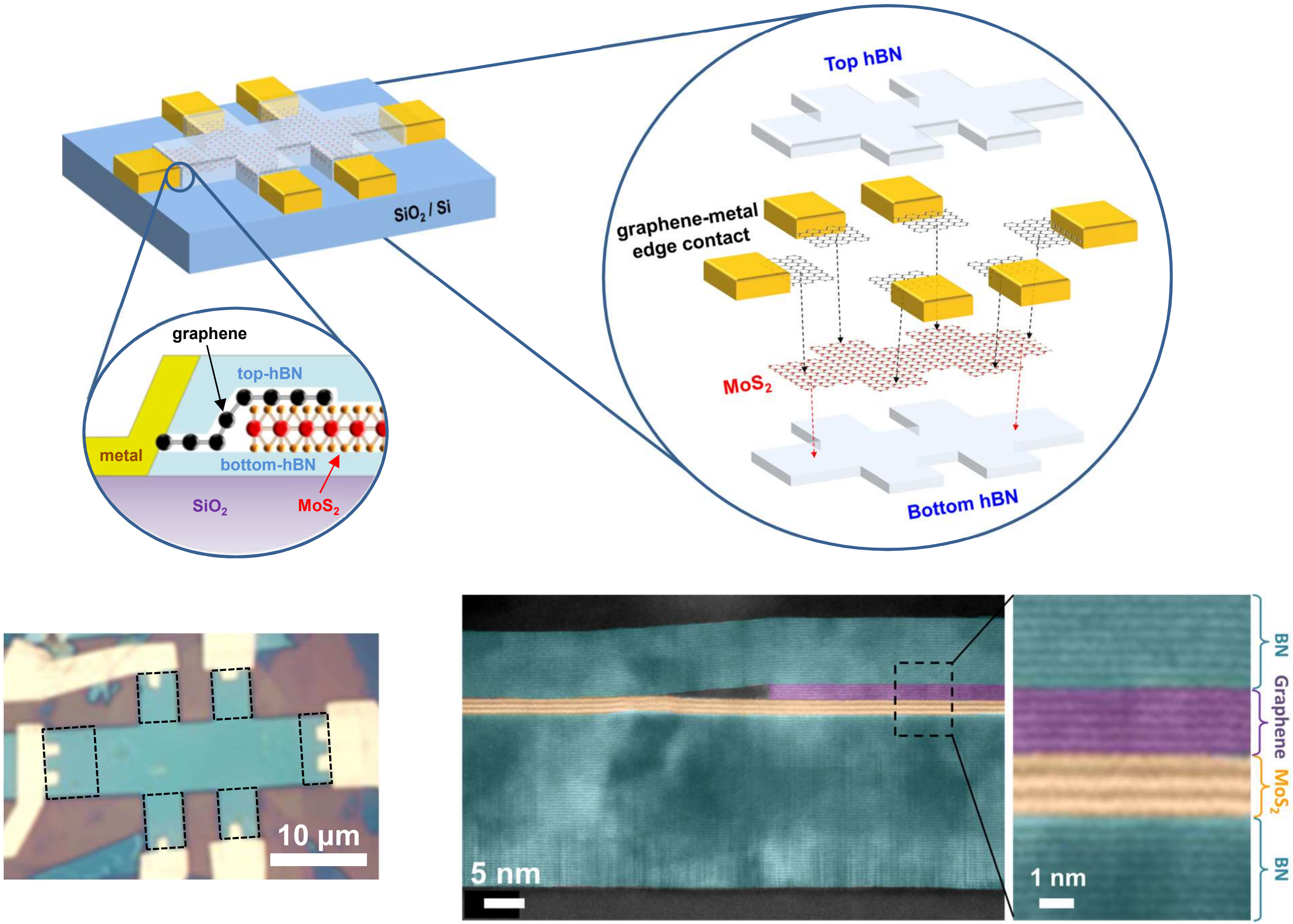

X. Cui et al. Nature Nanotechnol. (2015)

Electronic Transport of TMDs

Open structure device

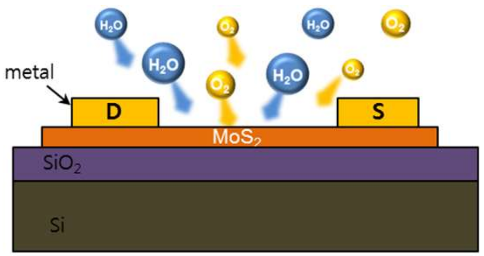

Encapsulated Device

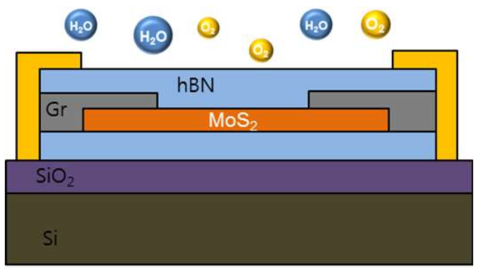

Perfect protection from environment

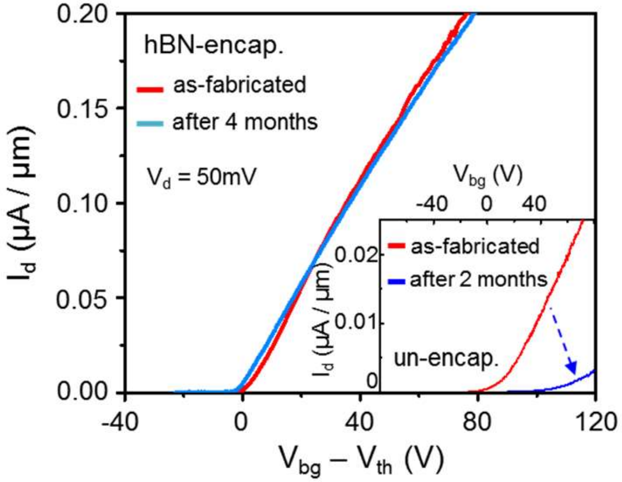

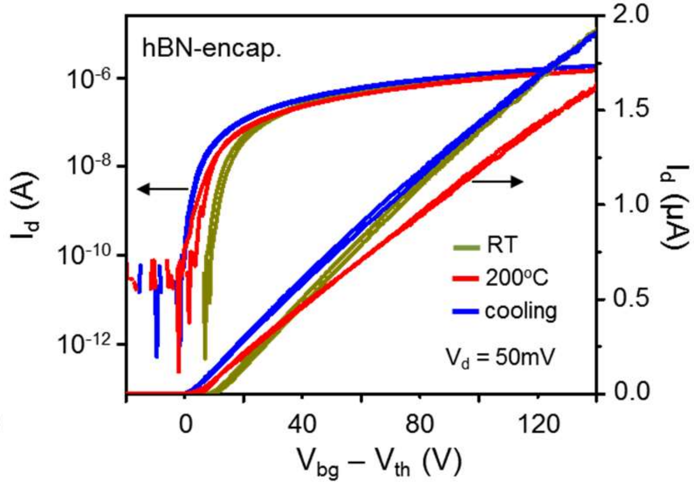

Gate-tunable graphene electrodes

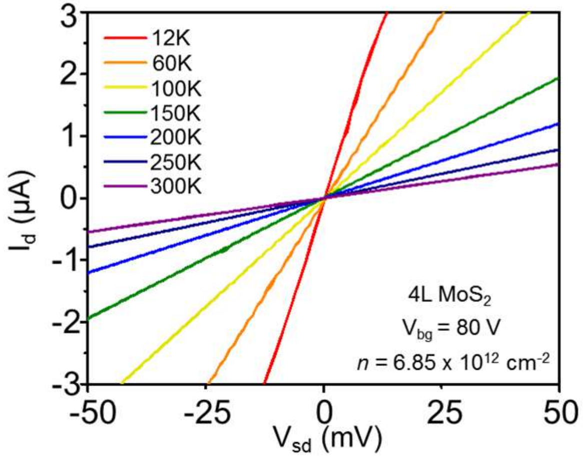

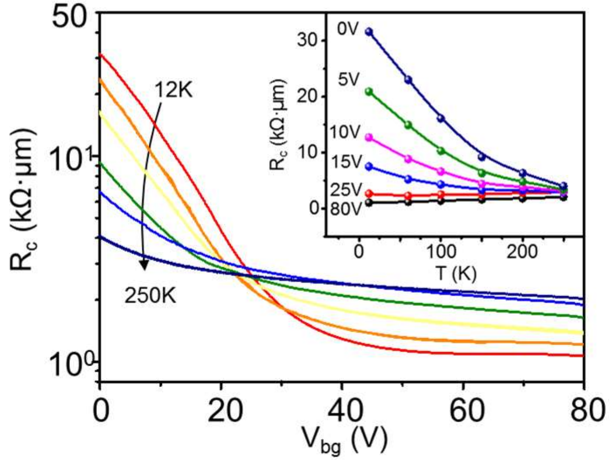

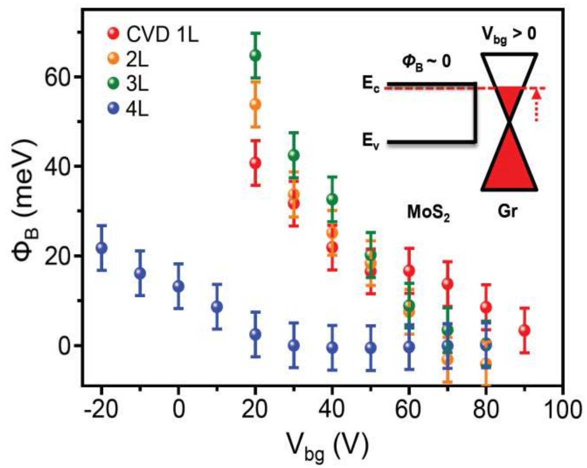

X. Cui et al. Nature Nanotechnol. (2015)

Electronic Transport of TMDs

Ultrahigh mobility in MoS_2

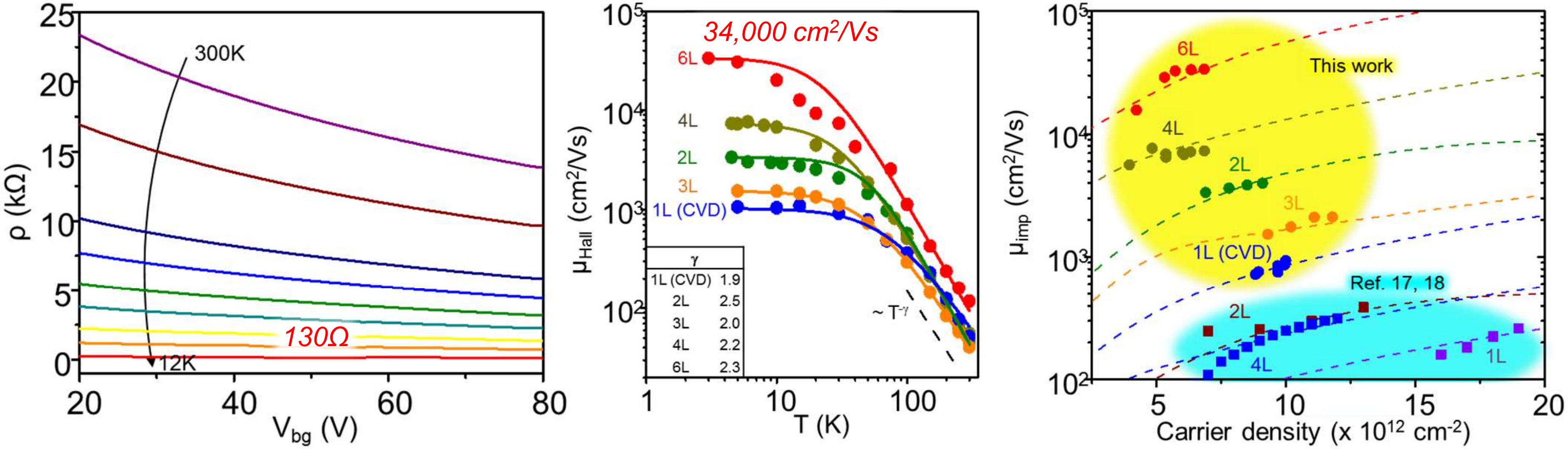

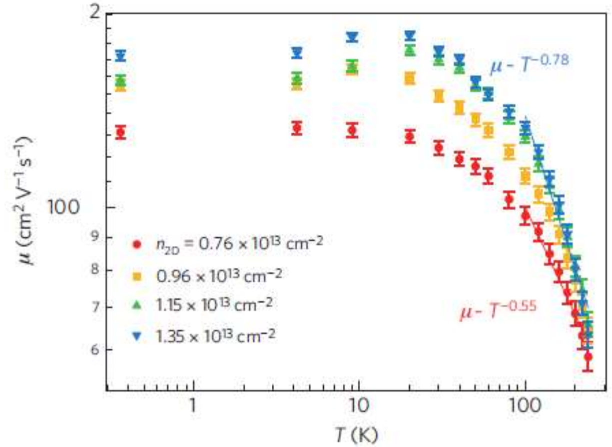

B. Radisavjevic et al. Nature Mater. (2014)

SdH Oscillations & QHE in MoS_2

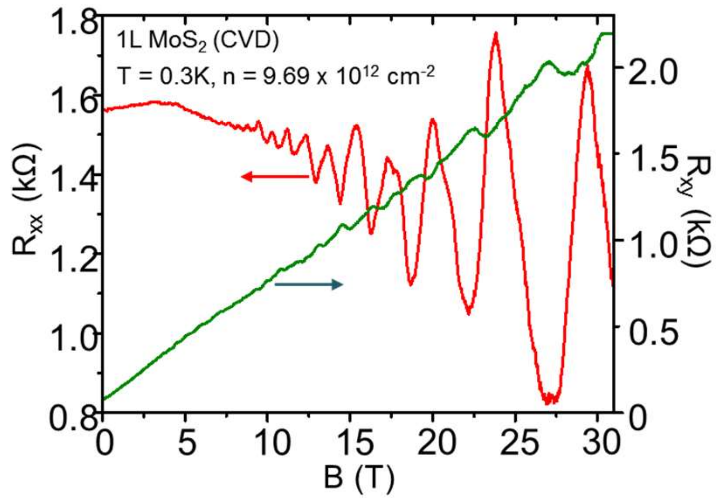

X. Cui et al. Nature Nanotechnol. (2015)

Electronic Transport of TMDs

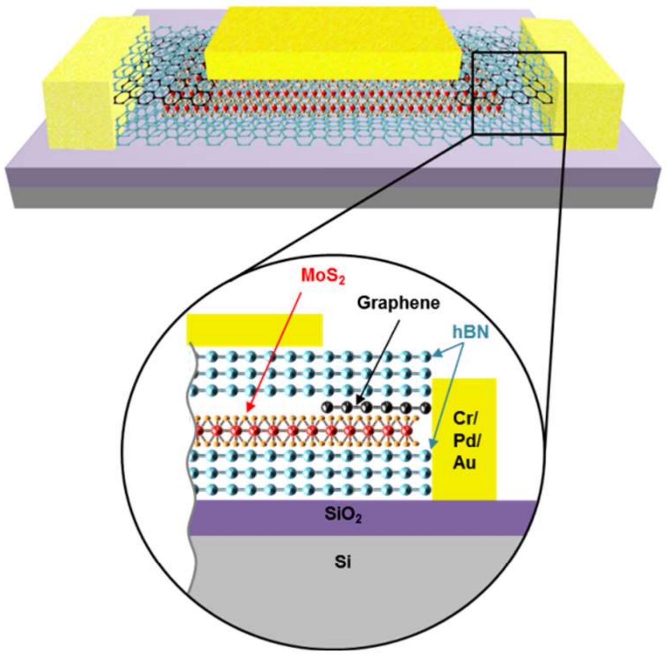

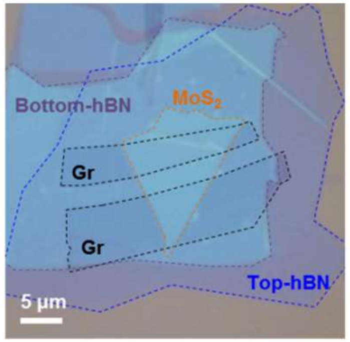

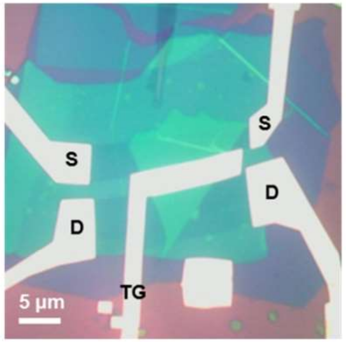

MoS$_2$ Thickness	2T Mobility (cm^2/Vs)	Fabrication Method
1L	94 (bottom-gate)	Pick-up
CVD 1L	19 (bottom-gate)	PDMS
2L	120	Pick-up
3L	69 (bottom-gate) 46 (top-gate)	Pick-up
3L	33 (bottom-gate) 37 (top-gate)	Pick-up
5L	52 (top-gate)	Pick-up
6L	96 (bottom-gate)	PDMS
45nm	151 (bottom-gate)	PDMS

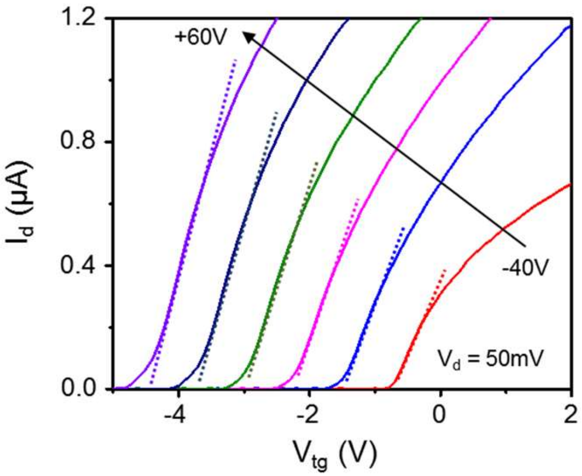

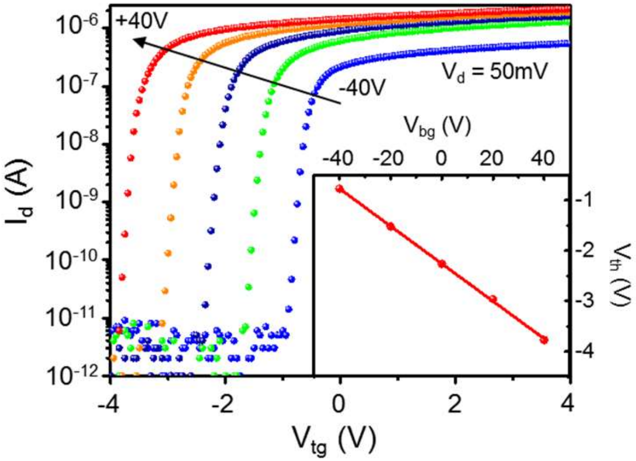

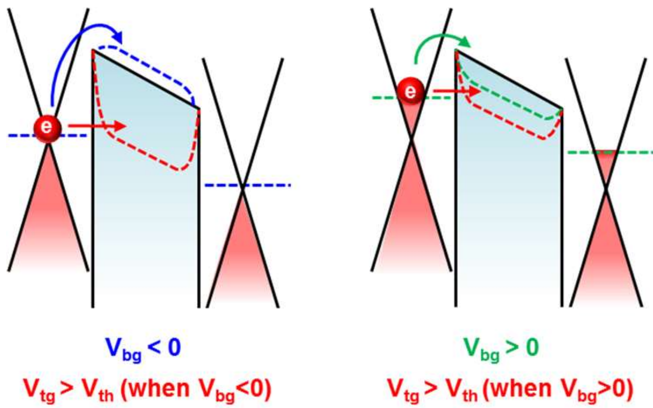

- *Tunable contact barrier (contact resistance)*
- *Tunable threshold voltage*

G.H. Lee, Y.J. Yoo, J. Hone et al. ACS Nano (2015)

Electronic Transport of TMDs

Subthermionic tunnel field-effect transistor

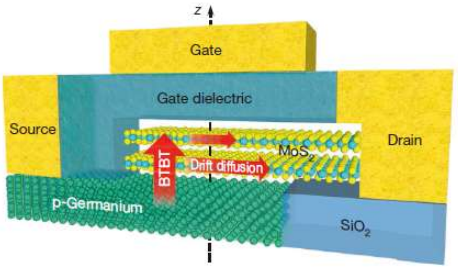

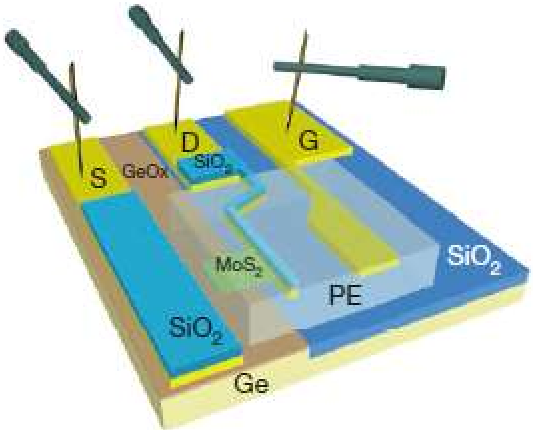

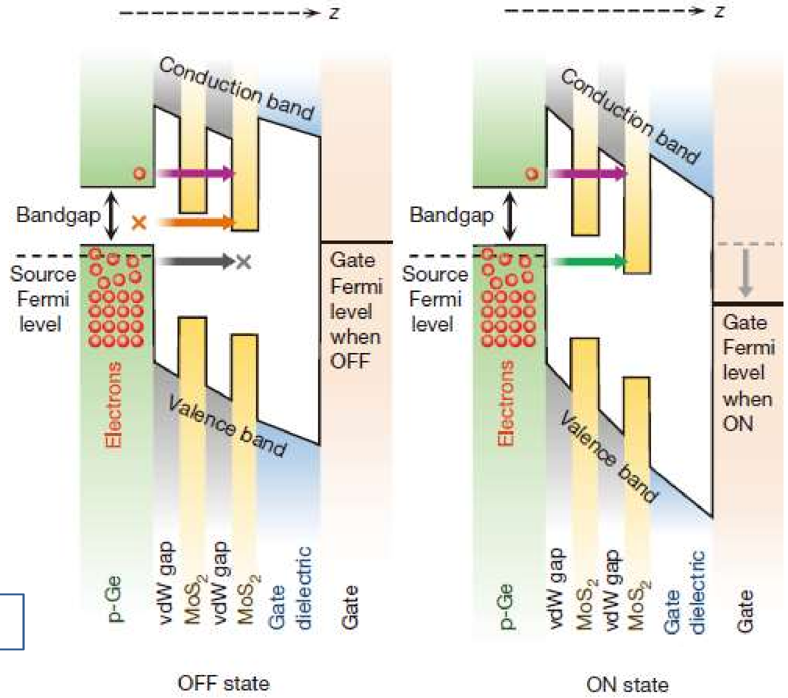

Tunnel current ∝ (Density of carriers × Empty states × tunnel probability)

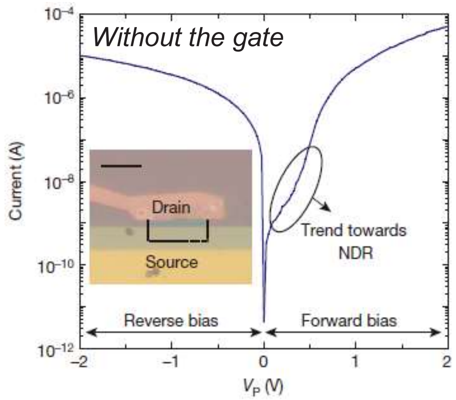

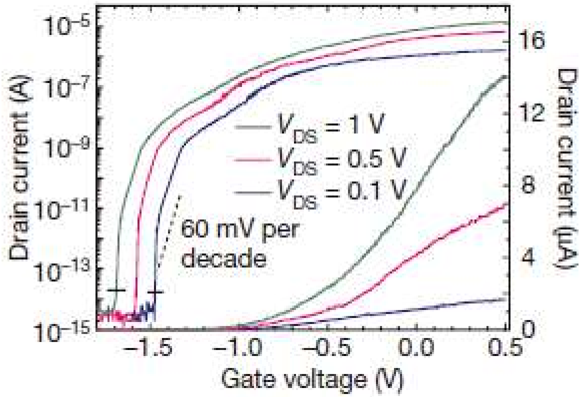

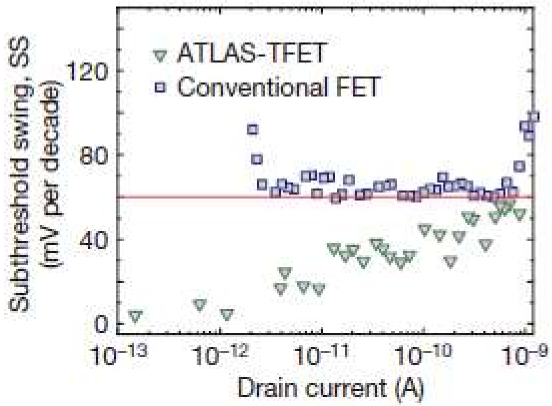

Deblina Sarkar et al. Nature (2015)

Piezoelectricity of MoS_2

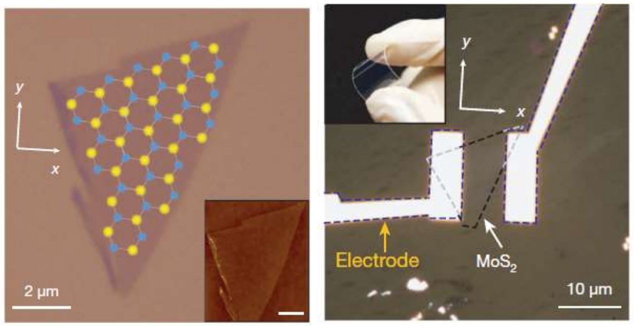

Directionality of piezoelectricity

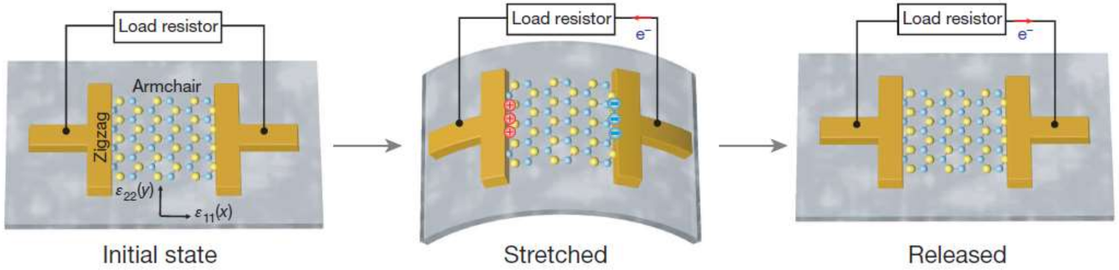

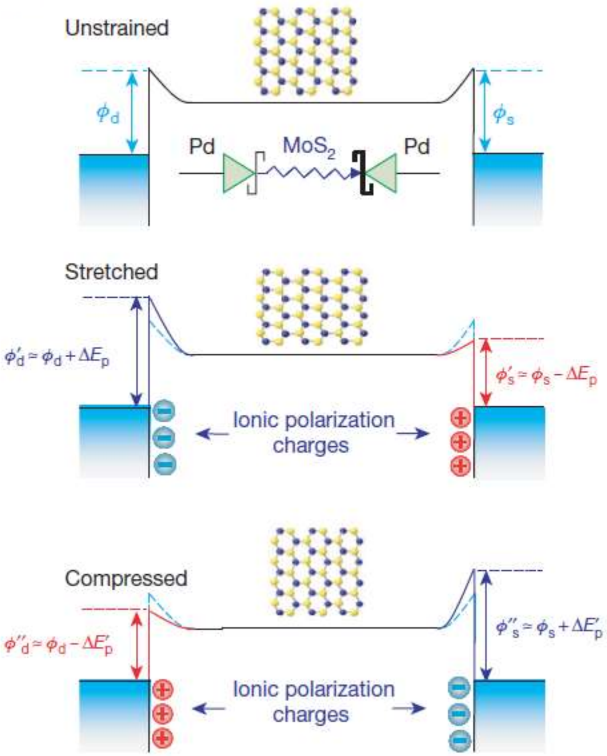

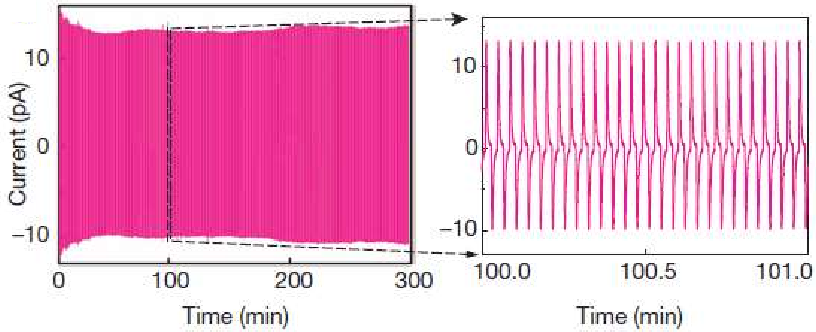

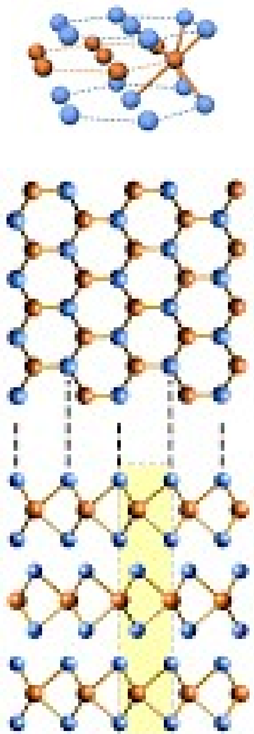

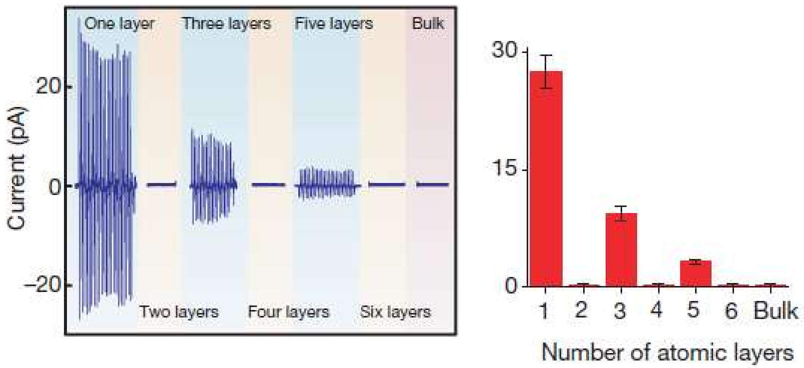

Dependence of layer number on piezoelectricity due to inversion symmetry breaking.

W. Wu et al. Nature (2014)

Spins, Valleys and Excitons in TMDs

Spin-orbit coupling

: TMDs have a strong spin-orbit coupling, which introduces a strong energy splitting between spin up and down states. The spin splitting in conduction band and valence band is in the meV range and several hundred meV, respectively.

Valley degree of freedom

: Confined carriers at different moment and same energy of local maximum/minimum on the valence/conduction band

Valley dependent optical selection rules

: A right circular polarized photon (σ^+) initialize a carrier in the K^+ valley and a left circular polarized photon (σ^-) initialize a carrier in the K^- valley.

Valleytronics

: The internal degree of freedom of valley is used to store, manipulate and read out bits of information using the multiple extrema of the band structure, so that the information of 0s and 1s would be stored as different discrete values of the crystal momentum.

Large binding energy of exciton

: In atomically thin 2D systems, there exist a strong confinement of electrons and holes in the layer plane, which dramatically enhances the Coulomb interaction between the electron and hole in TMD monolayers, leading to a large binding energy in the hundreds of meV range.

Trion

: Negatively charged trion consists of two electrons and one hole and a positively charged trion consists of two holes and one electron.

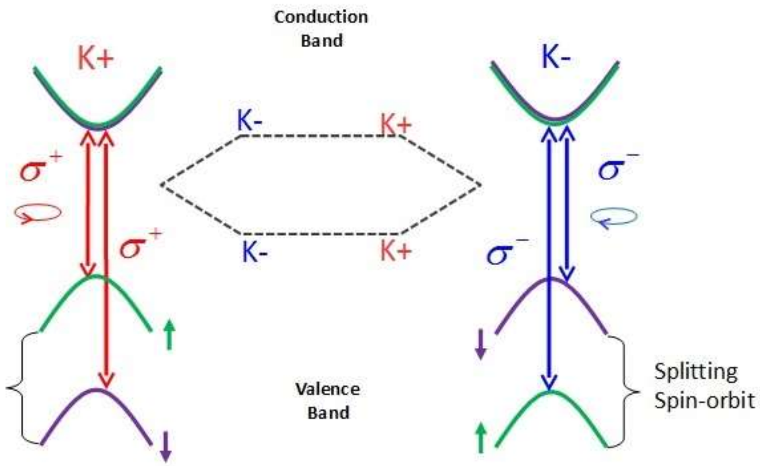

Electrically tunable trion density

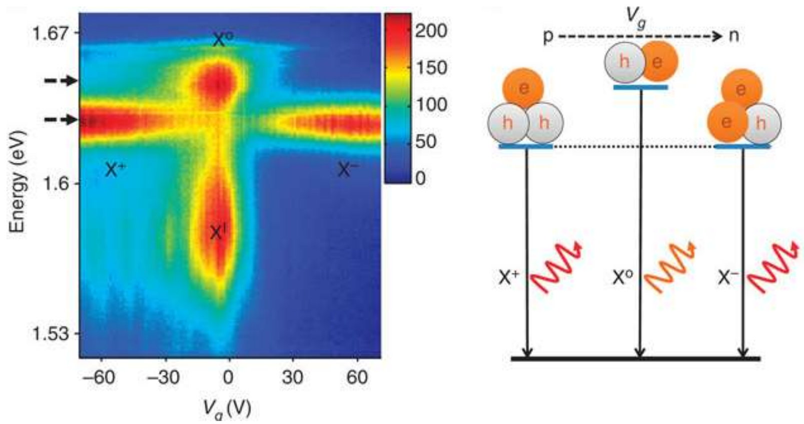

F. Xia et al. Nature Nanotechnol. (2014) & K. F. Mak et al. Nature Mater. (2014) & H. Fang et al. Nano Lett. (2012) & H. Zeng et al. Nature Nanotechnol. (2012)

Valleys in TMDs

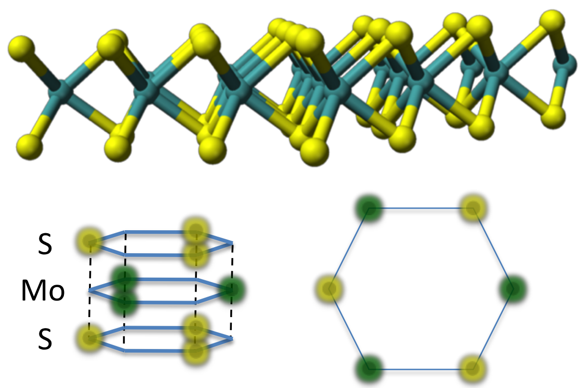

K. F. Mak et al. Nature Nanotechnology (2013)

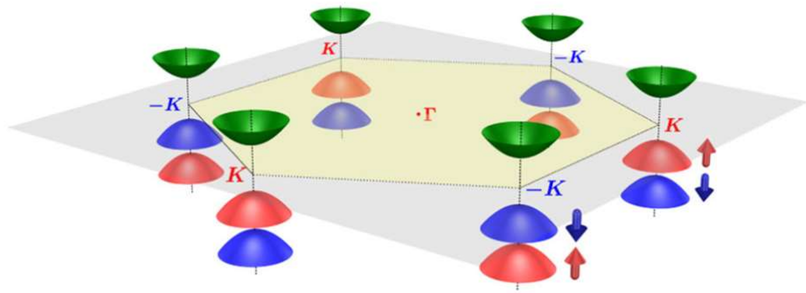

D. Xio et al. PRL (2012)

Honeycomb lattice with broken inversion symmetry induces the valley degree of freedom.

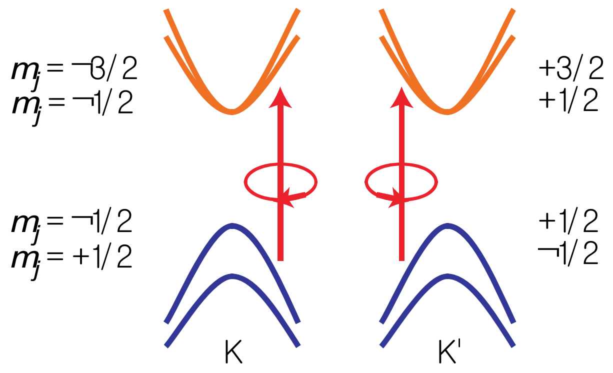

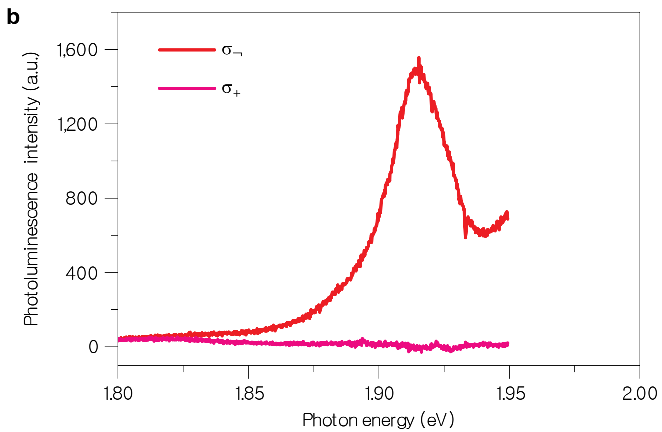

Valley dependent optical selection rule - accessed by circularly polarized light

Valleys in TMDs

Spin splitting by the strong spin-orbit coupling

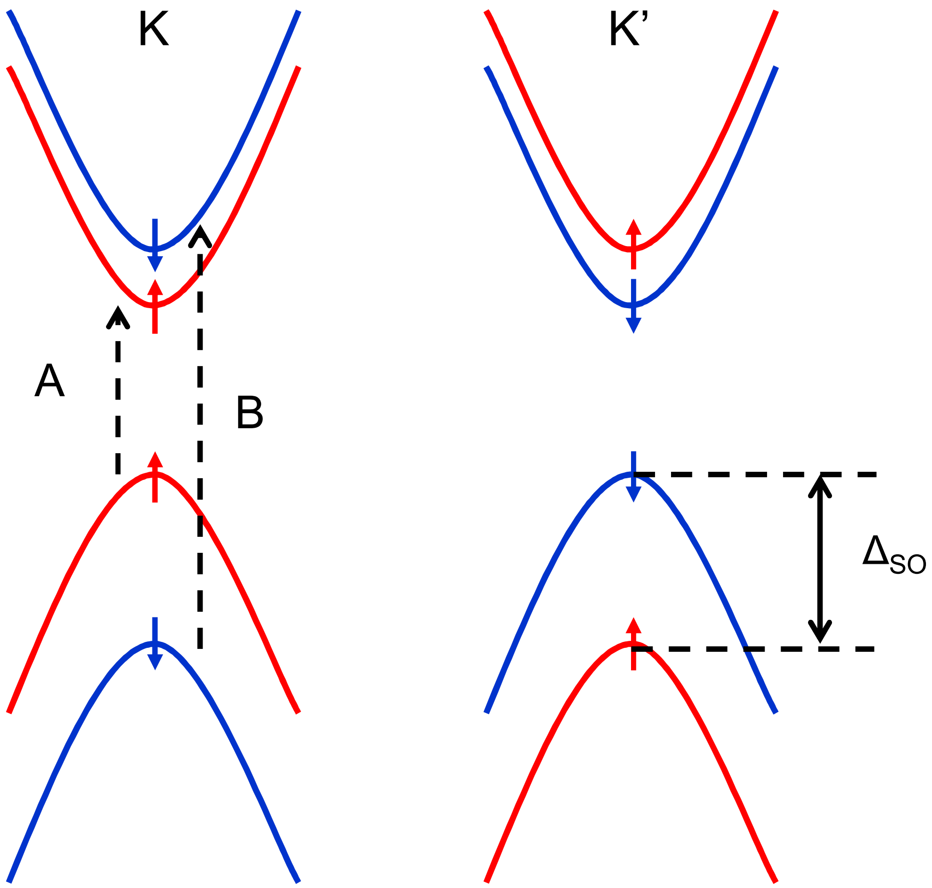

Optical absorption spectra

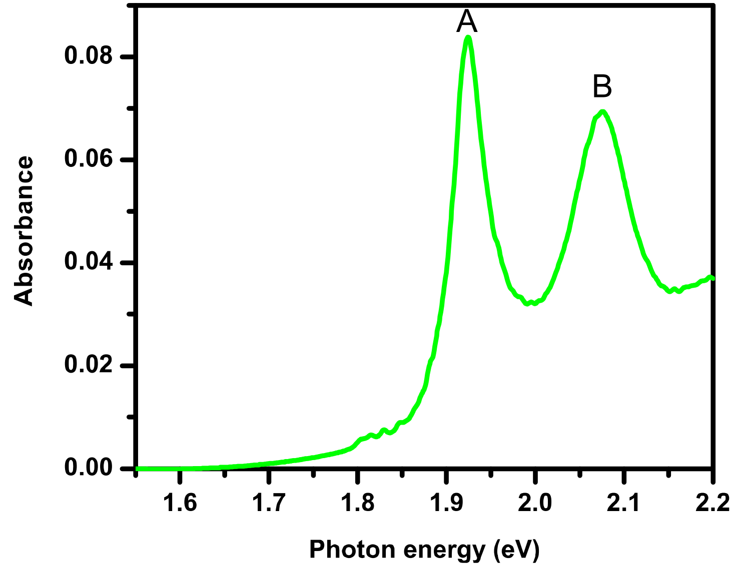

K. F. Mak et al. Nature Nanotech. (2013)

Valley Hall Effect in Monolayer TMDC

Valley polarization by circularly polarized light

:observation of Hall voltage by optical pumping

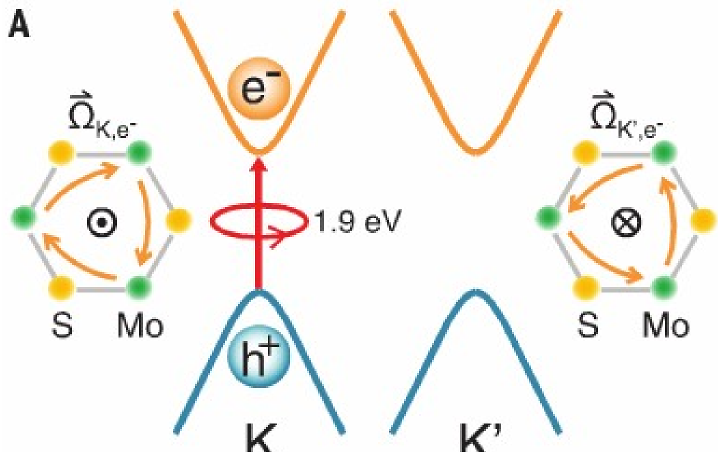

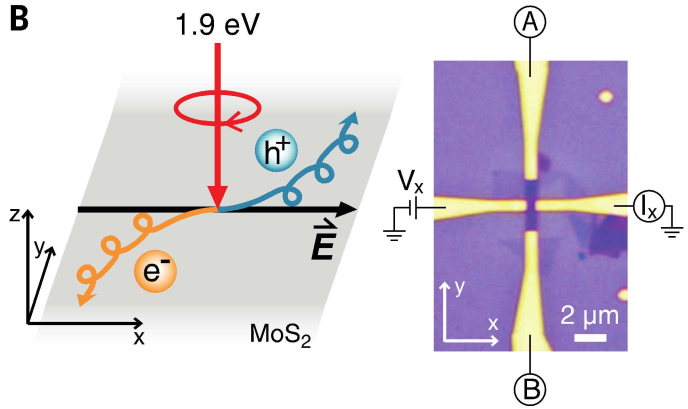

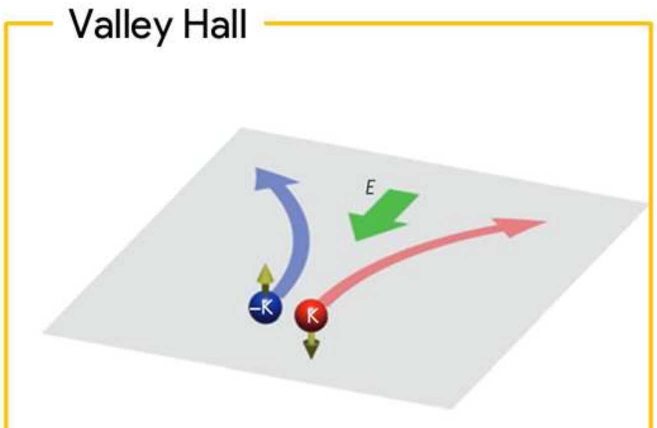

Xu *et al.*, Nat. Phys., **10**, 343 (2014).

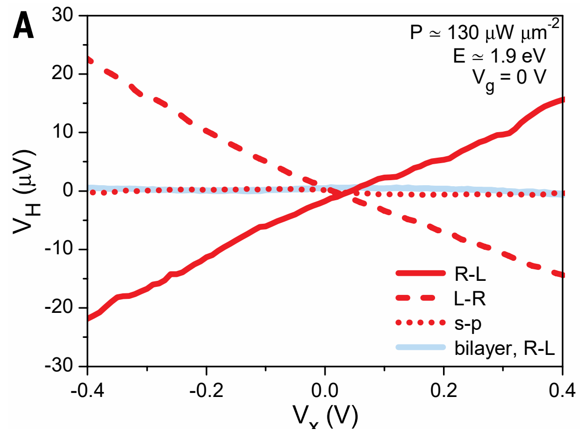

K. F. Mak et al., Science (2014)

Charge Carriers in TMDs

Ionic gel-gated MoS_2

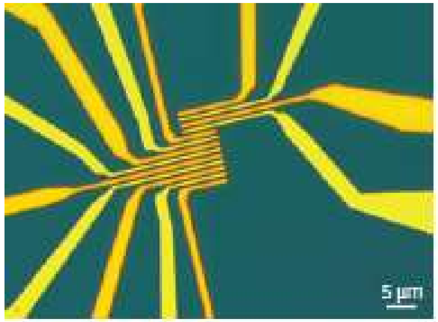

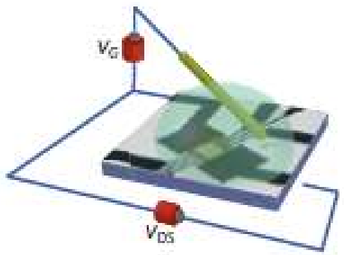

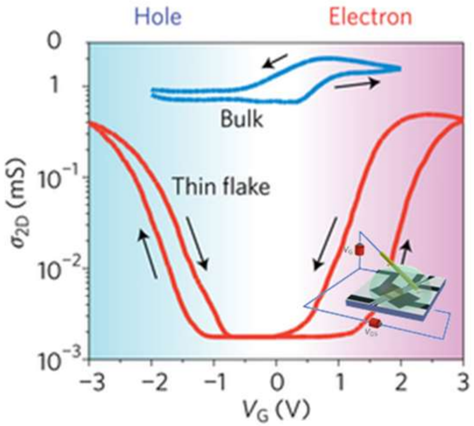

Y. Zhang et al. Nano Lett. (2012)

Ambipolar behavior

Tungsten Diselenide (WSe_2)

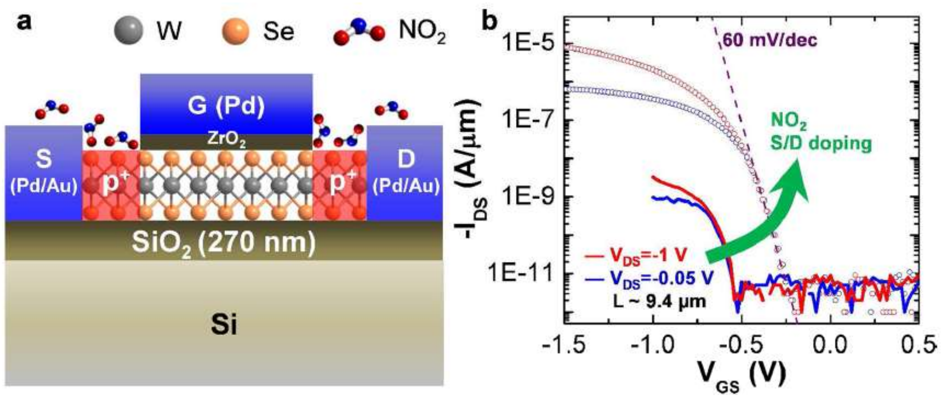

500cm²/Vs, ambipolar, 10⁴ on/off ratio

H. Fang et al. Nano Lett. (2012)

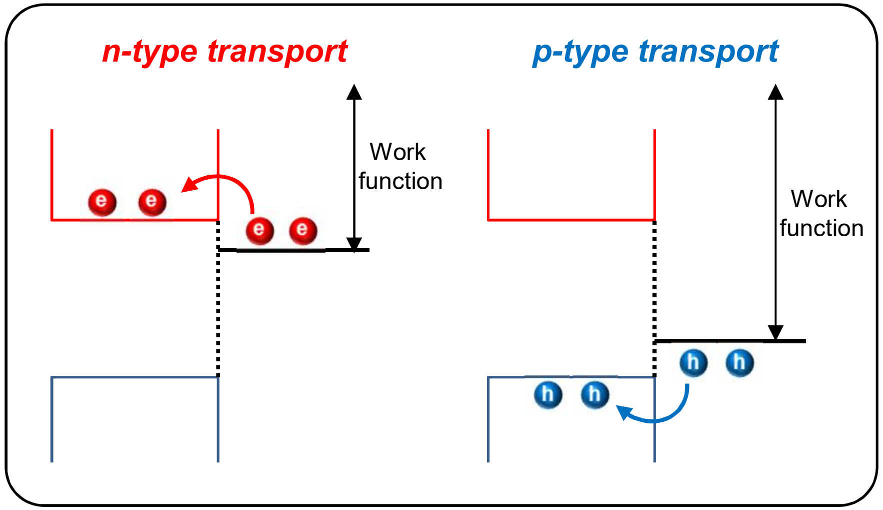

Carrier Type Control in TMDs: WF of Metal

Transfer curve of WSe_2 transistor with various metal contacts

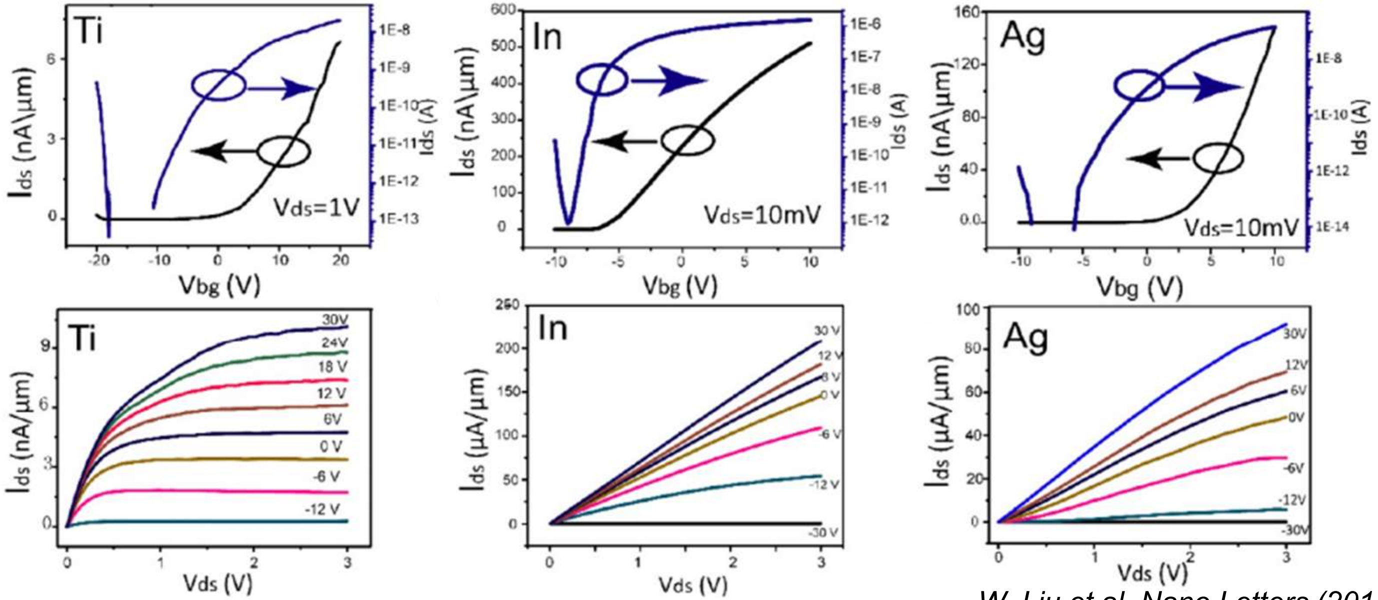

W. Liu et al. Nano Letters (2013)

Carrier type control with various metal contacts

- Band bending occurs through the alignment of the Fermi level of a metal electrode
- Carrier type controlled with different work function of various metals

High WF of Pd on WSe_2 → p-type WSe_2

Low WF of In on WSe_2 → n-type WSe_2

Band diagram for WSe_2 FETs

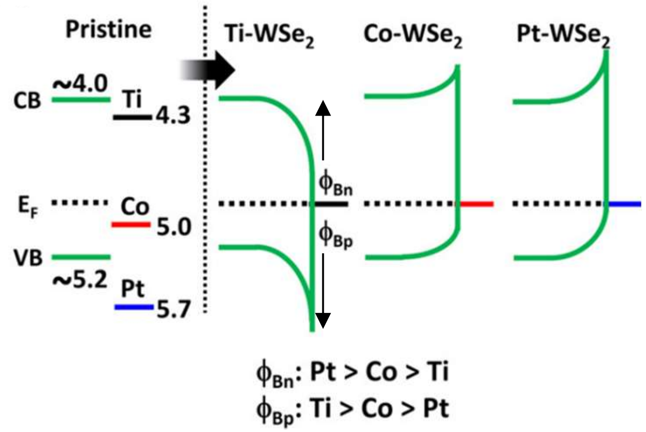

I. Lee et al. Nanotechnology (2015)

Carrier Type Control in TMDs: Thickness

Theoretical energy of monolayer to five-layer WSe_2

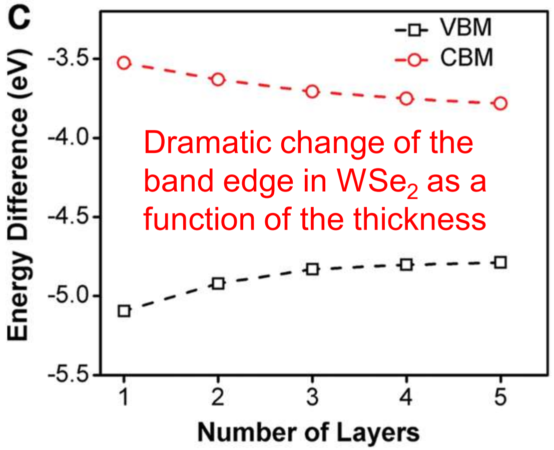

Transfer curves of WSe_2 transistors with various thicknesses

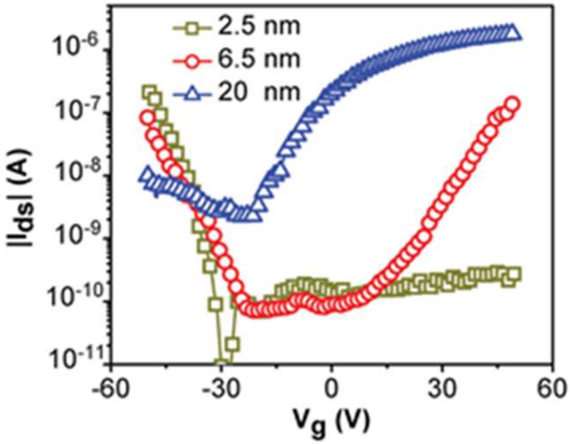

Carrier type control with various thicknesses

2.5 nm-thick WSe_2 → p-type WSe_2
6.5 nm-thick WSe_2 → ambipolar WSe_2
20 nm-thick WSe_2 → n-type WSe_2

2.5 nm

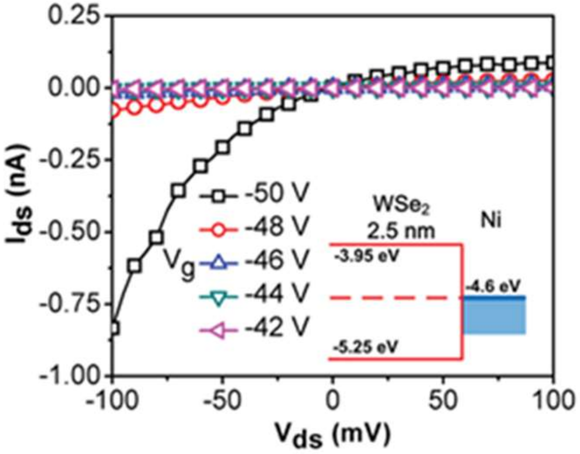

6.5 nm

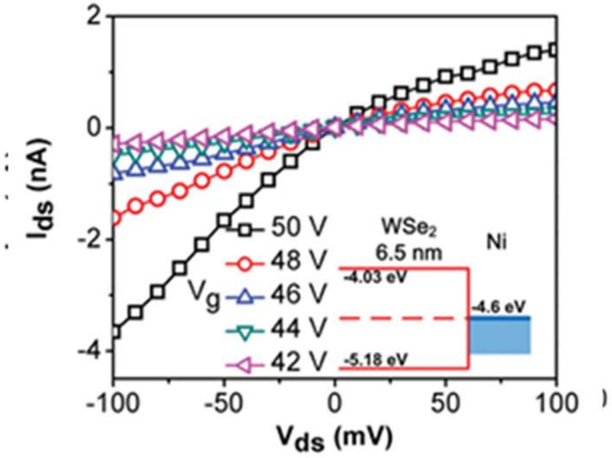

20 nm

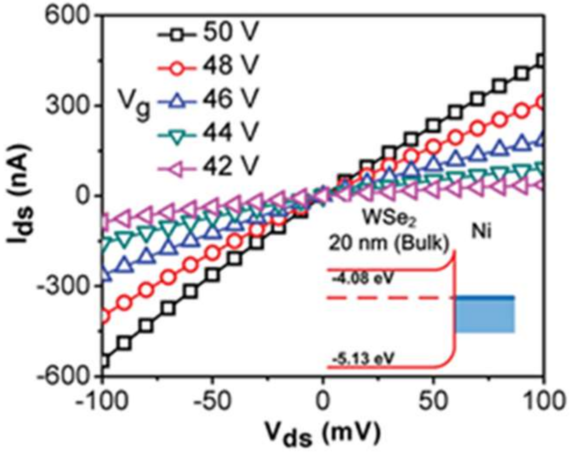

C. Zhou et al. Adv. Funct. Mater. (2016)

Carrier Type Control in TMDs: Defect

Intrinsic point defects in monolayer MoS_2

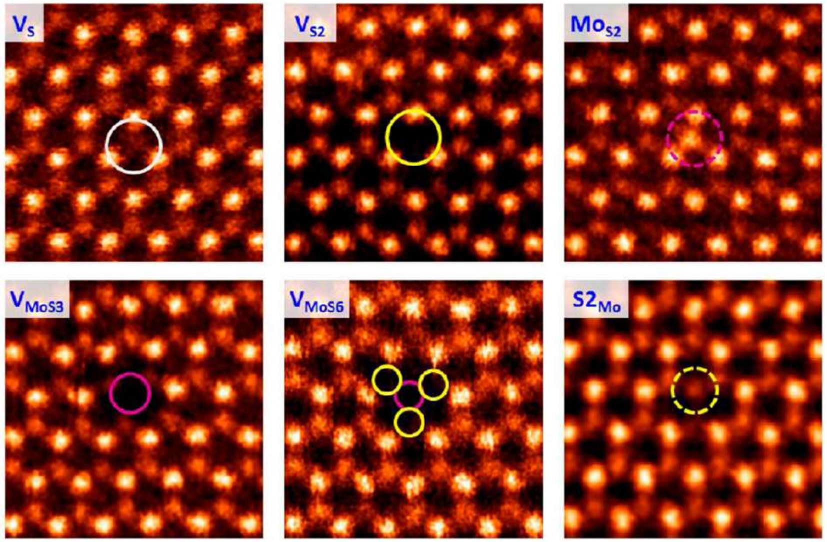

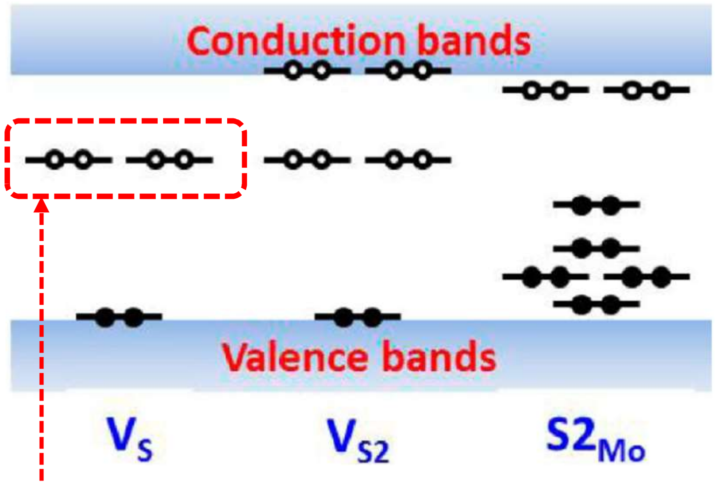

W. Zhou et al. Nano Letters (2013)

N-doping of TMDs by vacancies

- Sulfur vacancies have the lowest formation energy
- Sulfur vacancies introduce two unoccupied deep levels about 0.6 eV below the conduction

Sulfur vacancies act as a donor → n-type MoS_2

Emerging TMDs

Tin Disulfide (SnS_2)

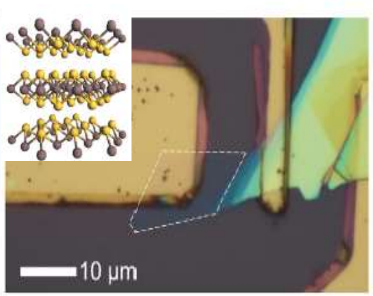

Thickness: ~ 0.6 nm per layer
Bandgap: 2.2 eV
SS: 80 mV/decade
On/Off ratio: ~ 10^6
Mobility: 5 cm^2/Vs

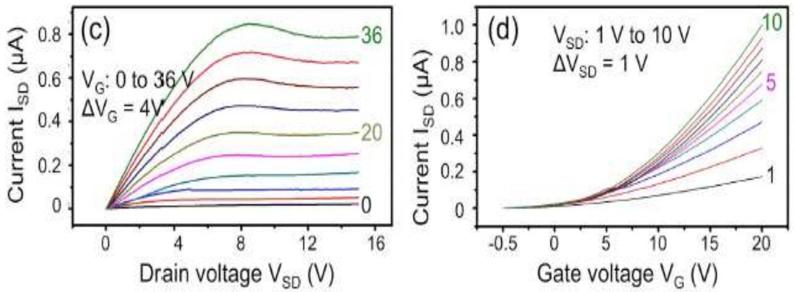

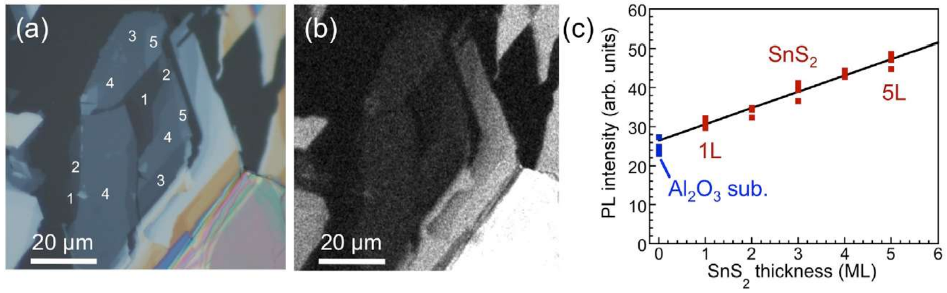

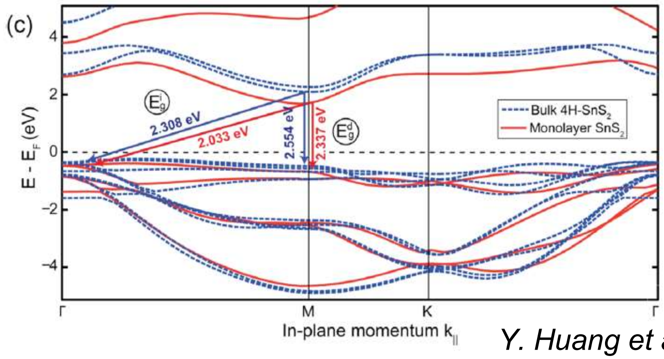

SnS_2 has indirect bandgap for both bulk and monolayer

Y. Huang et al. ACS Nano (2014)

Molybdenum selenide ($MoSe_2$)

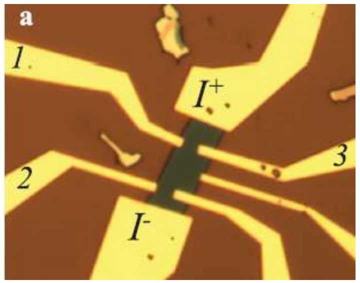

Thickness: ~ 0.7 nm per layer
Bandgap: ~ 1.41 eV
Mobility: ~ 200 cm^2/Vs (e^-)
~150 cm^2/Vs (h^+)

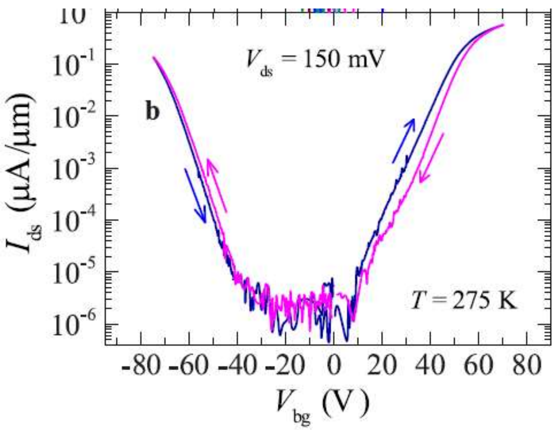

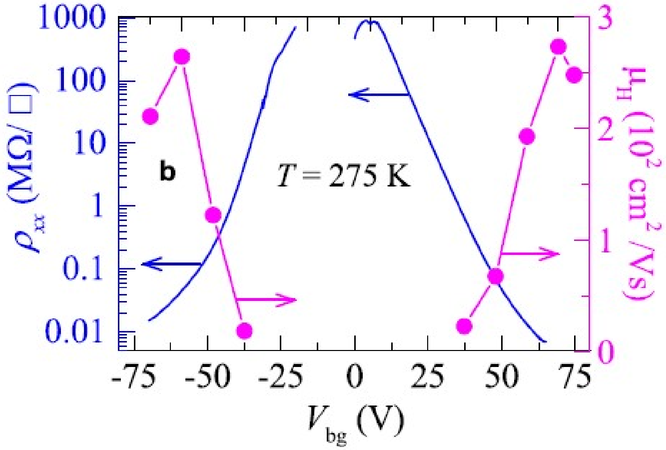

N. R. Pradhan et al. ACS Nano (2014)

Emerging TMDs

Molybdenum Ditelluride($MoTe_2$)

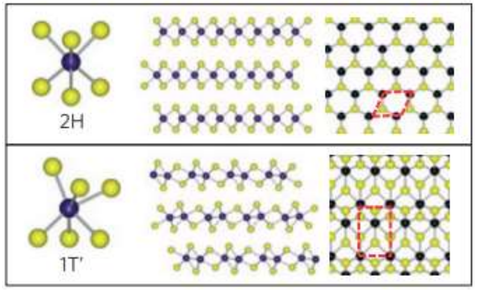

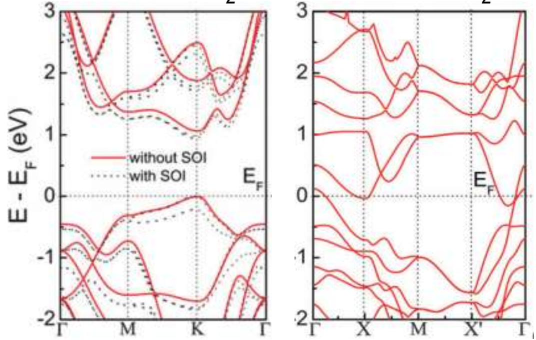

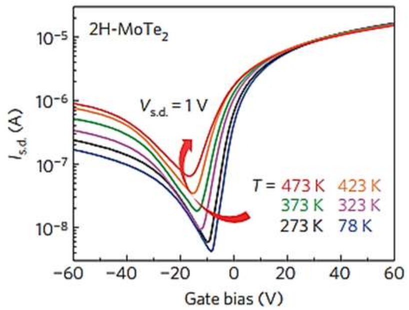

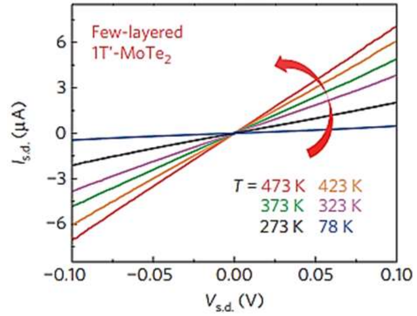

M. Kan et al. PCCP (2015) & D. H. Keum et al. Nature physics (2015)

Tungsten Ditelluride(WTe_2)

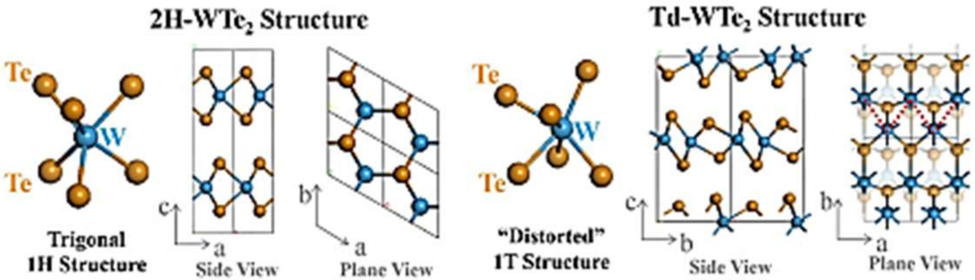

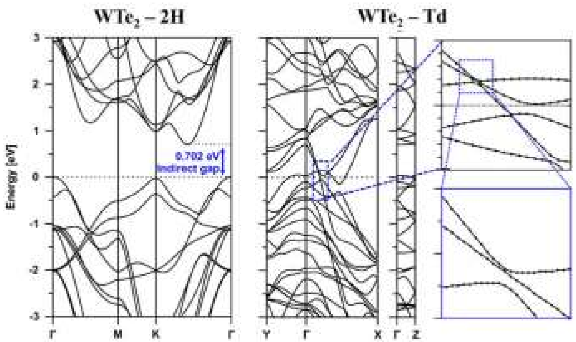

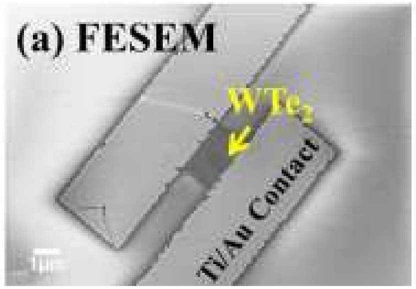

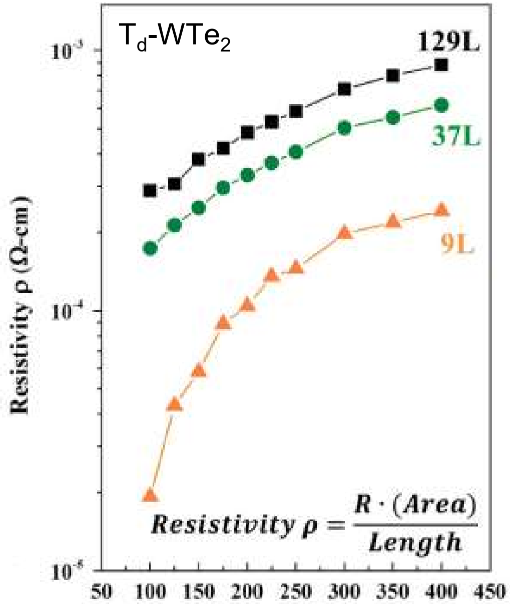

C.-H. Lee et al. Scientific reports (2015)

Optical Transparency of TMDs

CVD-MoS2

2L -> 4L -> 8L -> 12L

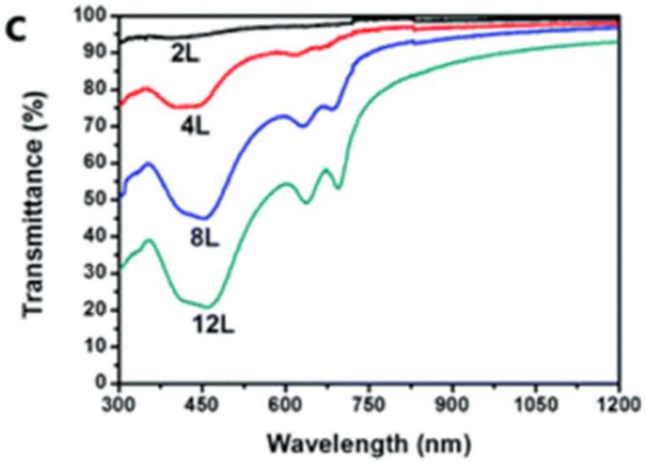

Over 90% transmission rate
@2L and visible range

Y. Lee et al., Nanoscale, 6, 2821 (2014)

Optical Response of TMDs

Highly efficient MoS_2 photodetector

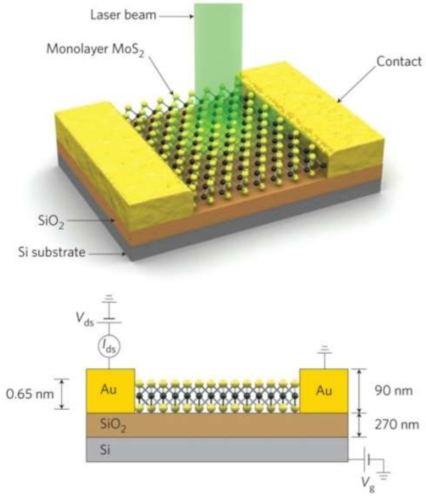

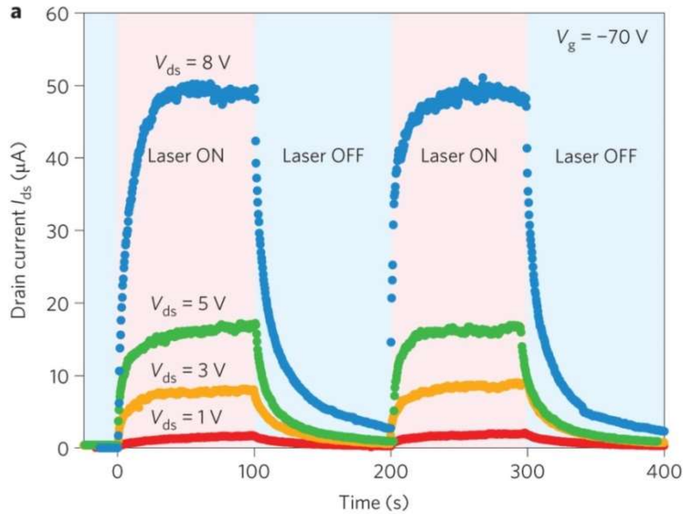

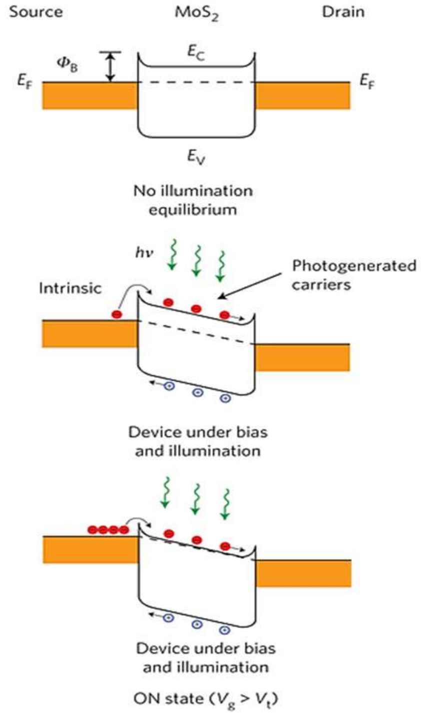

High efficiency: 880 A/W (cf. graphene: 0.5 mA/W)
High light absorption: 5 ~ 10%
Efficient charge separation due to limited dimension (ultrathinness)

O. Lopez-Sanchez et al. Nature Nanotechnol. (2013)

Mechanism of photocurrent in MoS_2

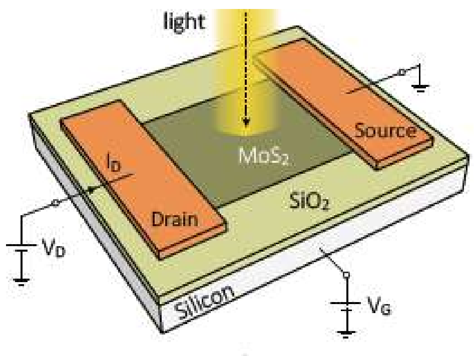

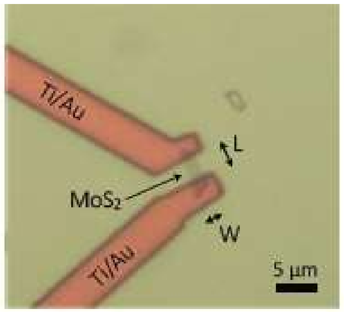

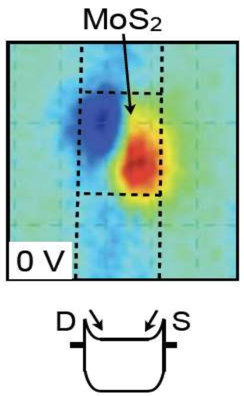

Photocurrent mapping

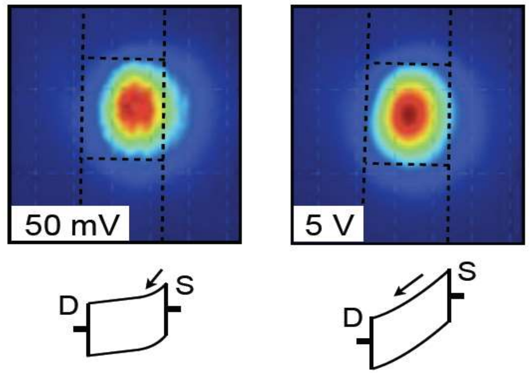

M. M. Furchi et al. Nano Lett. (2014)

Optical Response of TMDs

WSe_2 photodetector

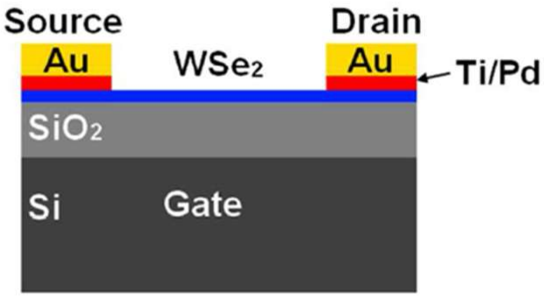

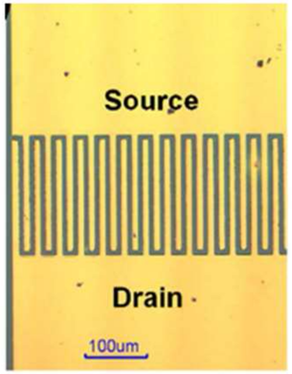

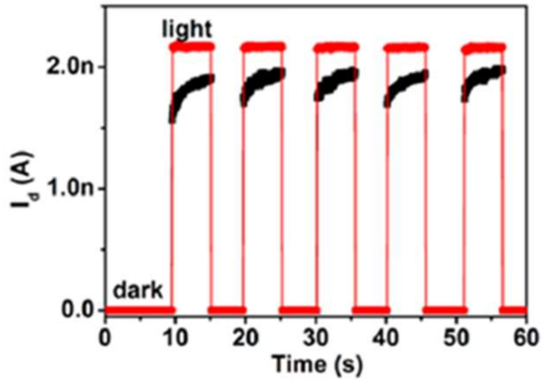

W. Zhang et al. ACS Nano (2014)

MoS_2/Graphene heterostructure photodetector

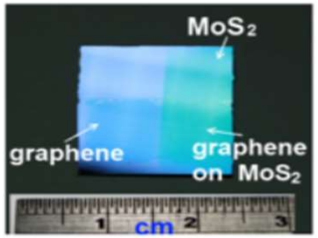

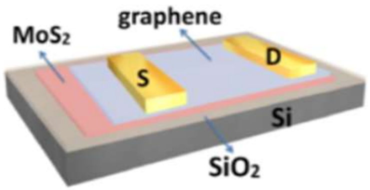

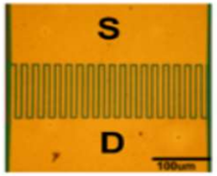

1. *Electron-hole pairs are produced in MoS_2.*
2. *Electrons moves to graphene due to effective electric field.*
3. *High photoresponsivity is obtained.*

Gate-tunability of photocurrent

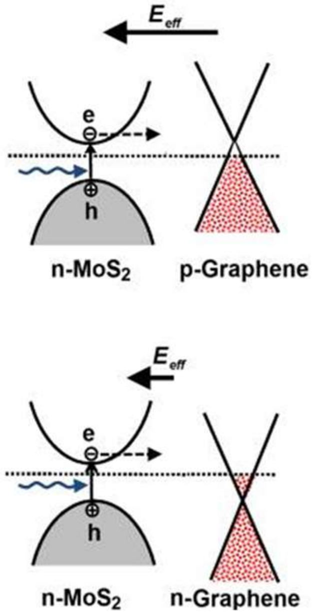

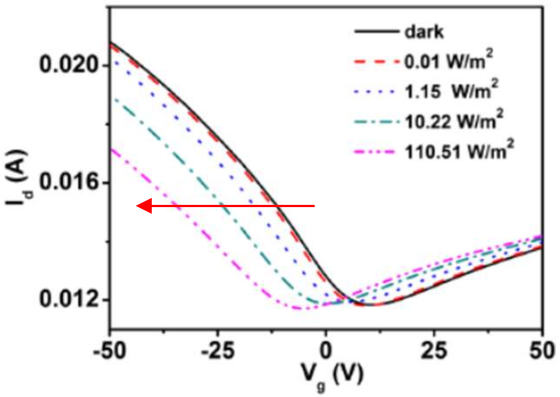

W. Zhang et al. Sci. Rep. 4, 3826 (2014)

Short Channel Effect

Subthreshold leakage

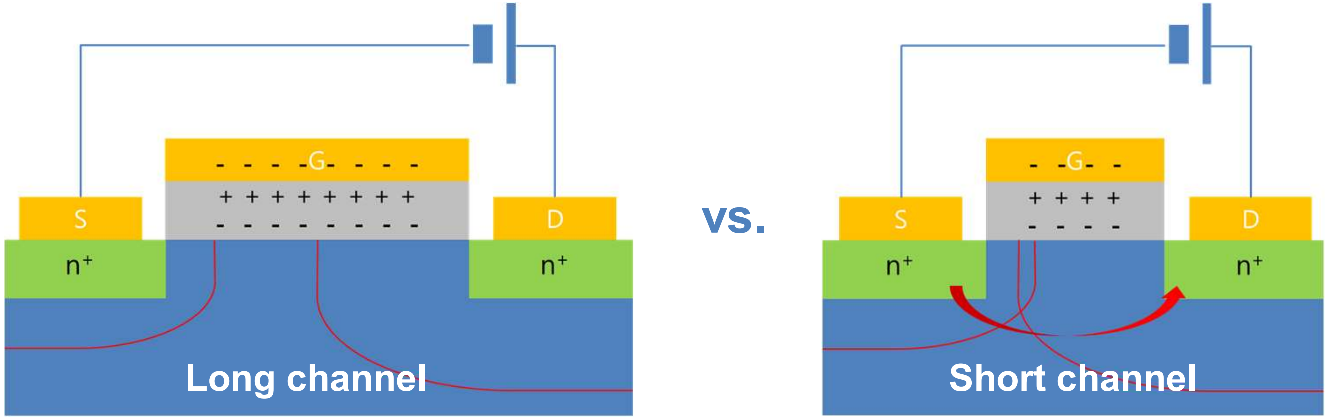

Electrons can flow at turn-off state (current leakage)

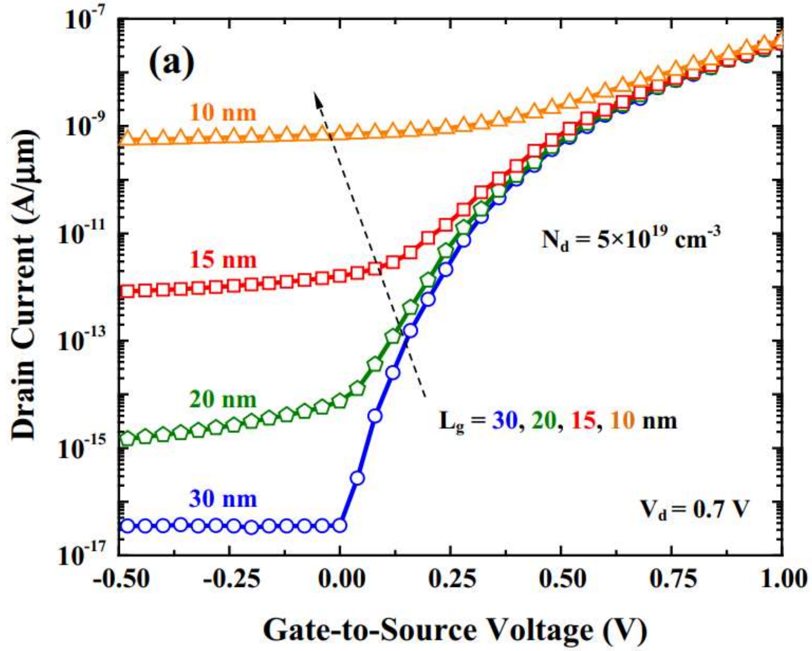

N.D. Chien et al, Microelectronics Reliability, 2015

Short Channel Effect

(1) Decreasing drain concentration

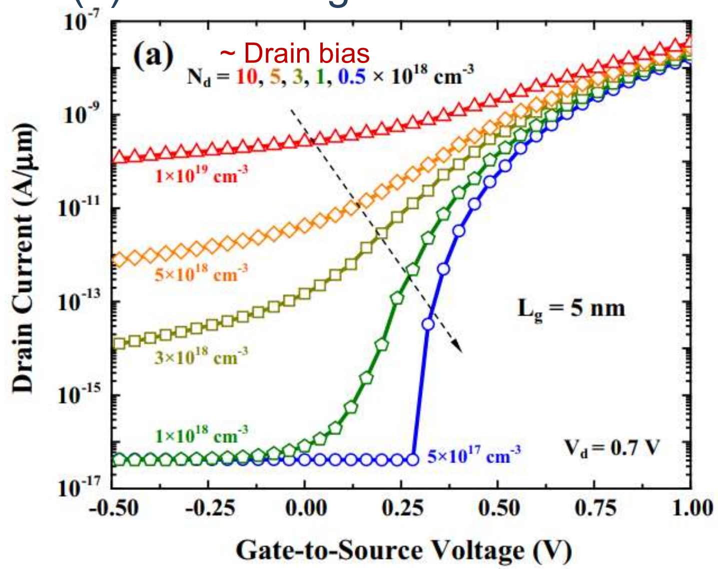

(2) Increasing doping concentration in p-Si

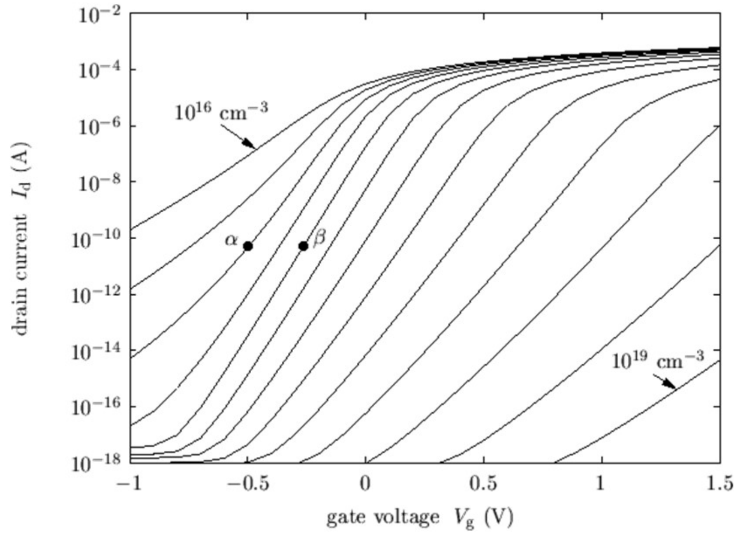

N.D. Chien et al, Microelectronics Reliability, 2015

Degradation of carrier mobility due to difficulty in overcoming of contact barrier and increase charged impurity scattering

Thin silicon on Insulator (higher gate capacitance)

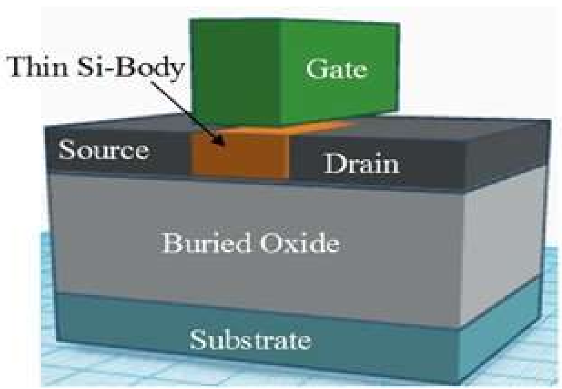

Dual gates

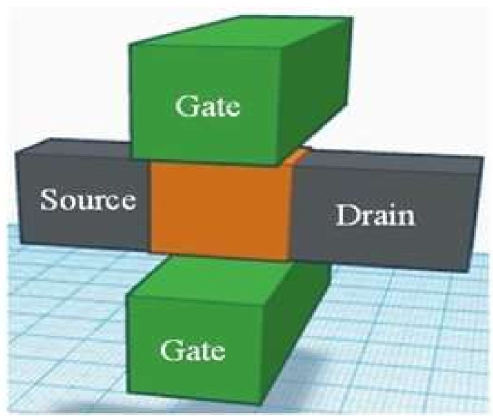

FinFET

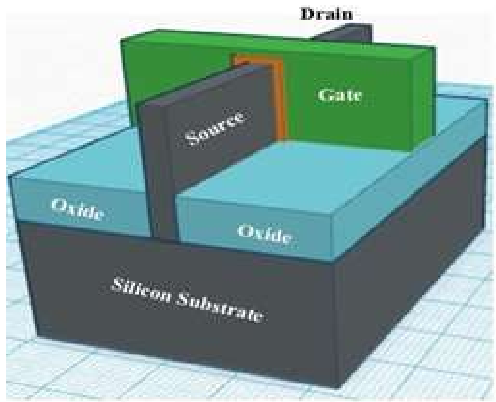

https://www.design-reuse.com/articles/41330/cmos-soi-finfet-technology-review-paper.html

2D semiconductors : Promising candidates beyond Si

Switching behavior of thin film FET

One-dimensional Poisson equation

$$\frac{d^2\varphi(x)}{dx^2} - \frac{\varphi(x)}{\lambda^2} = 0 \text{ with } \lambda = \sqrt{\frac{t_b t_{ox} \varepsilon_b}{\varepsilon_{ox}}},$$

Transistor size (λ) : ↓ → t_b : ↓ & ε_b : ↓

$\varphi(x)$: Potential distribution in the source/drain direction
λ : Transistor characteristic length
t_b : Thickness of the semiconductor body
ε_b : Dielectric constant of the semiconductor body
t_{ox} : Thickness of the dielectric layer
ε_{ox} : Dielectric constant of the dielectric layer

1. Atomically thin body thickness (t_b < 1nm)

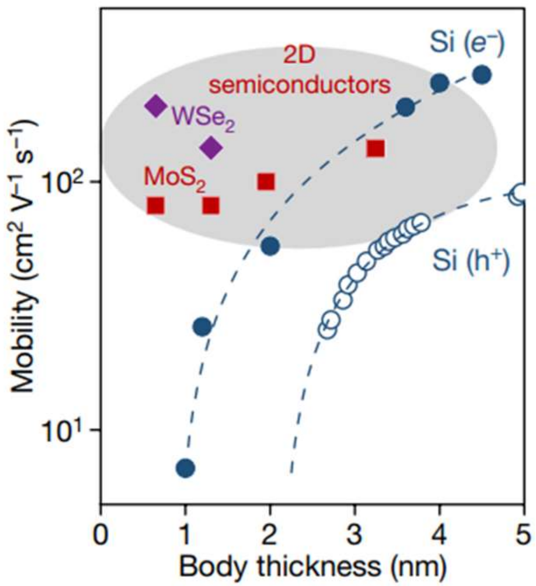

Silicon

- Surface dangling bond and roughness.

→ Strongly interface roughness scattering, leading to degradation of carrier mobility with decreasing t_b

2D semiconductor

- No dangling bond and ultra-flat interface

→ Little mobility variation with decreasing t_b

Nature 591,43 (2021)

2D semiconductors : Promising candidates beyond Si

2. Immunity to short channel effect of 2D semiconductor

- Low in-plane dielectric constant (ε_b : ↓)

→ ε_{MoS_2} : ~4 / ε_{Si} : ~11.7

- Larger effective mass & Larger bandgap

→ Effectively suppressing in direct tunnelling between source and drain electrodes in short channel devices, thus effectively suppressing leakage currents

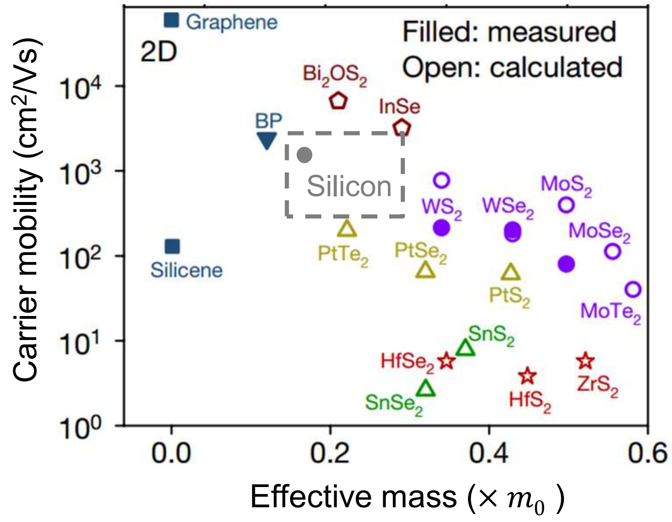

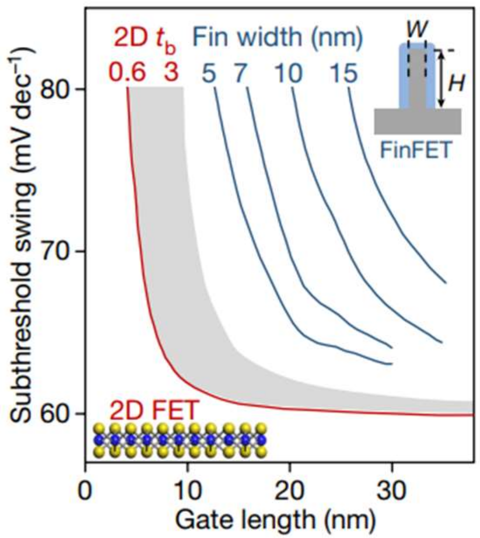

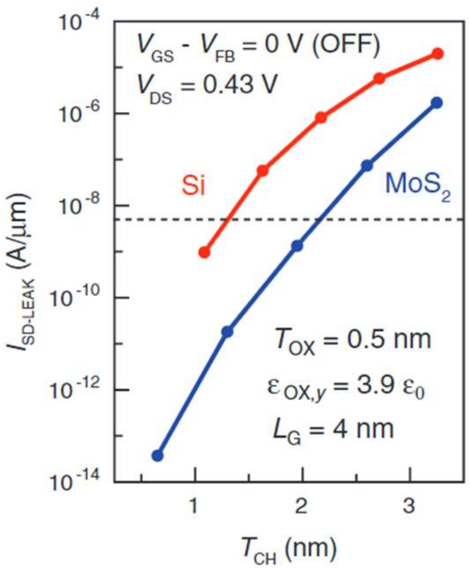

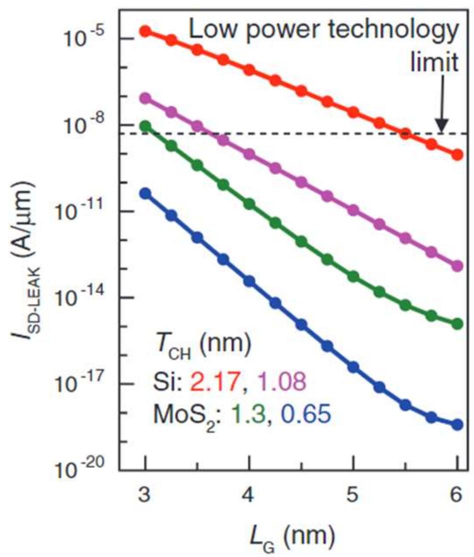

Nature 591,43 (2021) , Science, 354, 6308, 99-102 (2016)

No Short Channel Effect in 2D Channel

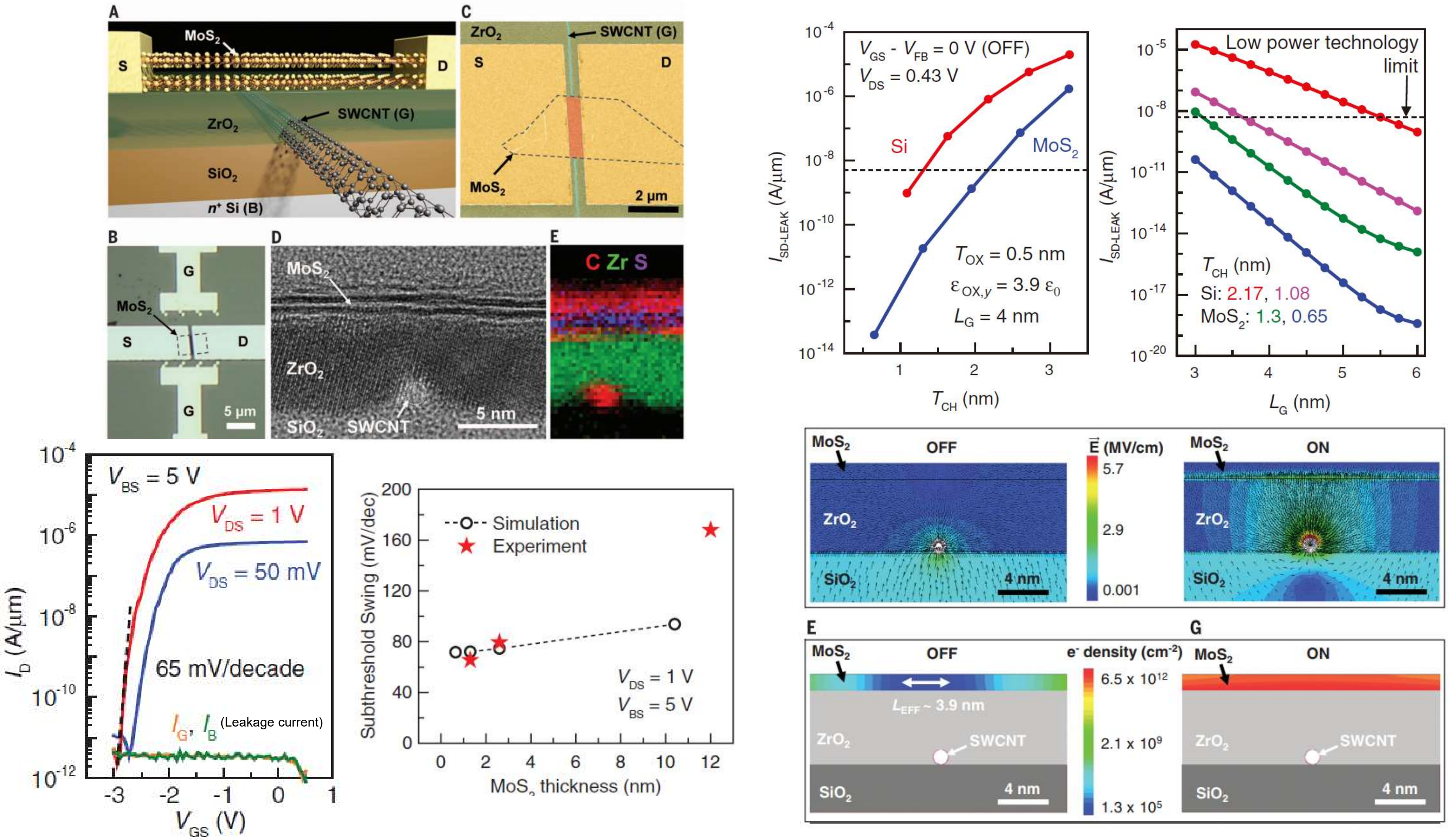

- Cause of low short channel effect, channel length can be scaled-down to nano-meter unit.
- TMD channels have high mobility(~hundreds $cm^2/V \cdot s$).
- However, high contact resistance makes device performance worse.
- Researches for reducing contact resistance are under way actively.

S. B. Desai et al, Science (2016)

Research Trend in 2D Devices

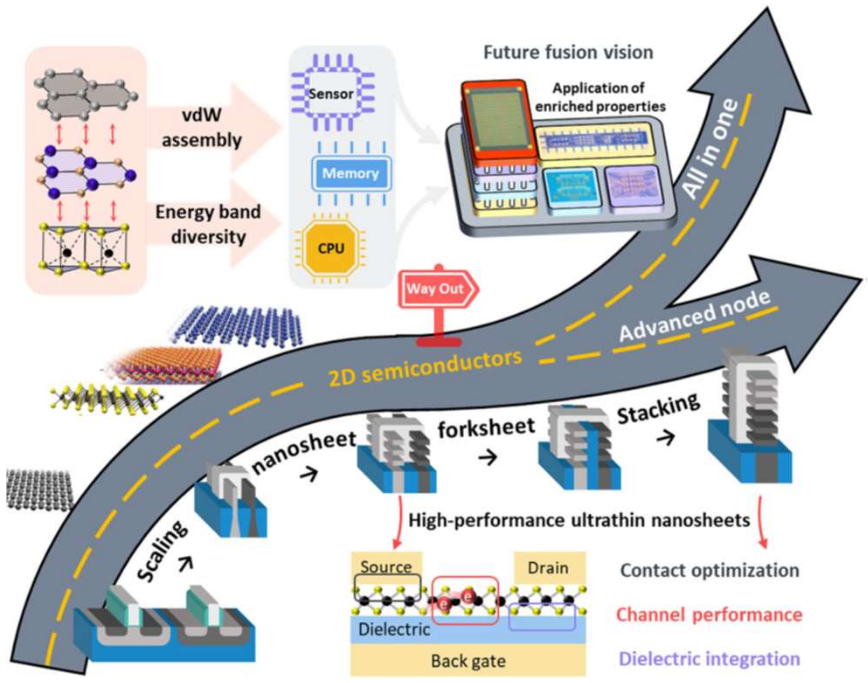

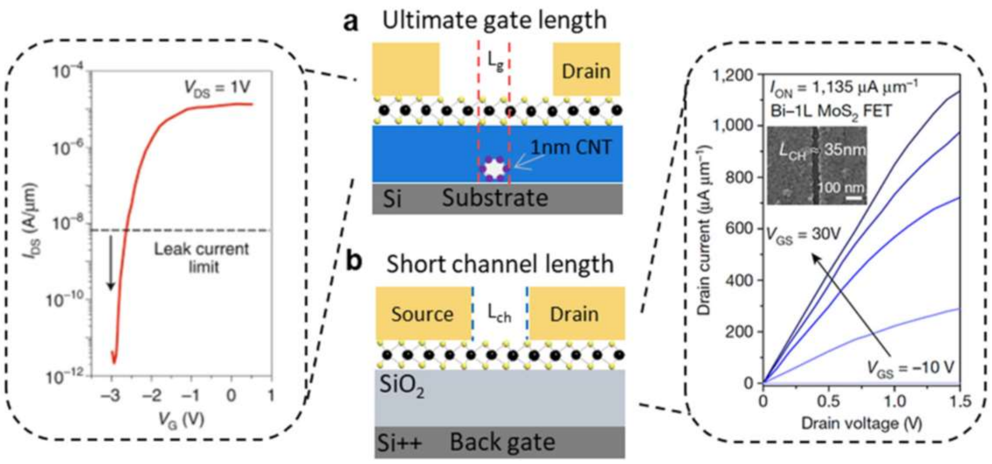

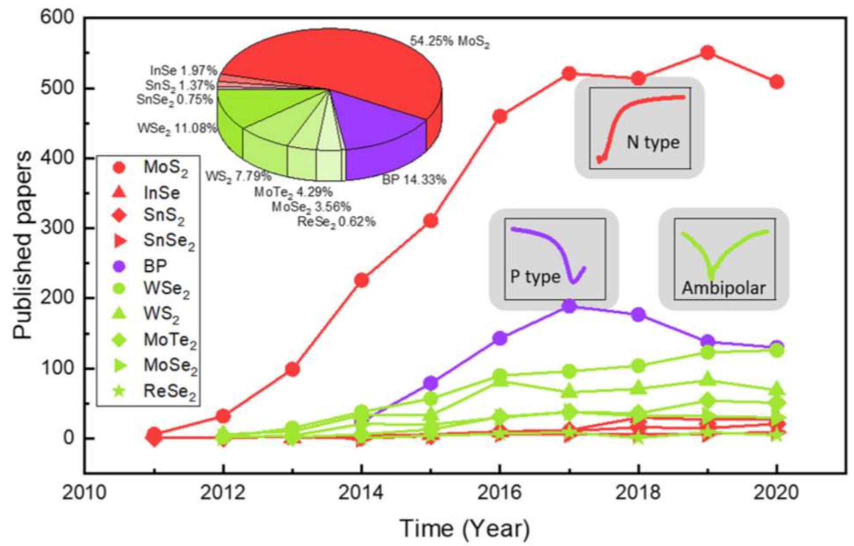

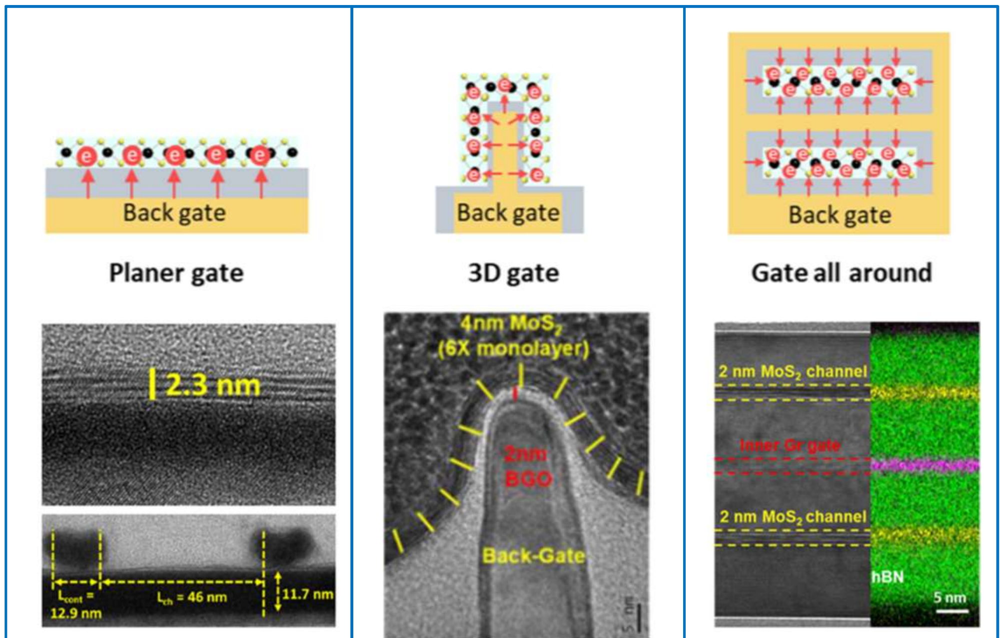

J. Elect. Dev. Soc. (2016)

npj 2D Mater. Appl. 51 (2022)

Breakthrough in 1nm process

2D semiconductors for next-generation FETs

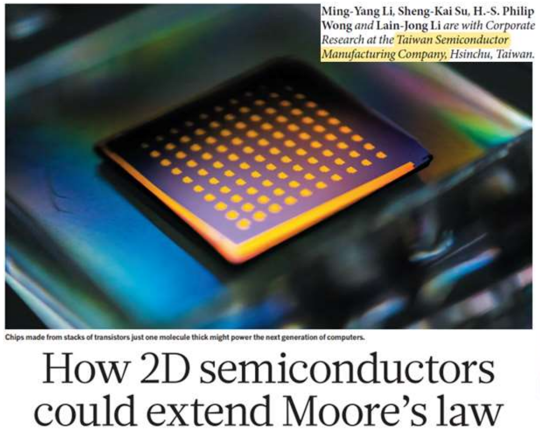

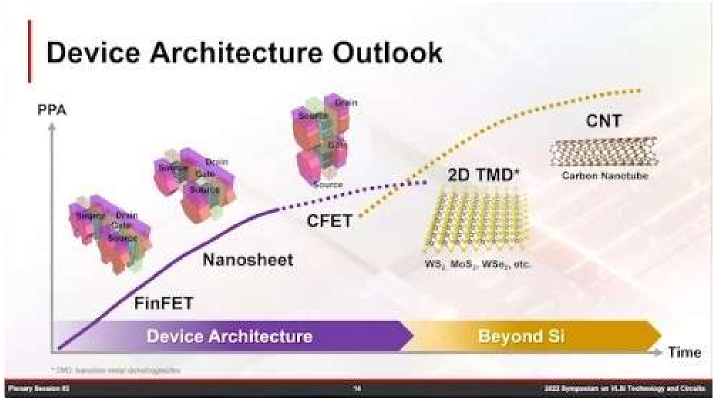

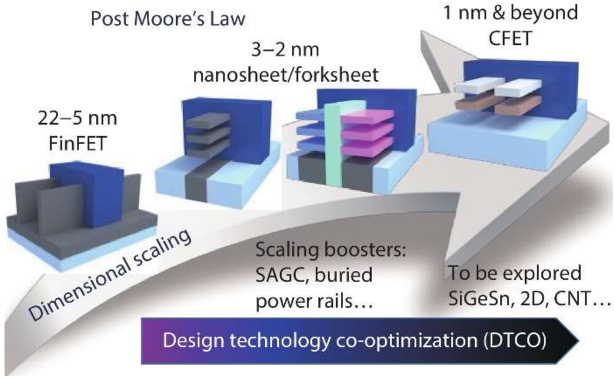

Nature, 567, 169-170 (2019) &TSMC at VLSI 2022

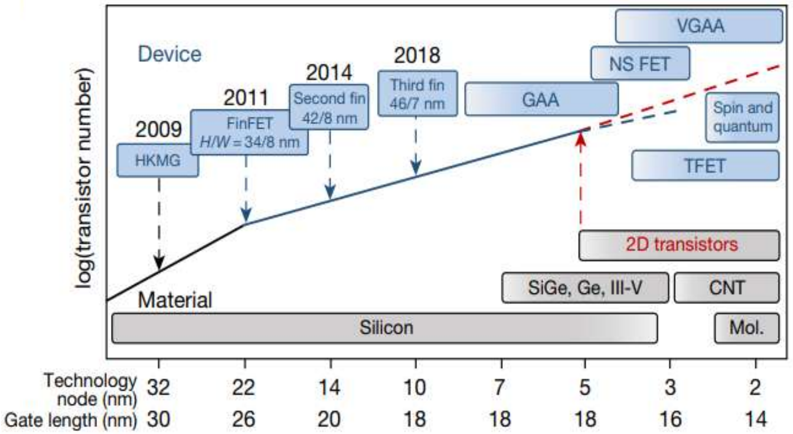

Nature 591, 43-53 (2021)

Papers from global semiconductor companies

Article
Ultralow contact resistance between semimetal and monolayer semiconductors

Article
High-κ perovskite membranes as insulators for two-dimensional transistors

Article
Wafer-scale single-crystal hexagonal boron nitride monolayers on Cu (111)

ARTICLE
https://doi.org/10.1038/s41467-022-31886-0 OPEN
Low-defect-density WS_2 by hydroxide vapor phase deposition

RESEARCH ARTICLE — ADVANCED MATERIALS
2D Materials-Based Static Random-Access Memory

REVIEW ARTICLE — nature electronics
https://doi.org/10.1038/s41928-021-00670-1
Transistors based on two-dimensional materials for future integrated circuits

ARTICLES — nature materials
https://doi.org/10.1038/s41563-020-0795-4
Ledge-directed epitaxy of continuously self-aligned single-crystalline nanoribbons of transition metal dichalcogenides

Schottky and Ohmic Contacts

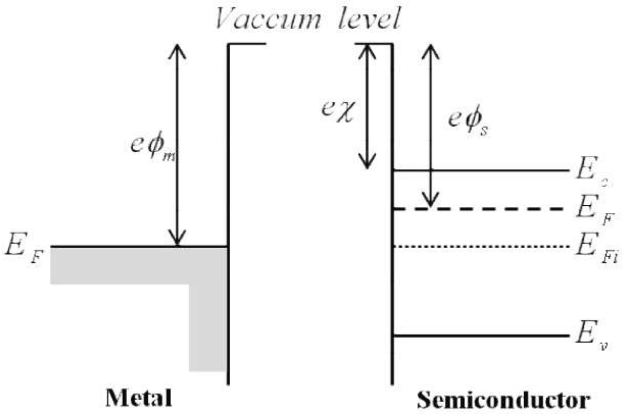

<before contact>

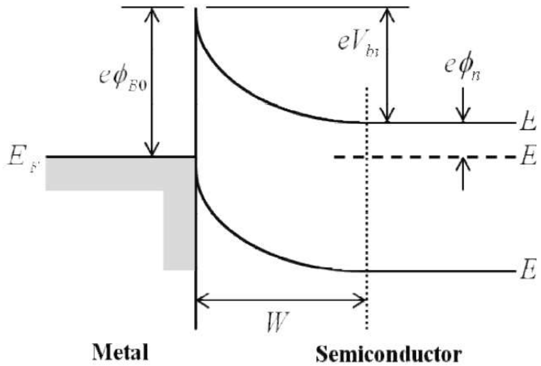

<after contact>

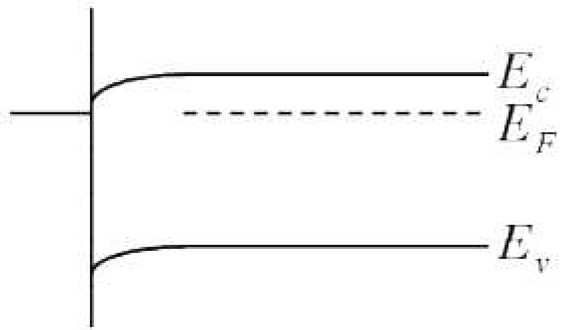

<Ohmic contact>

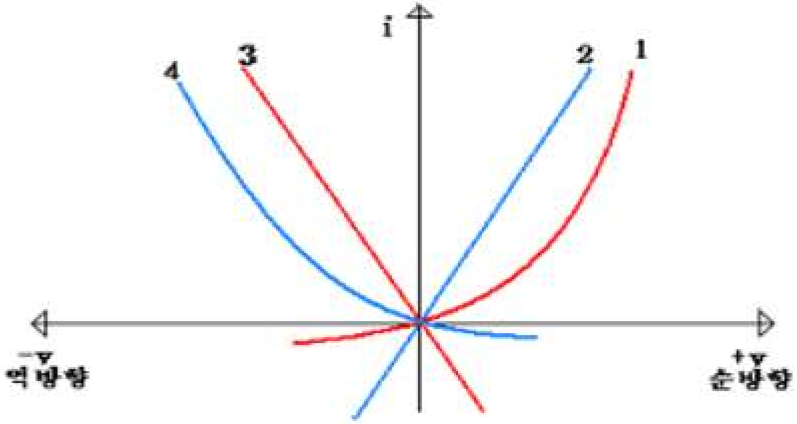

- Ohmic contact (2: n-type, 3: p-type)
  → Non rectifying
- Rectifying contact (1: n-type, 4: p-type)
  → Schottky contact

Schottky and Ohmic Contacts

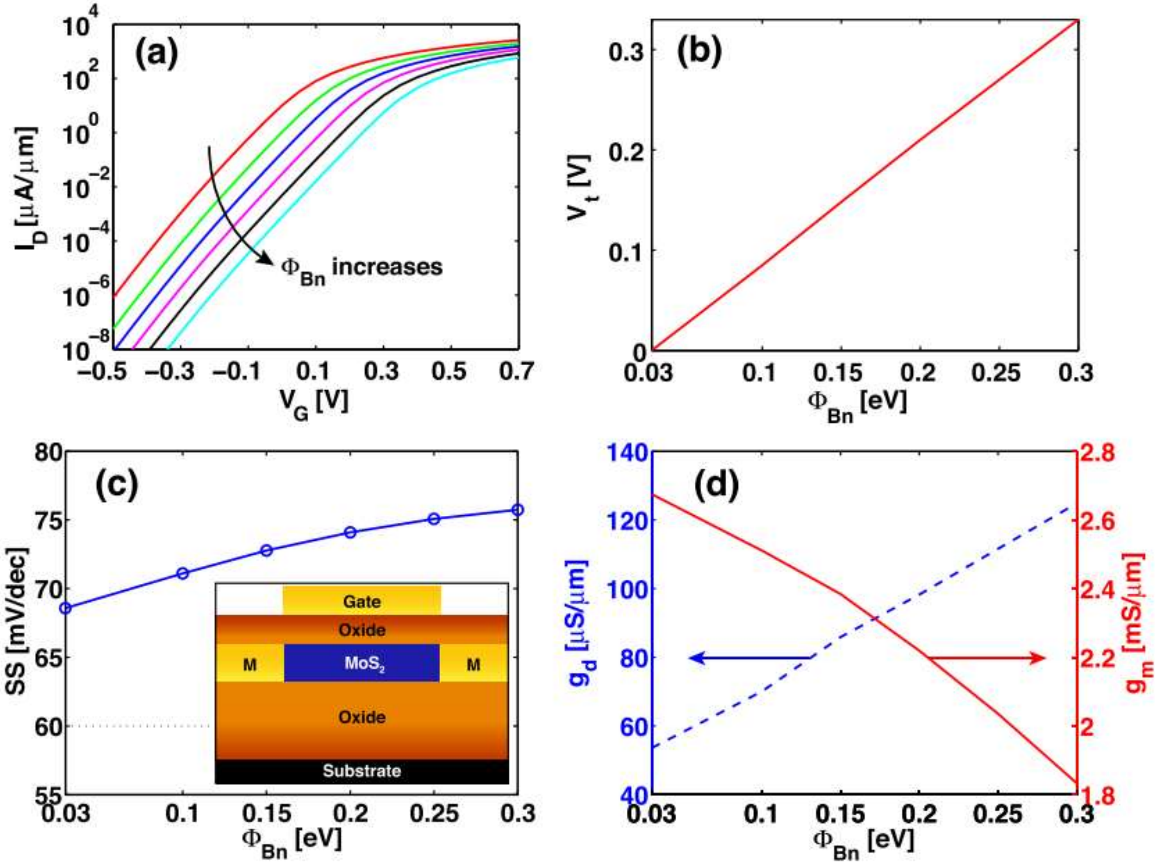

When Φ_{Bn} increases from 30 to 300meV

- Linear increase of threshold voltage(V_t)
  → Difficult to overcome the SB
- Subthreshold swing(SS) shows degradation by 10%

$$SS = \partial V_G / \partial \log_{10} I_D$$

- g_d (drain tunability) is increased by 130%

$$g_d = \partial I_D / \partial V_D$$

- g_m (gate tunability)is decreased by 30%

$$g_m = \partial I_D / \partial V_G$$

Better device performance can be achieved by using smaller Φ_{Bn}

G. Han et al. Appl. Phys. Lett. (2014)

Schottky and Ohmic Contacts: Effect of doping

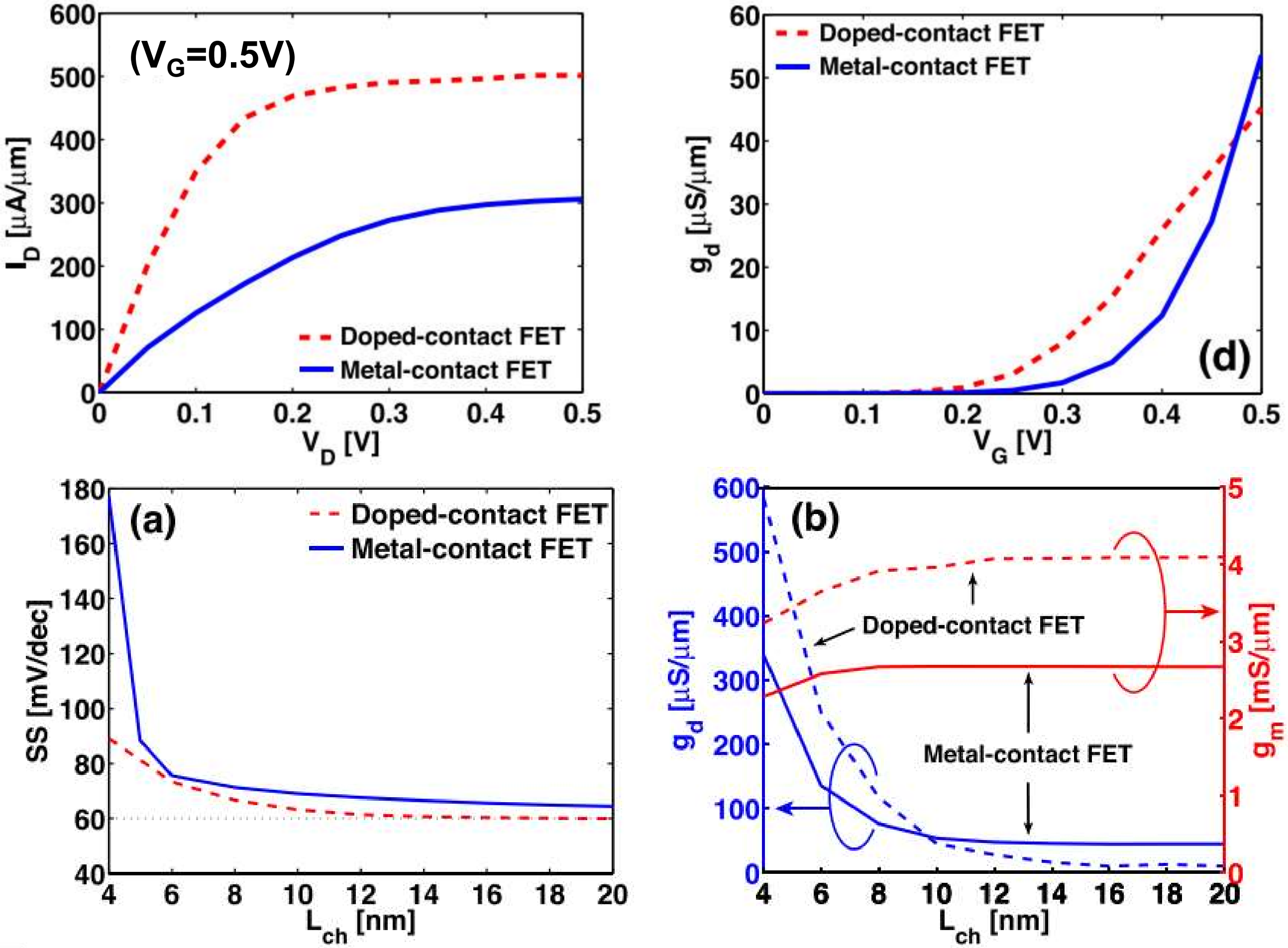

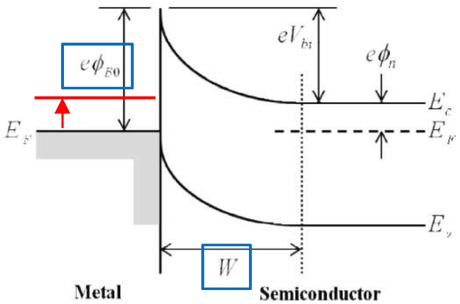

- At low gate voltages
  Thermionic current is more susceptible to the variation of V_D with doped contacts than with metal contacts
- At high gate voltages
  The Schottky barrier thickness is more sensitive to the V_D variation than the top of the barrier in doped-contact FETs

G. Han et al. Appl. Phys. Lett. (2014)

2D Semiconductor-Metal Contacts

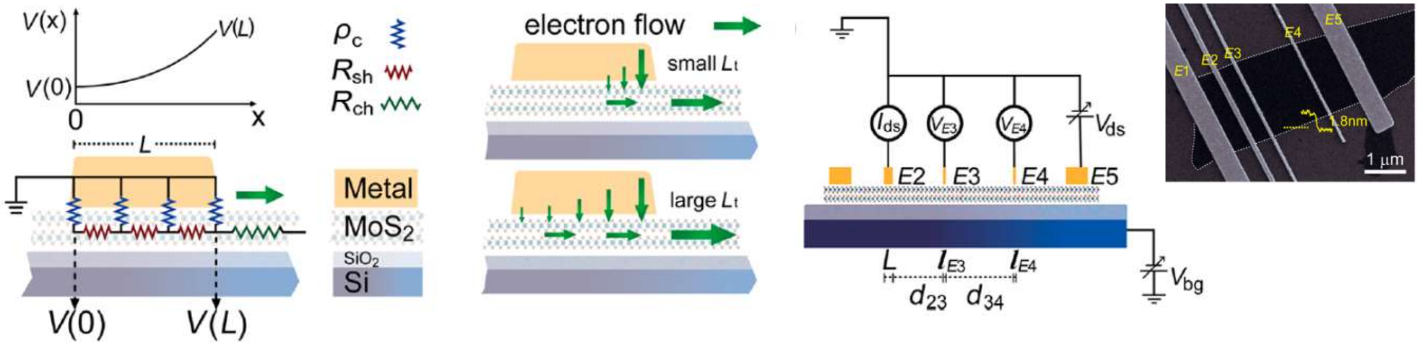

Contact Resistance

$$R_c = V(L)/I_{ds}$$

Effective conductive length

$$L_t = \sqrt{\rho_c/R_{sh}}$$

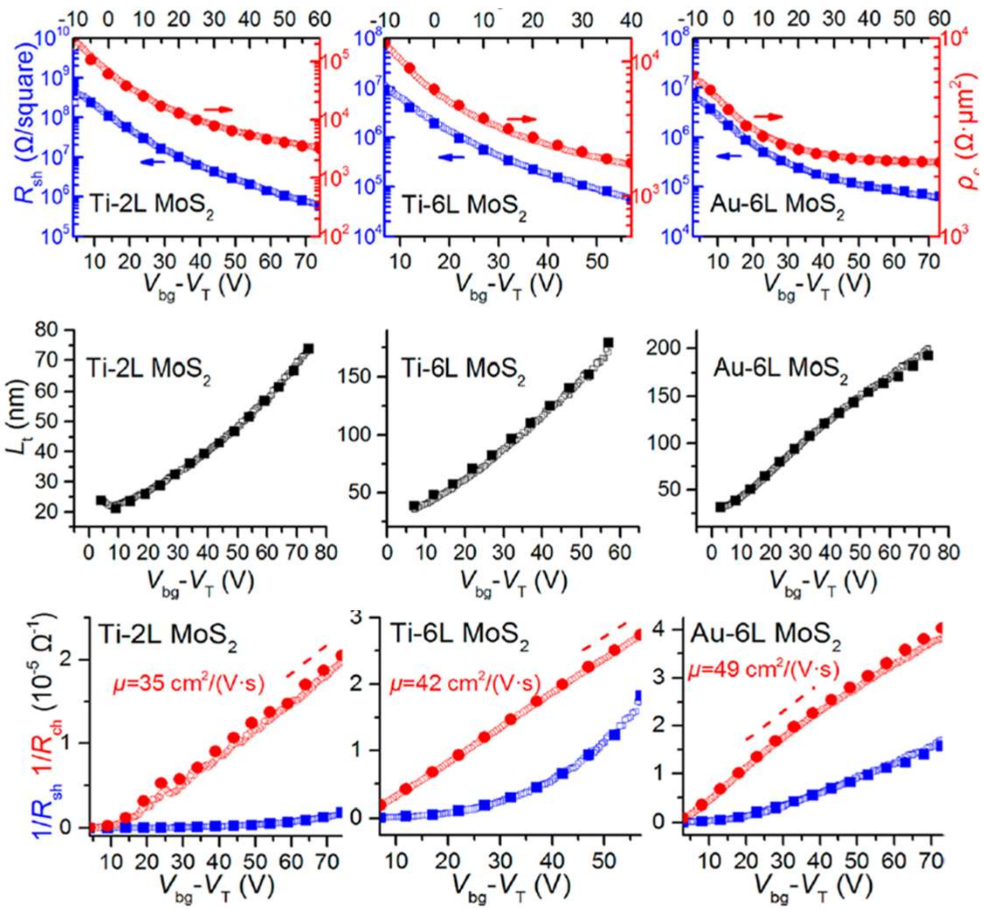

1. Contact Resistance increases with decreasing thickness.
→ Rise of the conduction band bottom

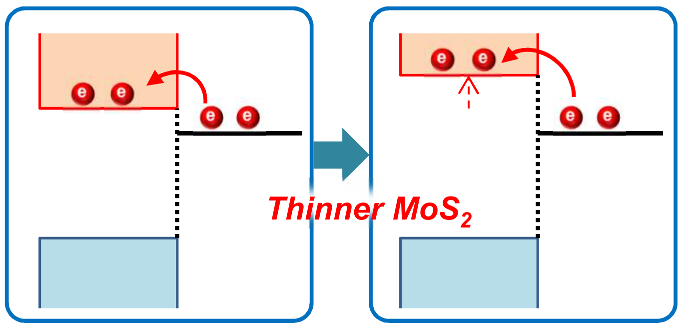

2. Effective conductive length (L_t) increases with V_{bg}.
→ R_{sh} drops more severely.

3. R_c / R become larger for shorter channel length.
→ In short channel devices, R_c is critical.

For low contact resistance (R_c)
1. L>>L_t
2. Engineering of dielectric environment (doping)
3. Band engineering in Interlayer between MoS_2 & metal

Y. Guo et al. ACS Nano (2014)

Schottky and Ohmic Contacts

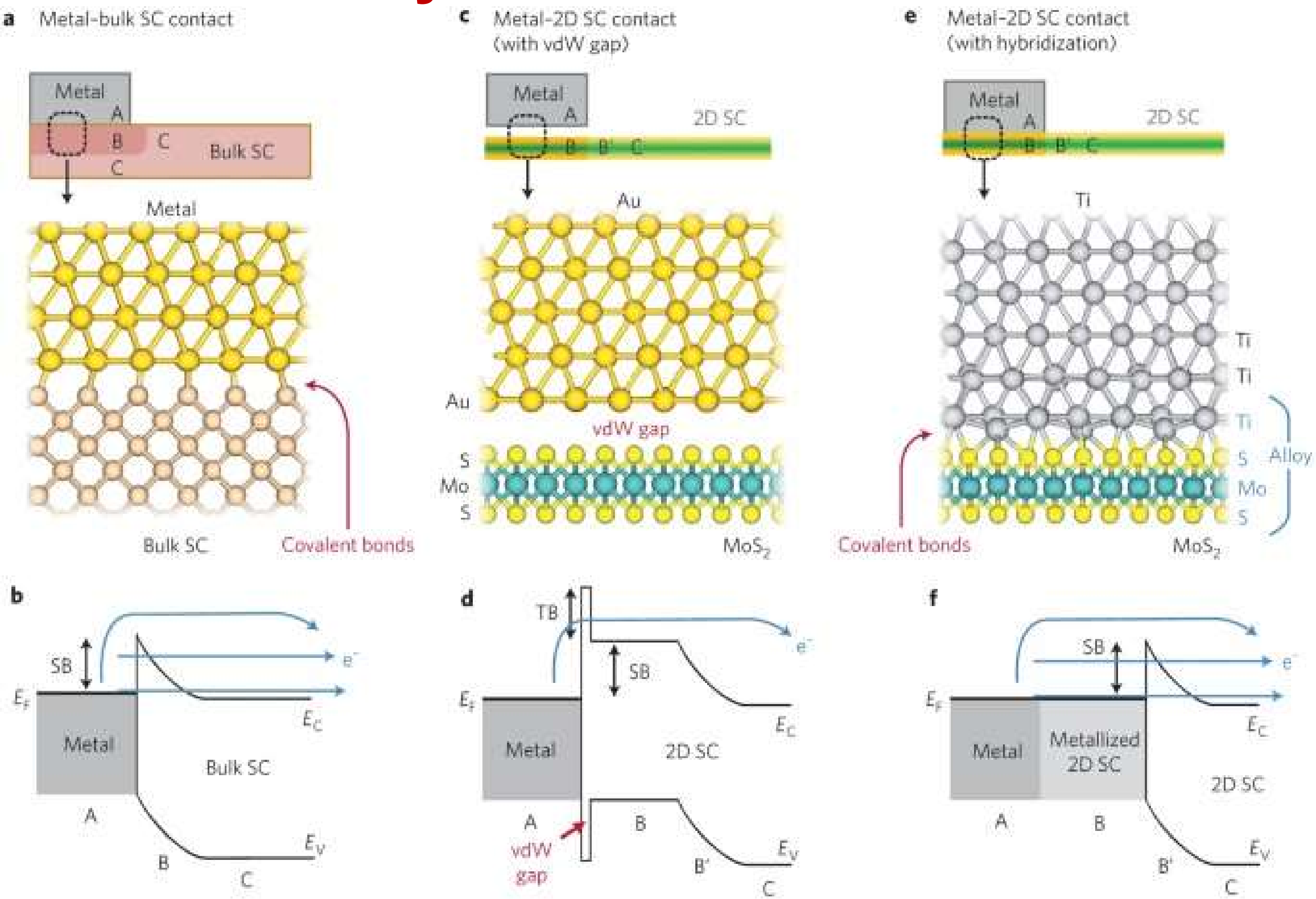

- vdW gap forms ***additional 'tunnel barrier'*** between 2Dchannel and metal.
- For device-to-device variability of metal-contact MoS_2 FETs, Schottky barrier height is a key device param eter that determines the overall performance of transistors.
- To reduce device-to-device variability in MoS_2 FETs, contact resistance should be reduced.
- Need to eliminate the vdW gap using metallized 2D SC.

A. Allain et al. Nature Mater. (2015)

1. vdW contact

Transfer of metal electrodes

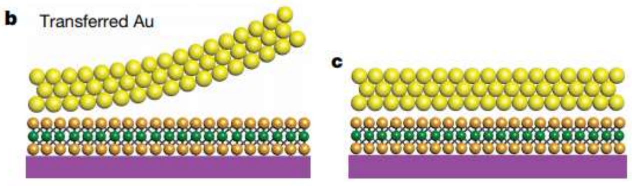

Nature (2018)

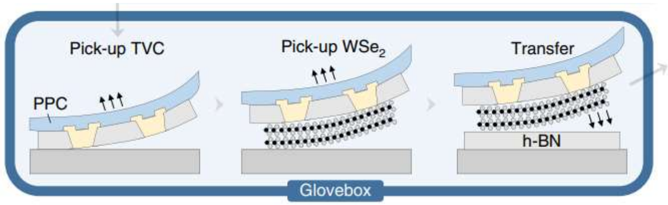

Nat. Electron. (2019)

Indium metal contact

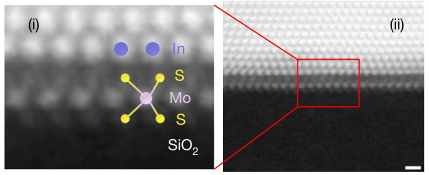

Nature (2018)

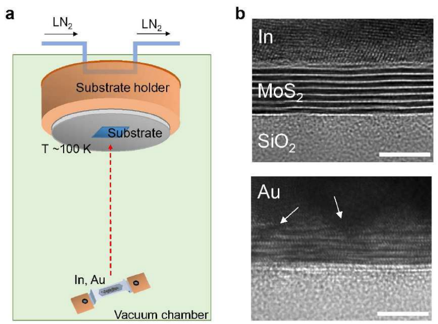

npj 2D Mater. Appl. (2021)

Stacked vdW contact

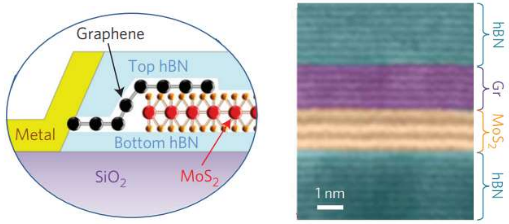

Nat. Nanotech. (2015)

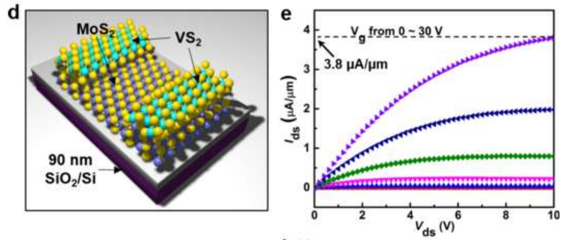

Nano Lett. (2017)

2. Chemically bonded contact

Contact via defects

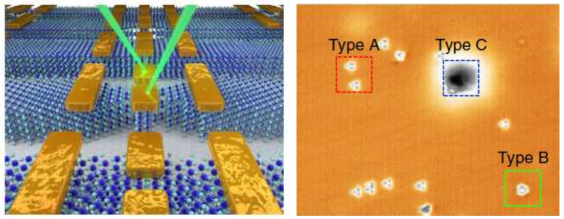

Nat. Electron. (2018)

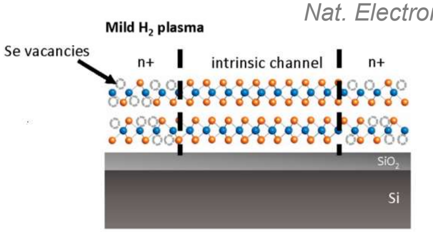

ACS Nano (2016)

Edge contact

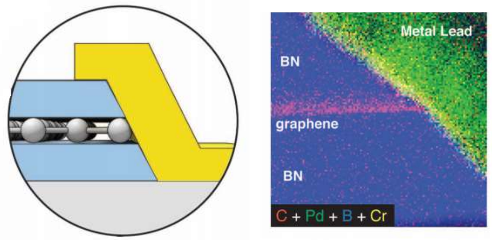

Science (2013)

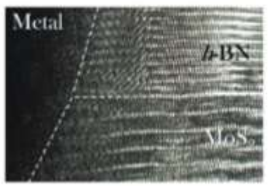

Adv. Mat. (2019)

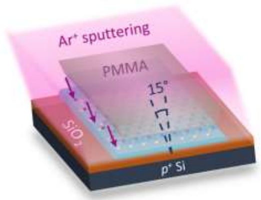

Nano Lett. (2019)

Contact with chemical bonding

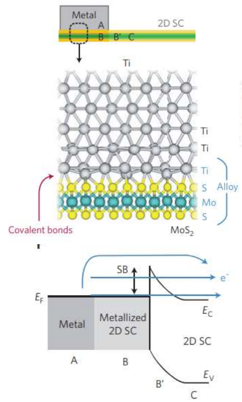

Nat. Mater. (2015)

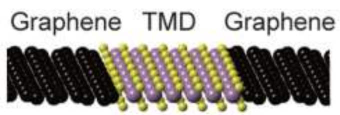

ACS. Nano (2016)

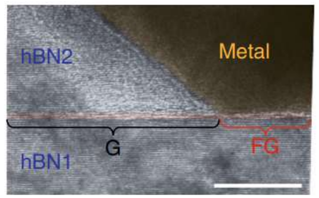

Nat. Comm. (2018)

3. Phase engineered contact

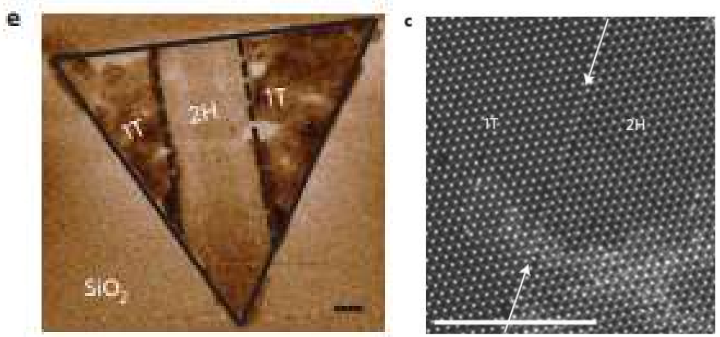

Nat. Mater. (2013)

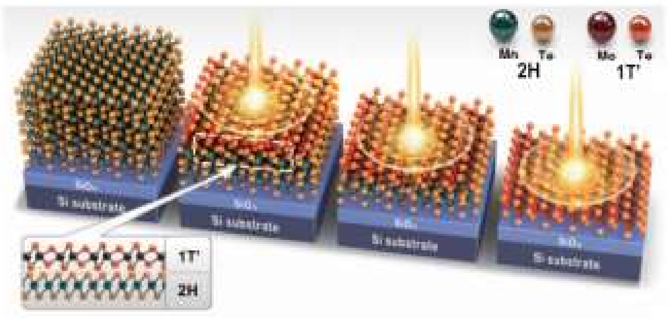

Science (2015)

4. Tunnel barrier contact

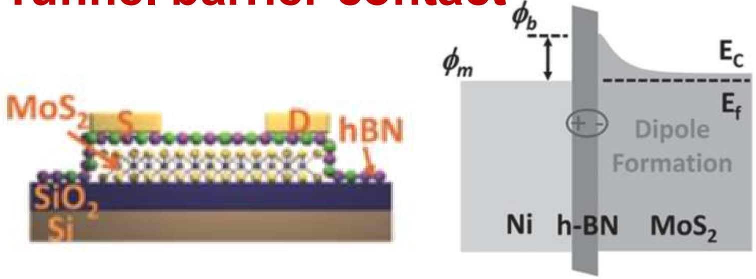

Adv. Mater. (2016)

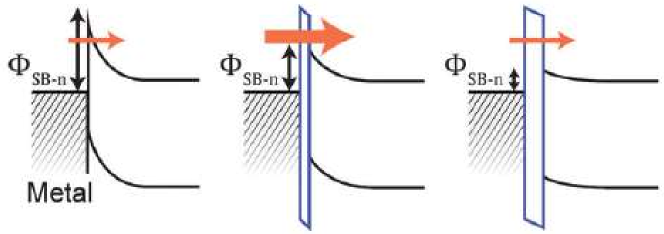

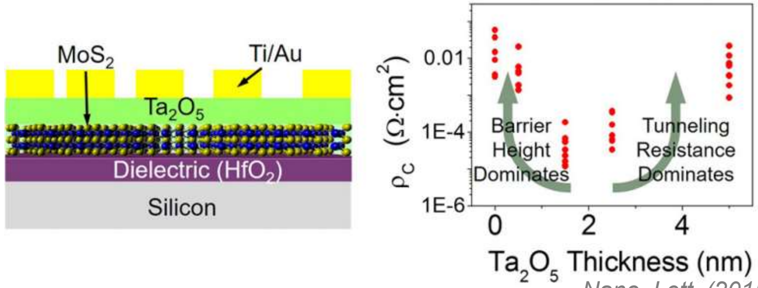

Nano. Lett. (2015)

- Phase transition can make one-dimensional contact between semiconducting and metallic phases.
  - laser exposure, solution exposure

- As inserting buffer layer between electrode and TMD channel, Schottky barrier can be reduced by tunnel contact.
  - Stack insulating 2D material(hBN) between electrodes and TMD channel
  - Deposit insulating interlayer materials directly

5. Contact improvement by doping

Molecular doping

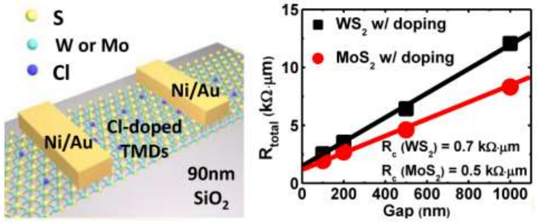

Nano. Lett. (2014)

MX_n	Dopant	Type	Concentration [cm^{-2}]	Mobility [$cm^2 V^{-1} s^{-1}$]
MoS_2	Nb	p	1.8×10^{14}	14
	P	p	10^{10}–10^{12}	137.7
	Re	n	5.5×10^{12}	—
$MoSe_2$	W	p	4.0×10^{11}	1.6
WS_2	N	p	3.83×10^{11}	1.7
	Cl	n	6.0×10^{11}	60
WSe_2	S	n	—	68.2
SnS_2	Fe	—	—	8.15
	Se	n	—	4.6
$SnSe_2$	Cl	n	$> 10^{12}$	167

Nanoscale Horiz. (2019)

Intercalation doping

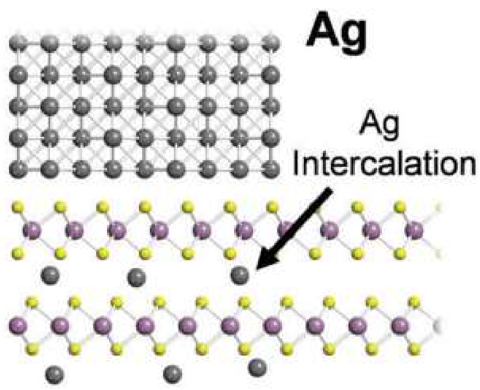

J. Appl. Phys (2017)

Ion implantation

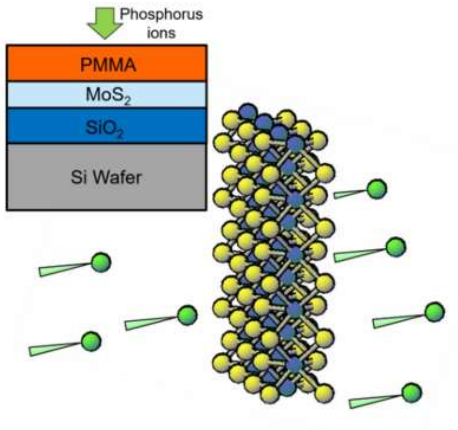

Semicond. Sci. Technol. (2017)

6. Semi-metal contact

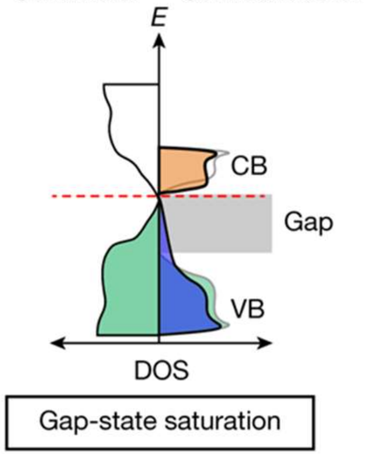

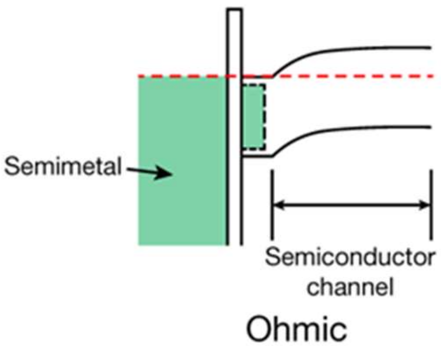

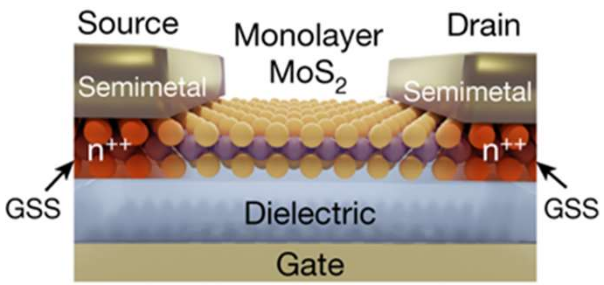

P.C. Shen et al. Nature (2021)

Low Work Function Metal for Contact

Contact Barrier of various metals

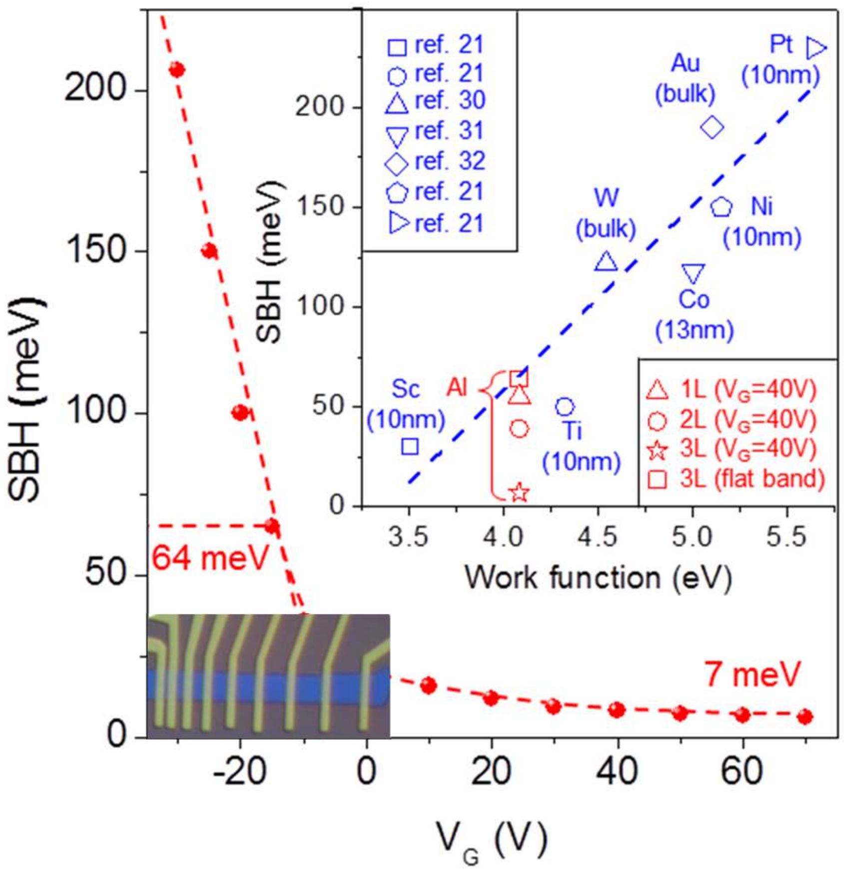

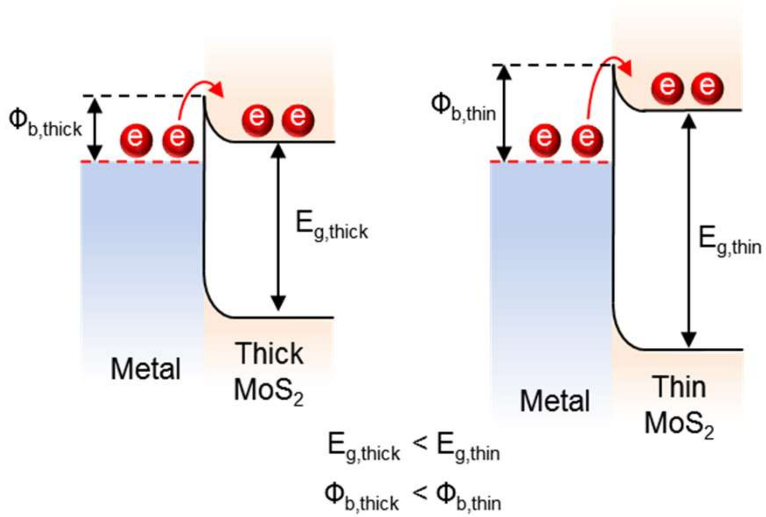

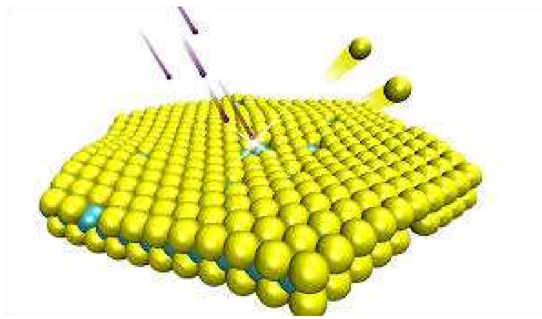

- ❑ Al contacts to MoS_2 are gate-voltage- and thickness-dependent.
- ❑ Still high contact resistance due to pinning at MoS_2-metal interface

J. Y. Kwon, G. H. Lee **Nanoscale** (2017)

Van der Waals Contact

Fermi level pinning

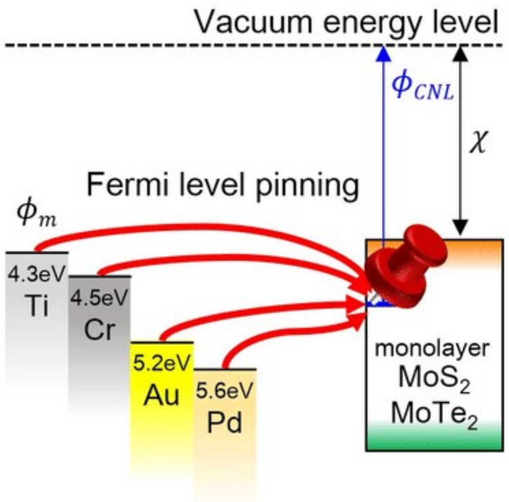

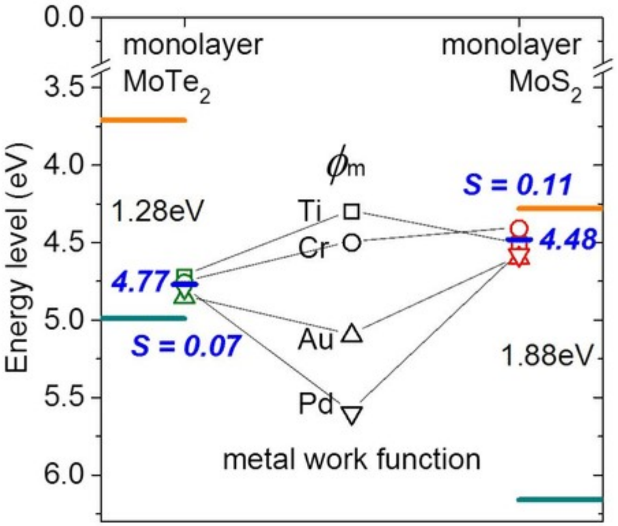

C. Kim, et al. ACS Nano (2017)

Deposited contact

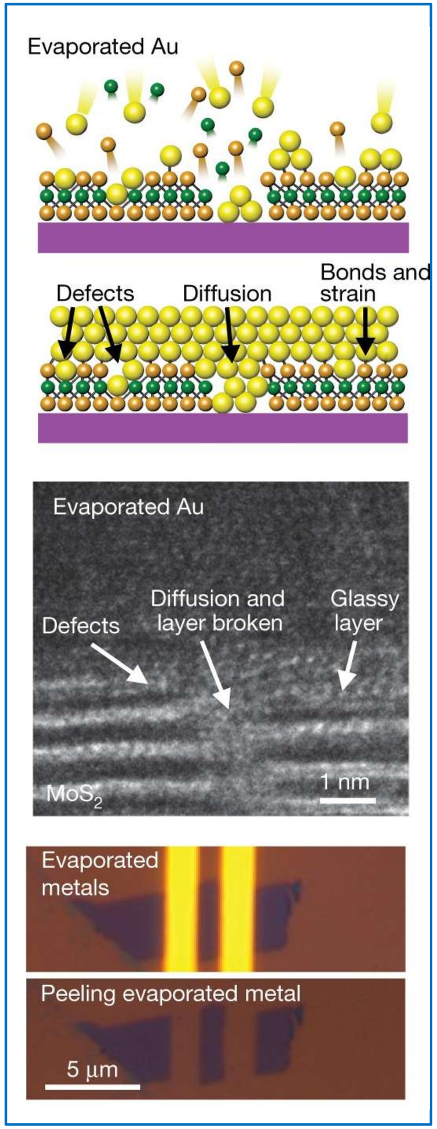

vdW contact

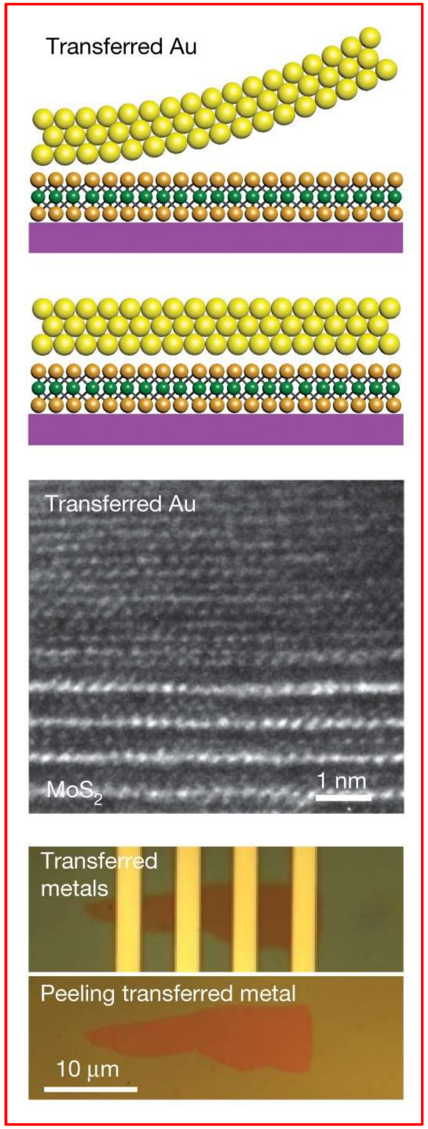

Y. Liu, et al. Nature (2018)

Van der Waals Contact

Indium contact by thermal evaporation (low energy)

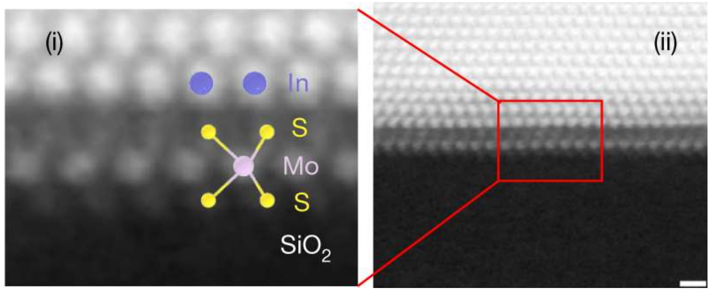

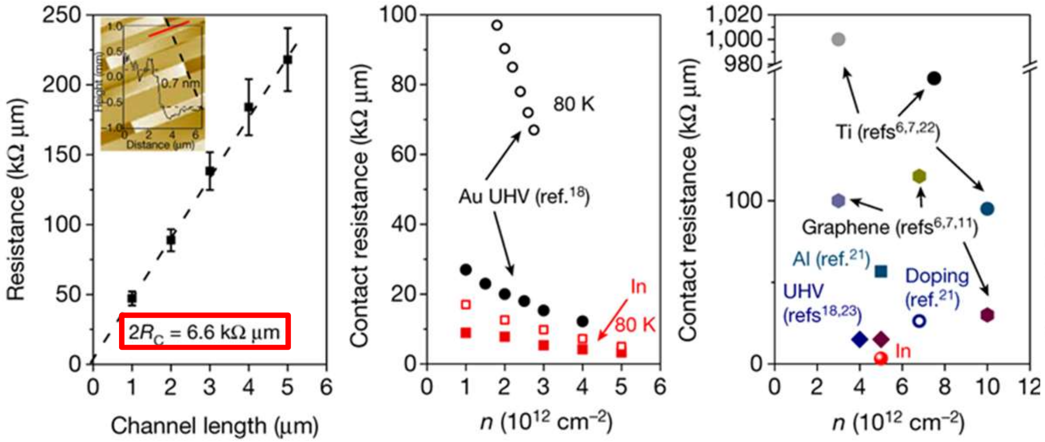

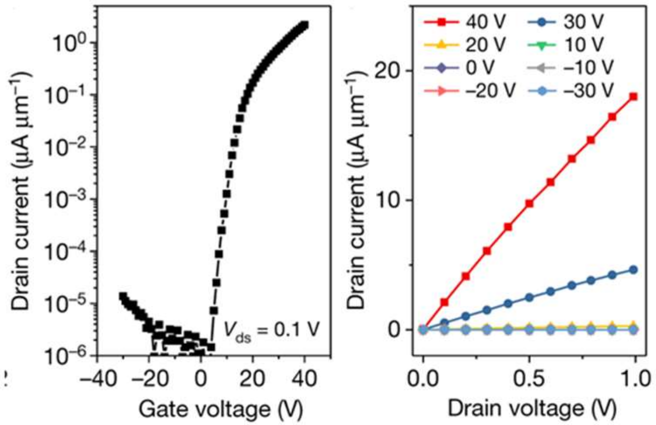

Nature 568, 70–74 (2019)

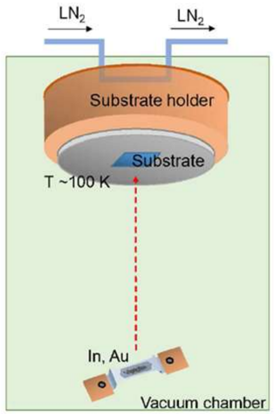

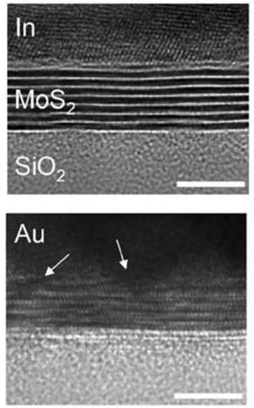

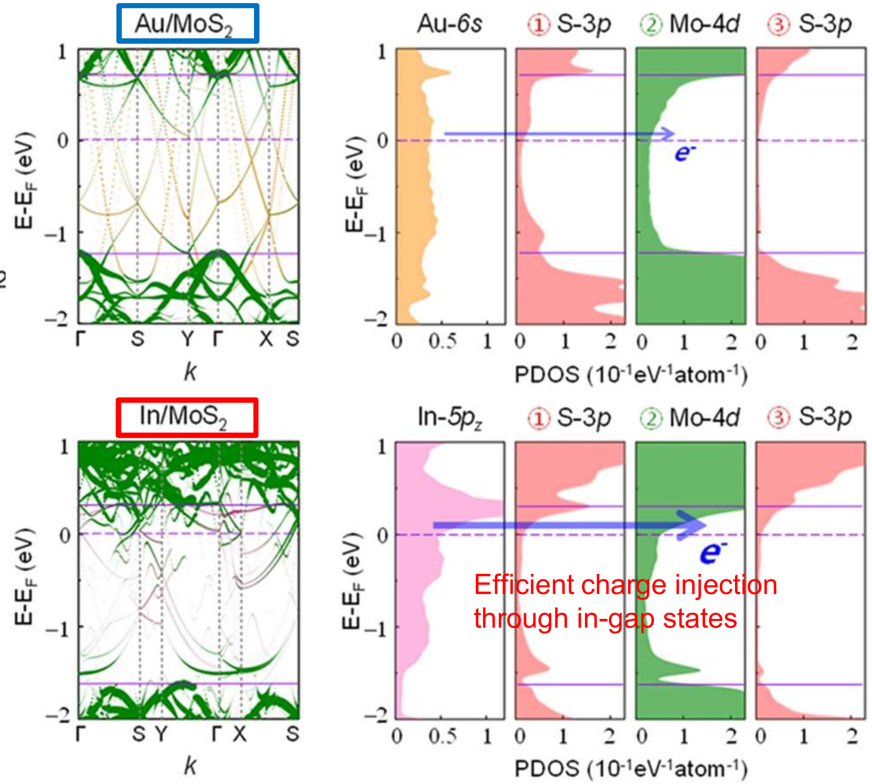

npj 2D Mater. Appl. (2021)

Nanoscale Heterogeneous Transition Metal Dichalcogenide–Au Interfaces

Schottky barrier measurement of WS_2 on deposited Au

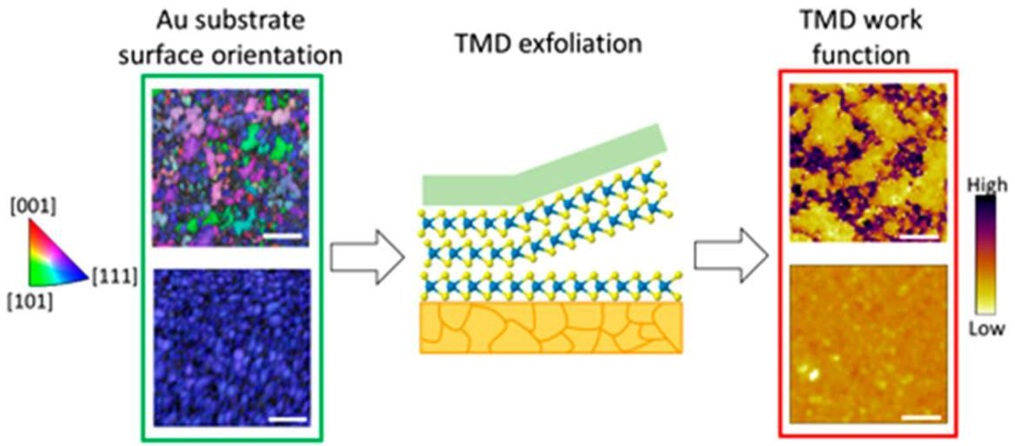

Photoemission electron microscopy (PEEM) for WS_2 on Au

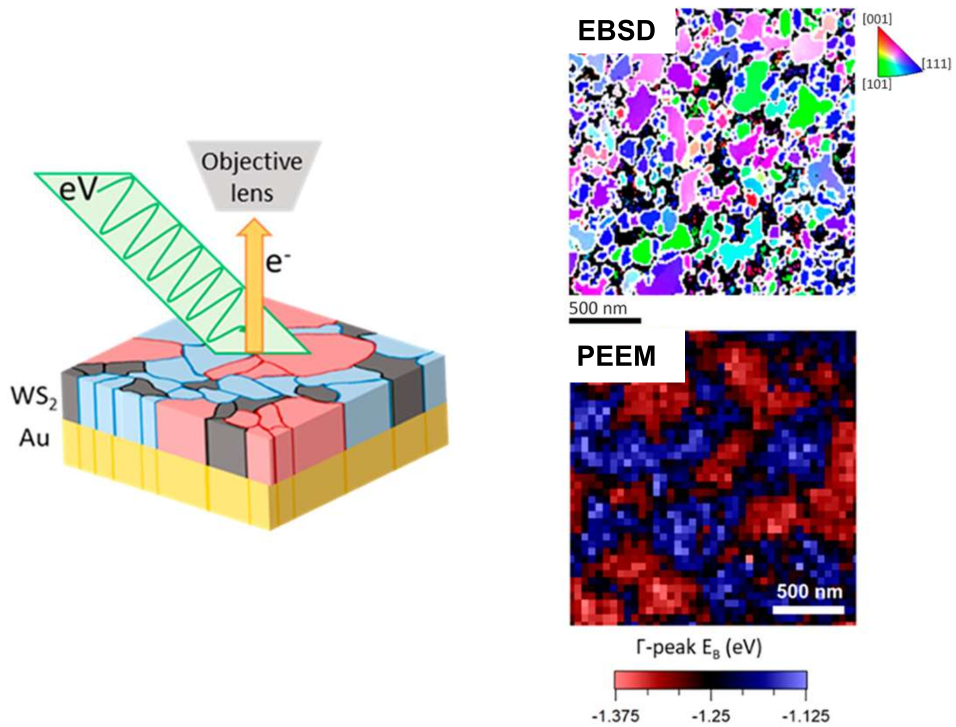

Local variation of barrier

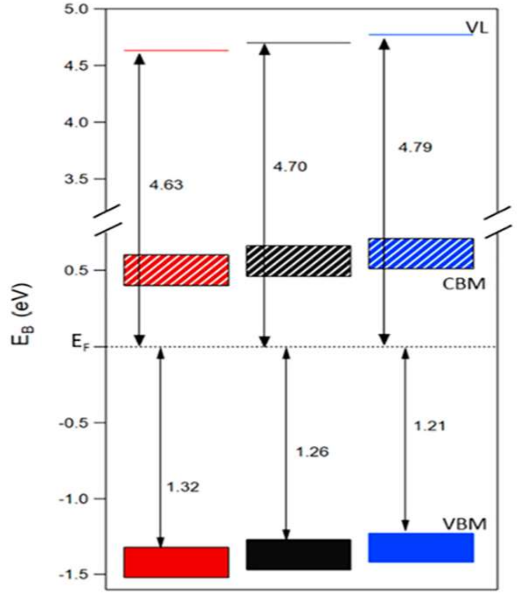

Layer-dependence of barrier

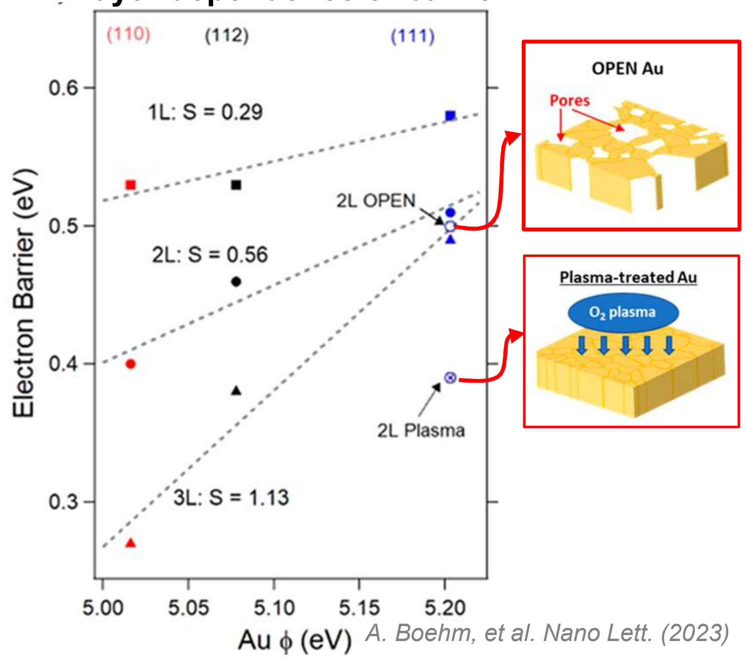

A. Boehm, et al. Nano Lett. (2023)

Semimetal–semiconductor Contact

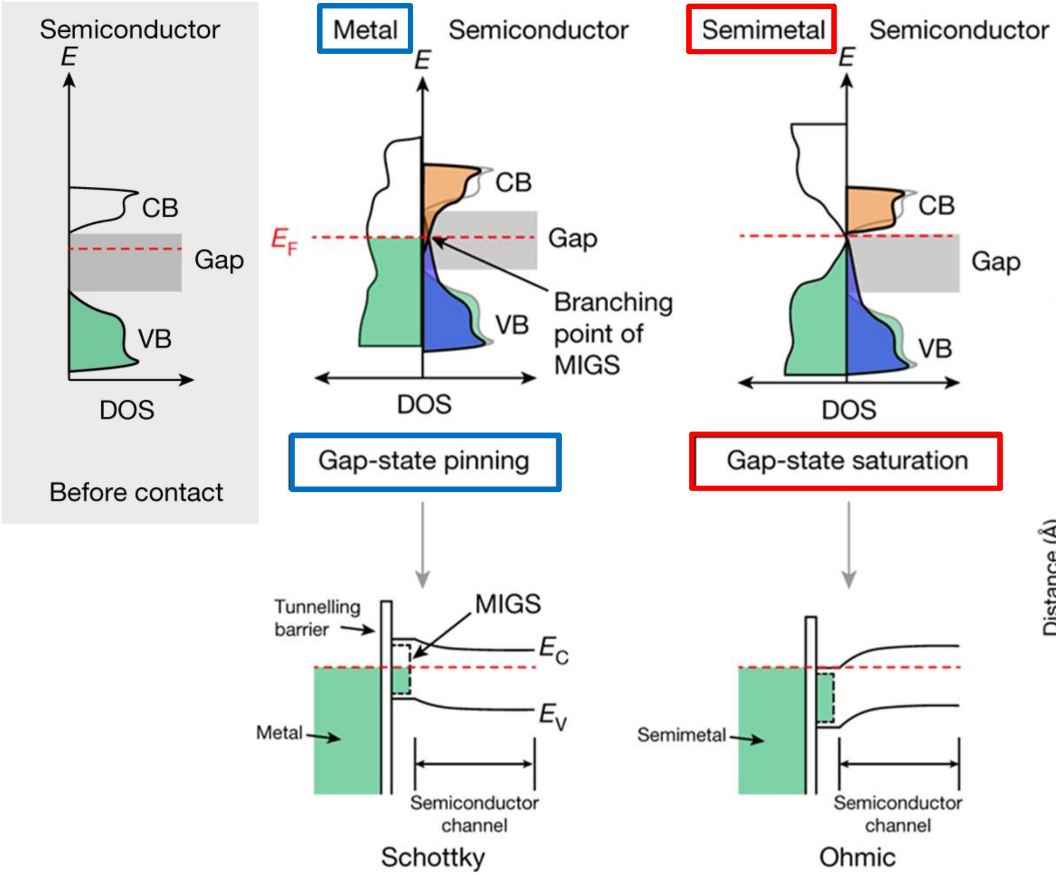

MoS$_2$ FET with semimetal (Bi) contacts

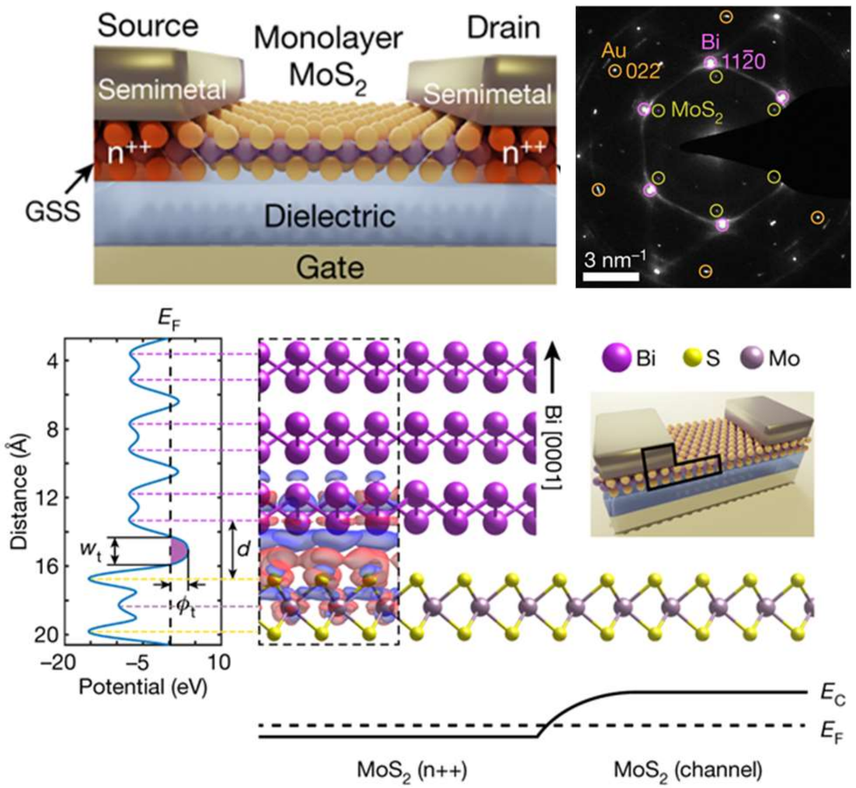

Interface of metal and semiconductor

- Due to the metal-induced gap states (MIGS), the Fermi level (E_F) is pinned around the branching point of the MIGS, leading to gap-state pinning. The Schottky barrier is induced as a result of gap-state pinning.

Interface of semimetal and semiconductor

- Because the Fermi level of the semimetal aligns with the conduction band of the semiconductor and the DOS at the Fermi level of the semimetal is near-zero, conduction-band-contributed MIGS are suppressed and the branching point is elevated into the conduction band. The MIGS, now mostly contributed by the valence band, are saturated, leading to gap-state saturation. The Ohmic contact is induced due to gap-state saturation.

P.C. Shen et al. ***Nature*** *(2021)*

Semimetal–semiconductor Contact

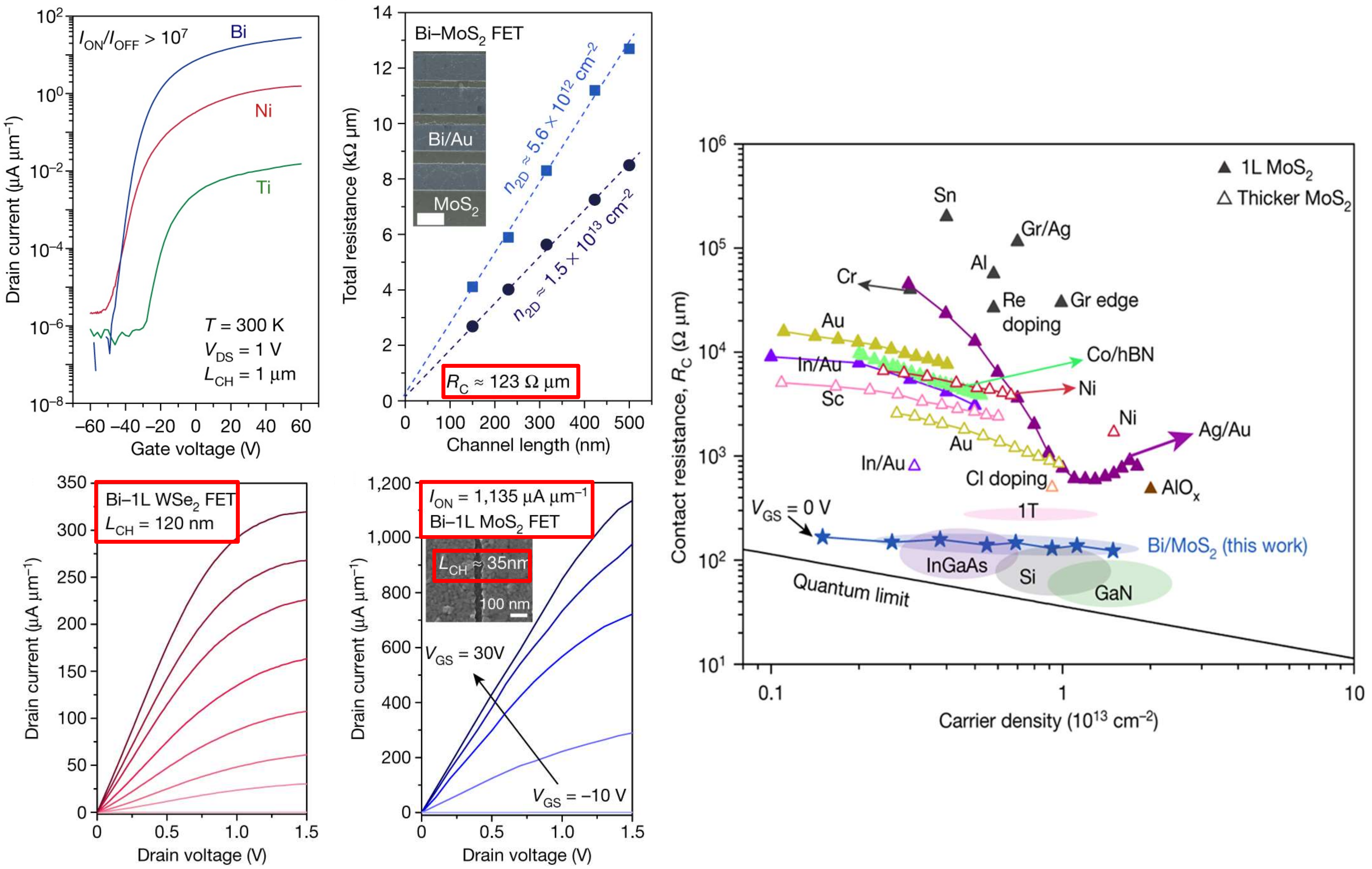

P.C. Shen et al. ***Nature*** *(2021)*

Vertical Schottky-junction TMD Photovoltaics

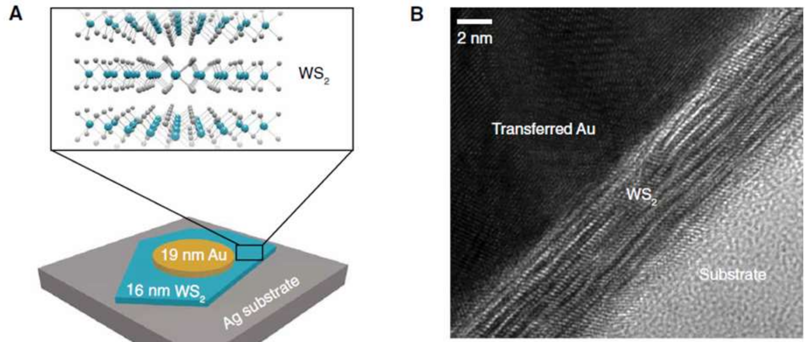

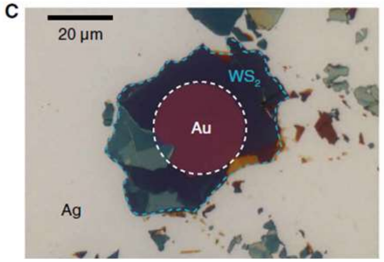

Fully depleted

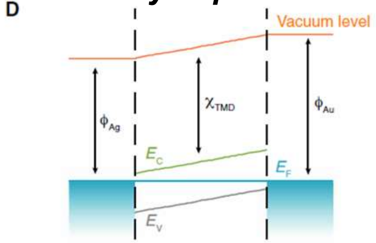

No Fermi-level pinning

Transferred device

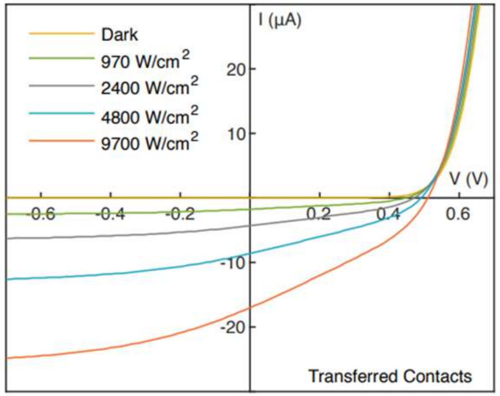

Rectifying behavior
due to the difference between WF_{Au} and WF_{Ag}

Evaporated device

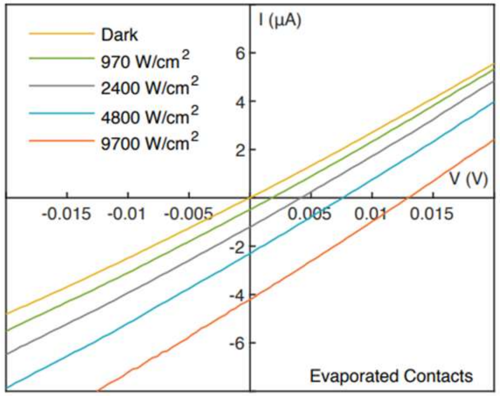

resistive behavior
due to $\phi_{evaporated\ Au} \approx \phi_{transferred\ Ag}$ by E_F pinning

C. M. Went et al. Sci. Adv. (2019)

Forming van der Waals contacts to eliminate the Fermi-level pinning by metal transfer process.

1. *No Fermi-level pining by metal transfer*
2. *Fully depleted by vertical structure (~19 nm of WS_2)*

Rectifying behavior → photovoltaic property

Fermi-level pinning by conventional metal evaporation

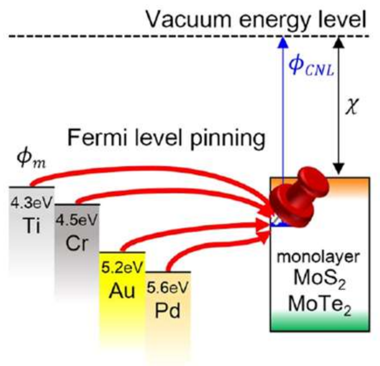

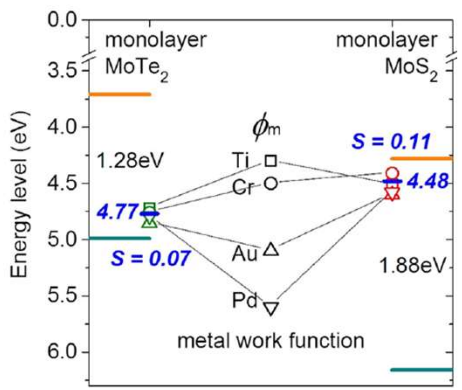

C. Kim et al. ACS Nano (2017)

Phase Transition of MoS_2

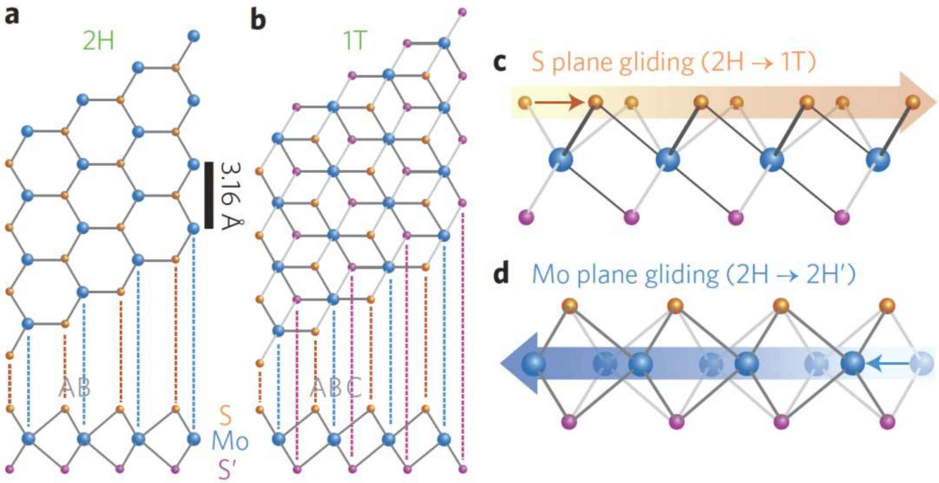

Phase transitions from 2H to 1T in one-atom thick layer alter the properties of a material.

1. Stable semiconducting (2H) phase
2. Metastable metallic (1T) phase

Difference only by a transversal displacement of one of its two Sulphur planes

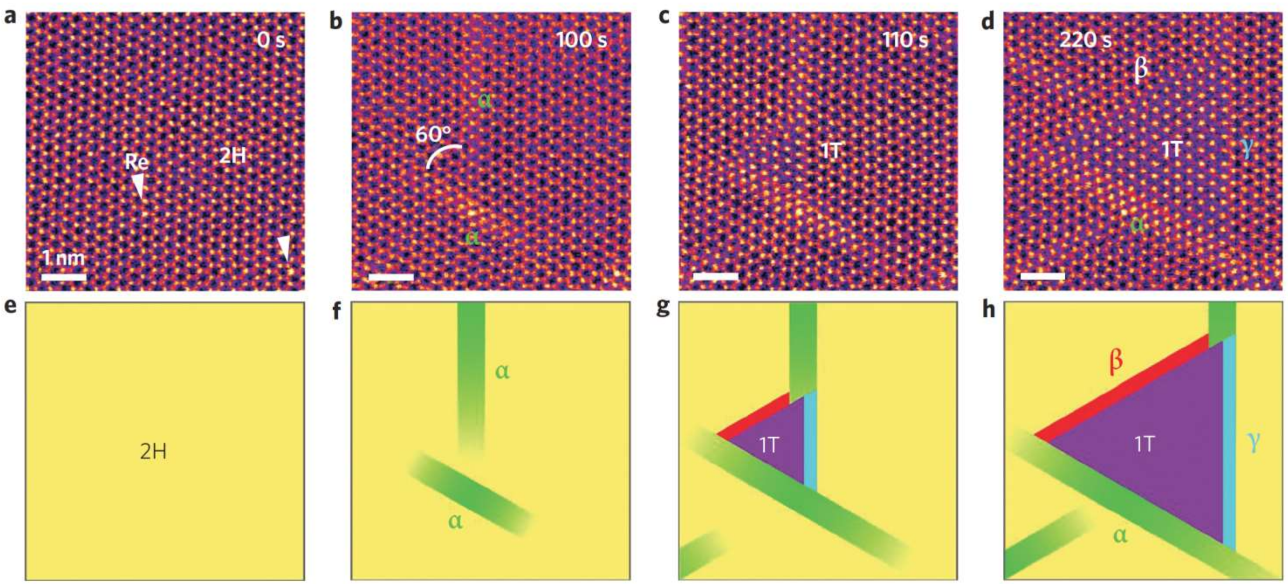

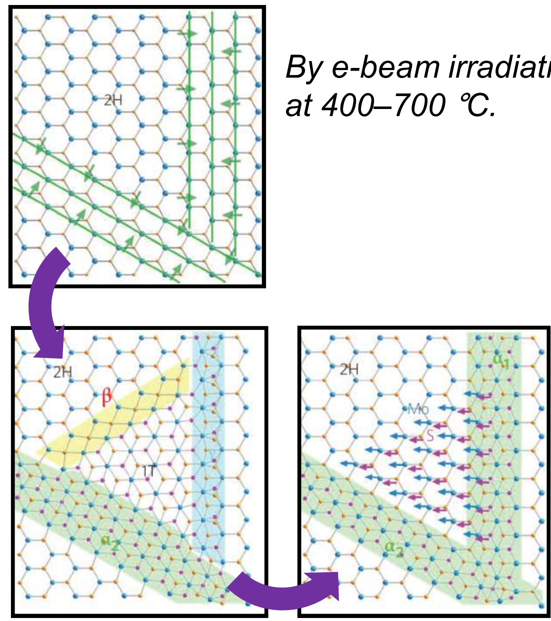

By e-beam irradiation at 400–700 ℃.

Y. –C. Lin et al. Nature Nanotechnol. (2014)

Phase Engineering of MoS_2

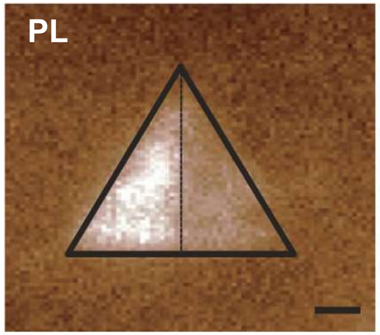

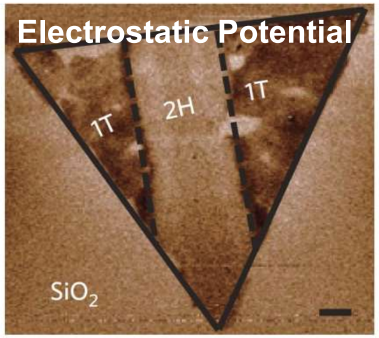

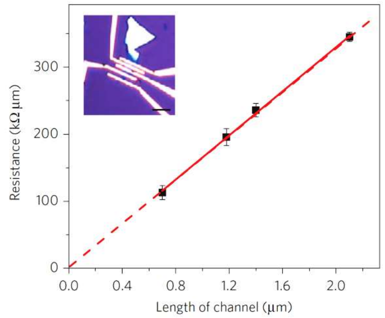

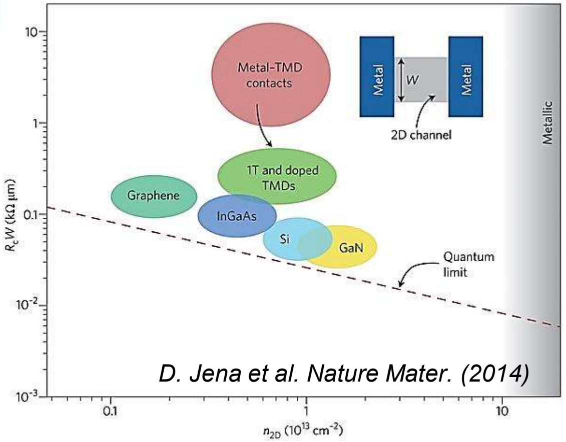

D. Jena et al. Nature Mater. (2014)

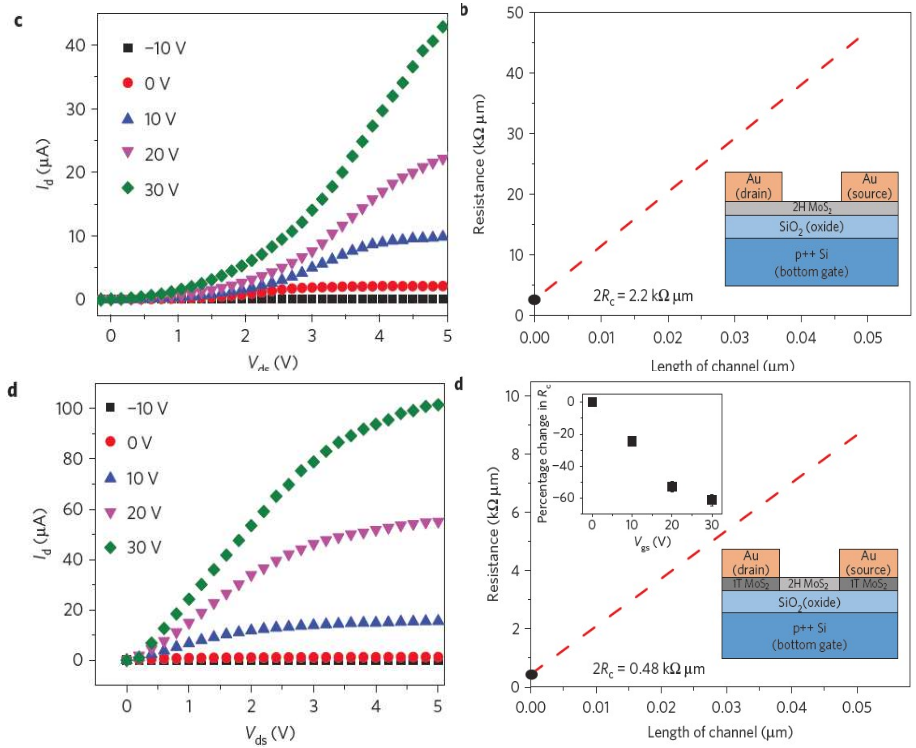

Traditional methods for low contact resistance

1. Heavy doping of semiconductor
2. Use of metal with appropriate work function
3. Large semiconductor contact region
4. Reduction of barrier thickness by large bias

<u>Unconventional method</u> to address contact resistance problem, based on the local conversion of MoS_2 semiconducting layers into a metal.

Chemical method for phase transition: Treating the MoS_2 with an organometallic solution containing n-butyl lithium. Lithium donates electrons to the 2H MoS_2, converting it into the 1T metallic phase.

Contact resistance drops from ~ 1–10 kΩ µm to ~ 0.2–0.3 kΩ µm

R. Kappera et al. Nature Mater. (2014)

Strain Induced Phase Transition of TMDs

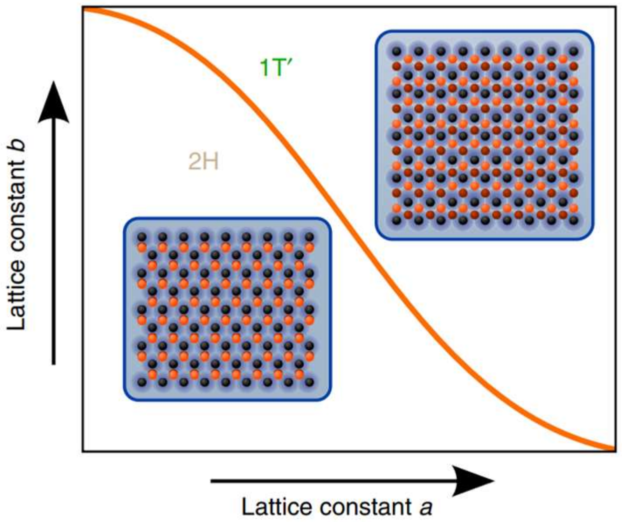

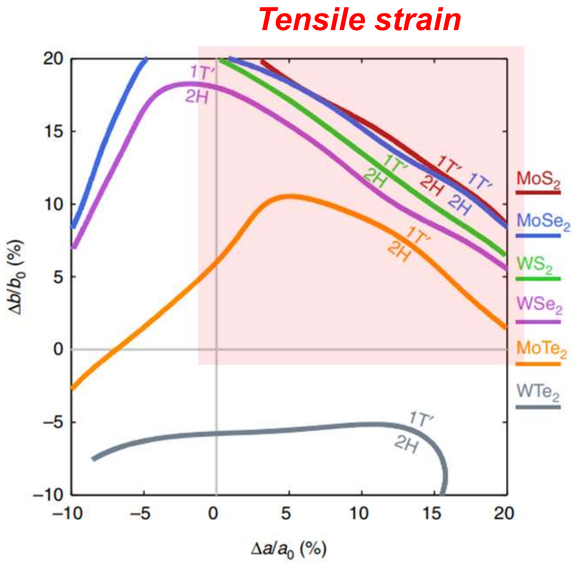

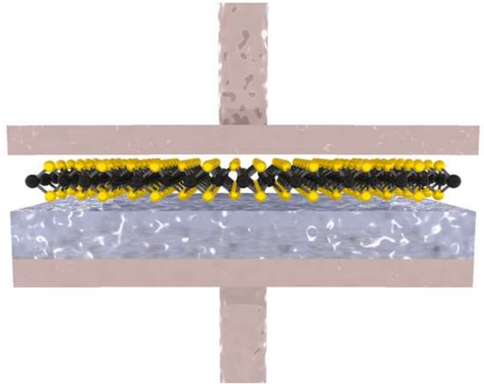

Phase transition of TMDs by strain

1. In 2D system, lattice constants can be independently controlled with underlying substrate
2. In spite of compression in 2D is problematic, still phase transition can be occurred through tensile strain in 2D materials.

Tendency to lower the internal energy, U → phase transition

K. -A. N. Duerloo Nat. Commun. (2014)

Ion-gating Induced Phase Transition of $MoTe_2$

Ionic liquid gating → high doping level

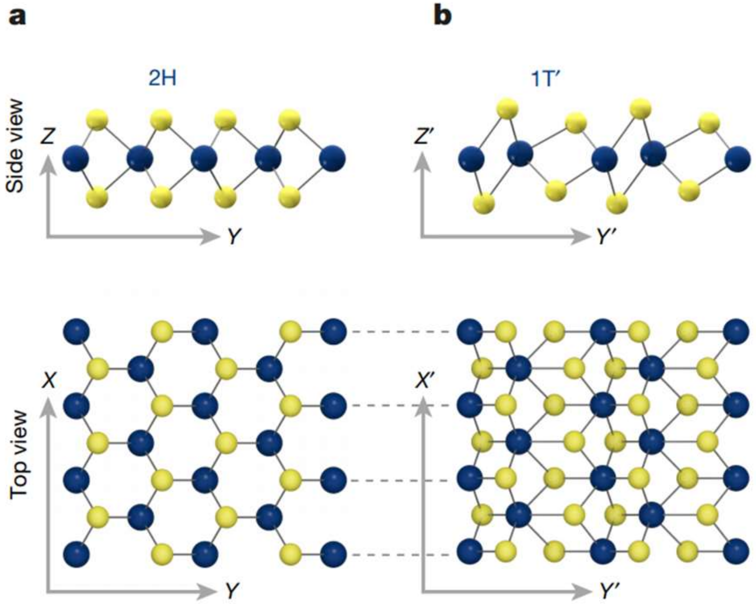

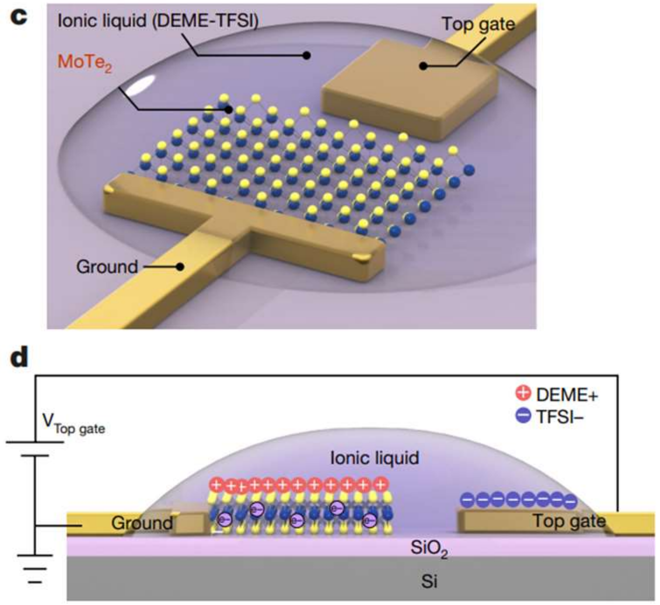

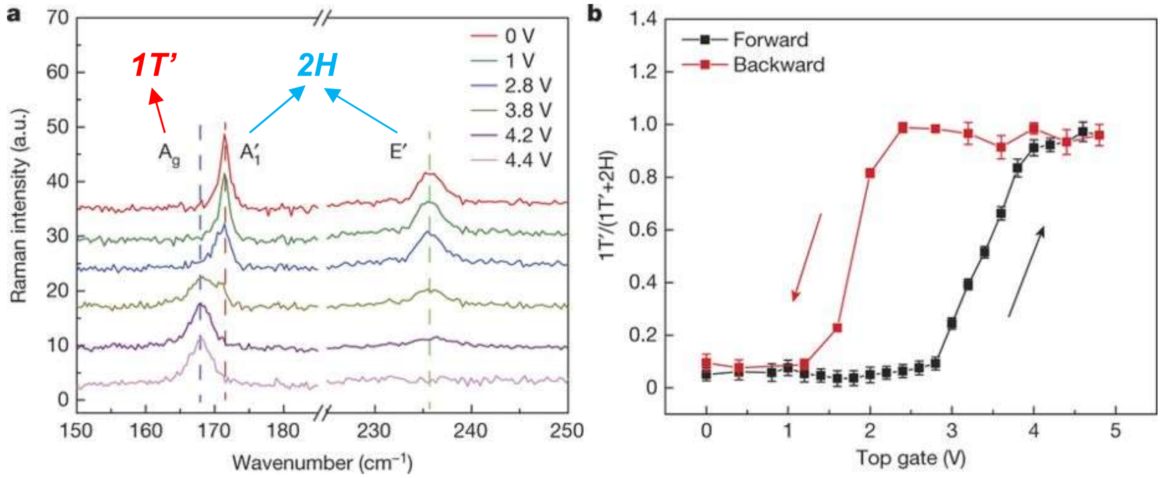

Y. Wang et al. Nature (2017)

Phase transition of $MoTe_2$ by excessive electrons doping

1. Doping level up to 10^{14} electrons/cm^2 in mono layer $MoTe_2$
2. In the condition of high charge density, 1T' phase become thermodynamically stable phase

High doping → 2H to 1T' phase transition

Electric-field Induced Phase Transition of Te-based TMDs

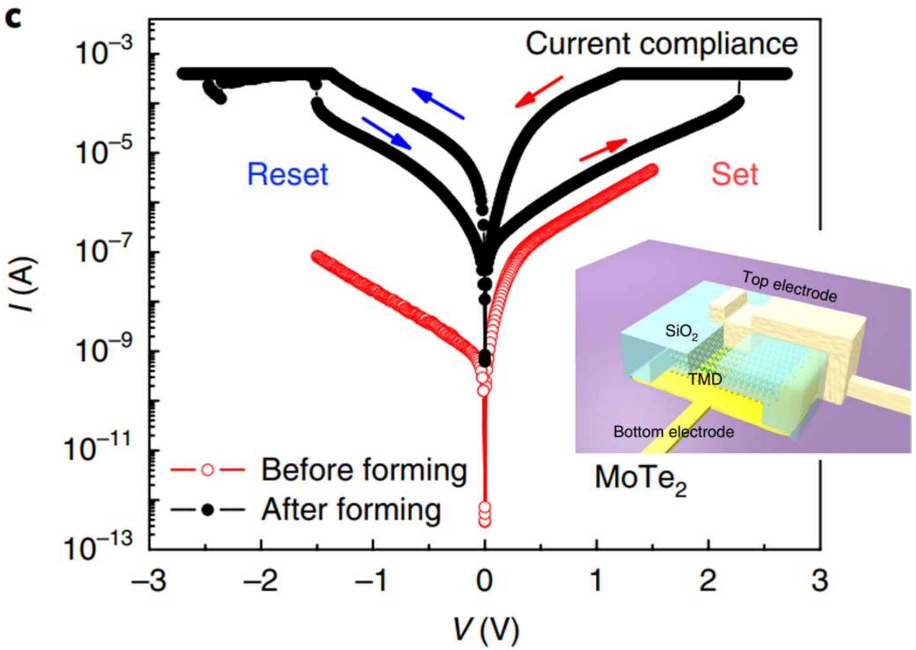

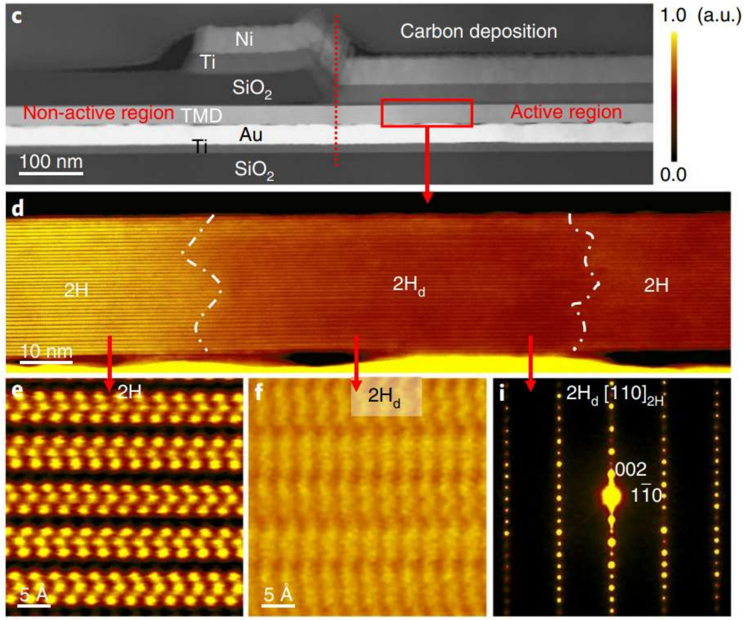

Phase transition of Te-based TMDs by electric field

1. $2H_d$ phase conductive path is formed in 2H phase structure
2. For the bipolar switching, the main driving force is the electric field, rather than Joule heating

Electric field → 2H to $2H_d$ phase transition

Main driving force: electric field

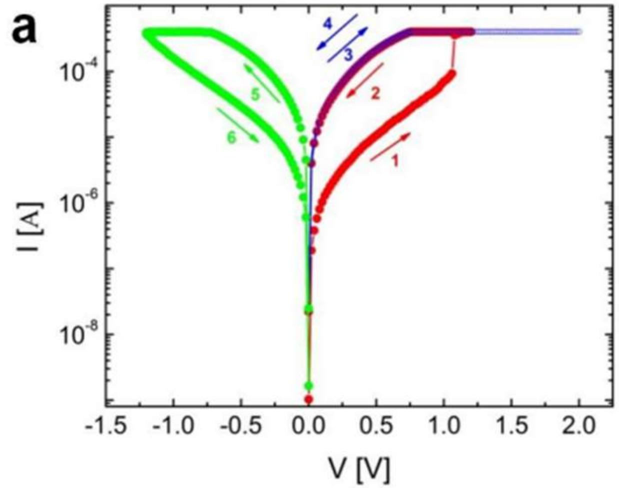

Formation of Low Resistance Contacts by Phase Transition

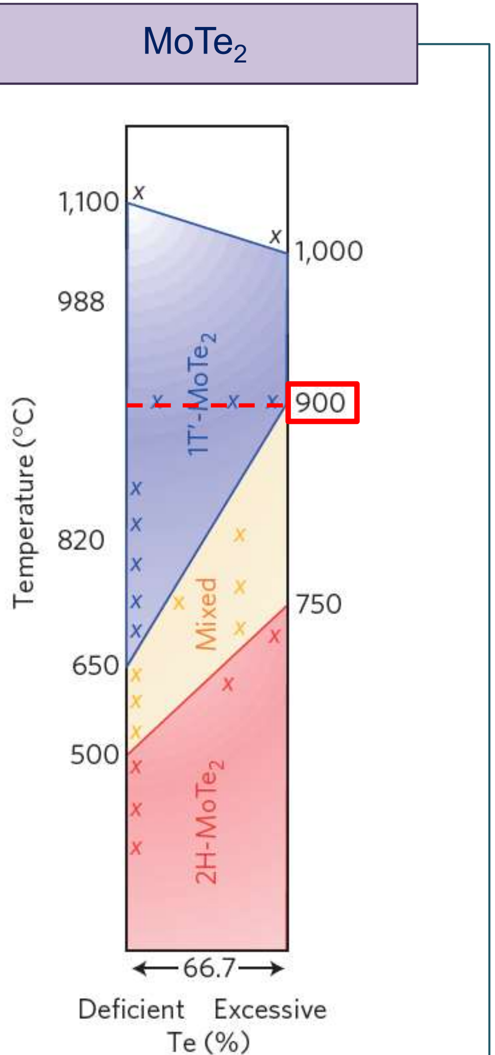

- Chemically active
- Unstable at high T

Nature Physics 13, 931–937 (2017)

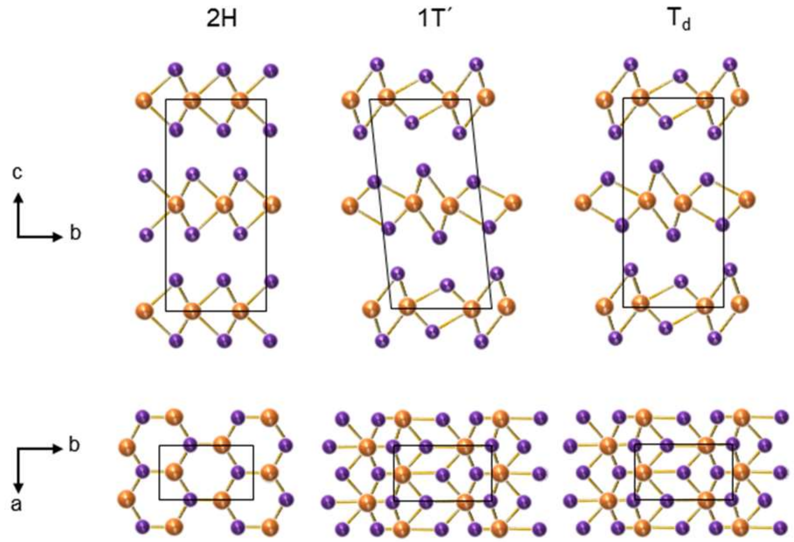

After annealing at 1000°C

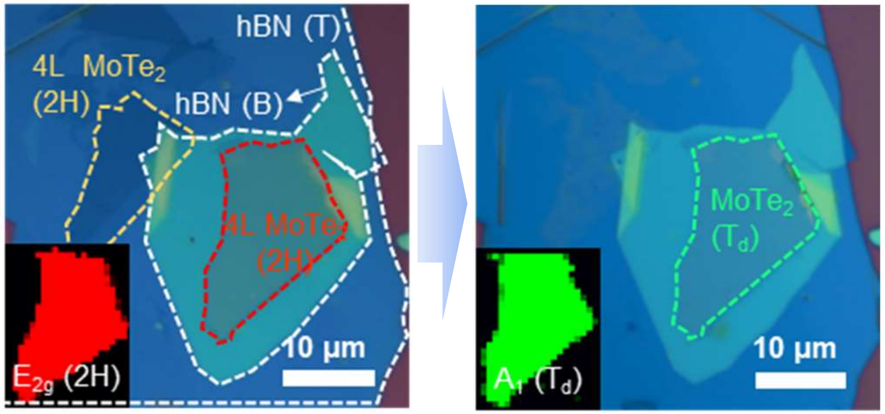

H.J. Ryu, …, K.P. Kim, H. Cheong, Y.W. Son, G.H. Lee, **Advanced Functional Materials** (2020)

Formation of Low Resistance Contacts by Phase Transition

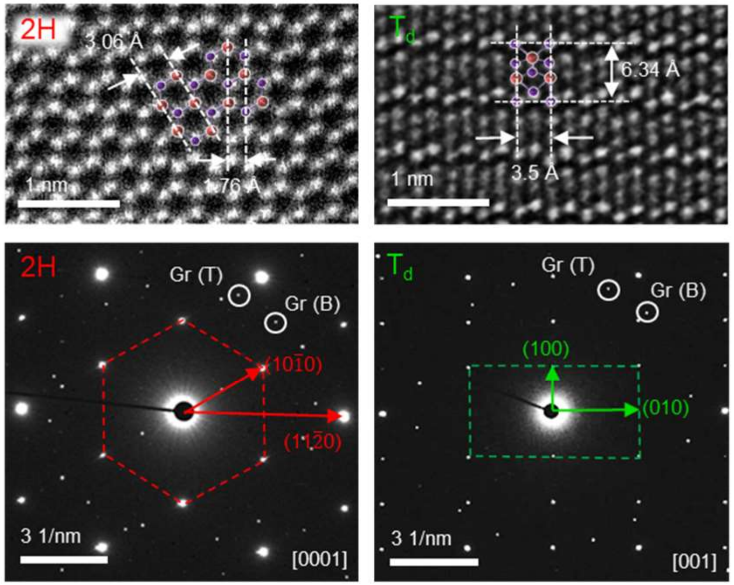

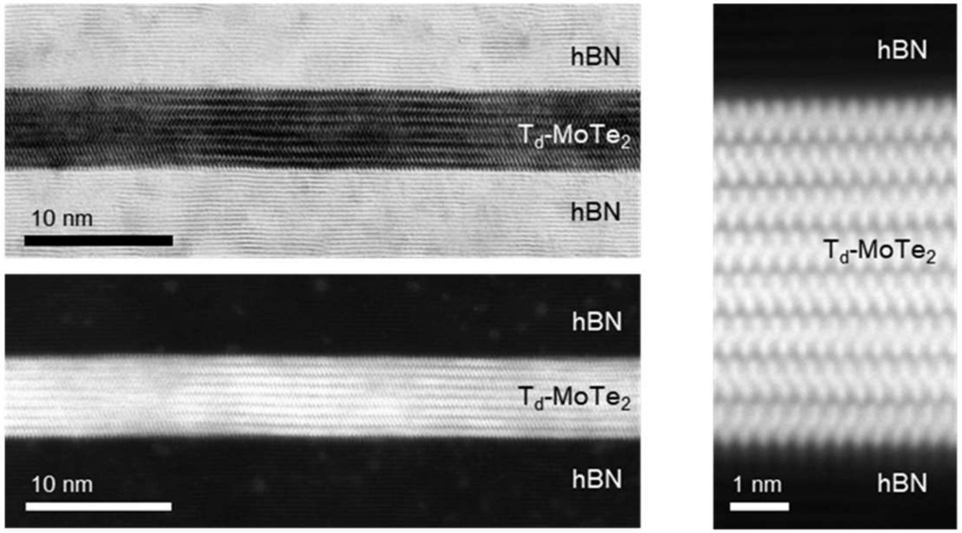

Polycrystalline T_d-$MoTe_2$

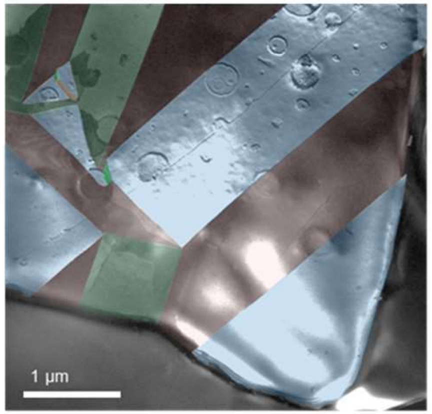

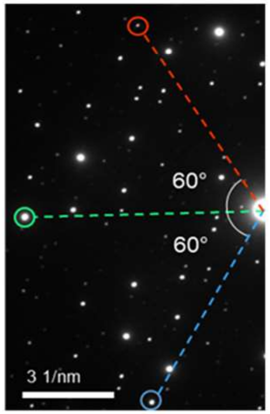

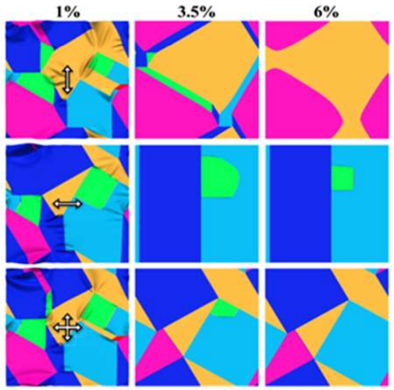

Phys. Rev. Mater. 2, 114002 (2018)

Grain boundary structure

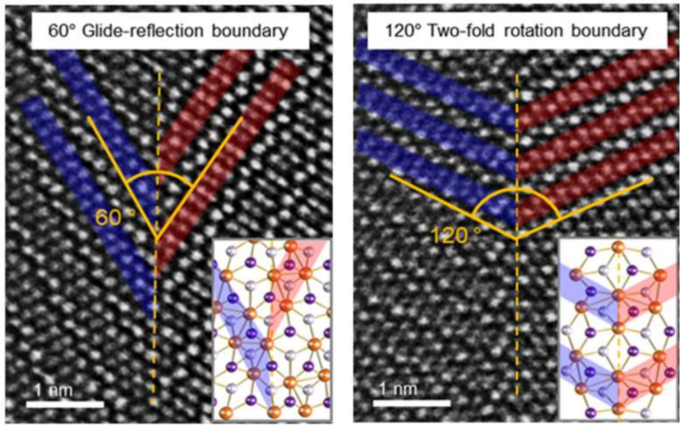

H.J. Ryu, …, K.P. Kim, H. Cheong, Y.W. Son, G.H. Lee, **Advanced Functional Materials** (2020)

Formation of Low Resistance Contacts by Phase Transition

Phase transition of $MoTe_2$ with different thicknesses

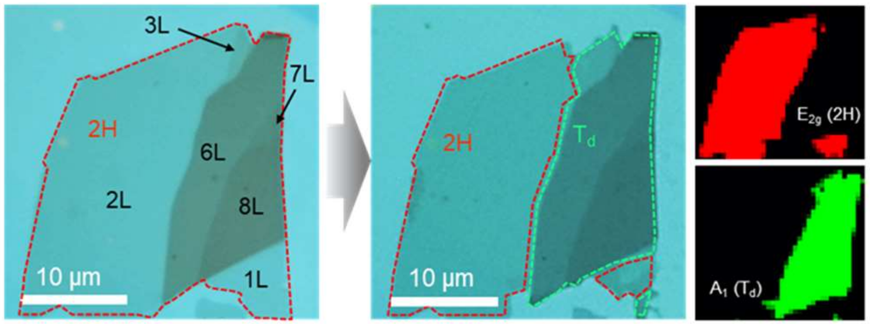

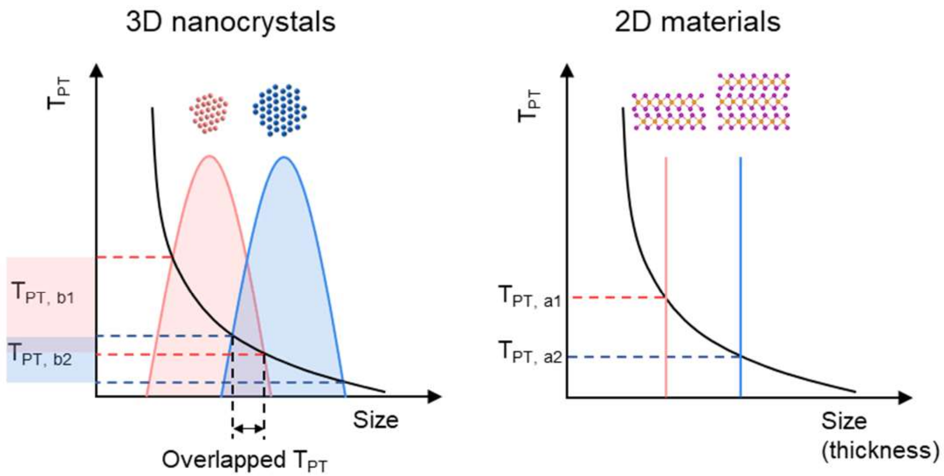

Layer-dependent PT temperature

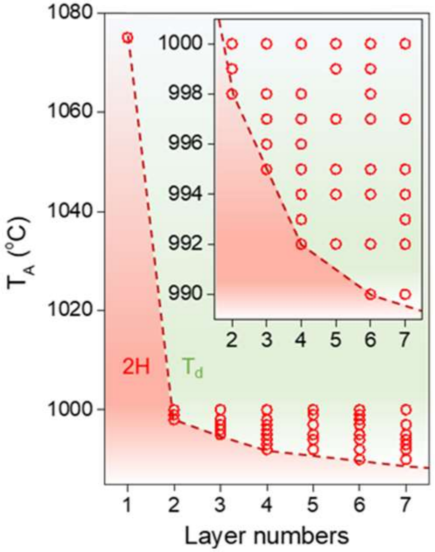

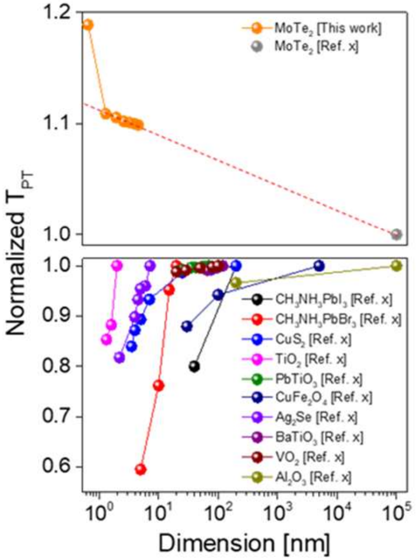

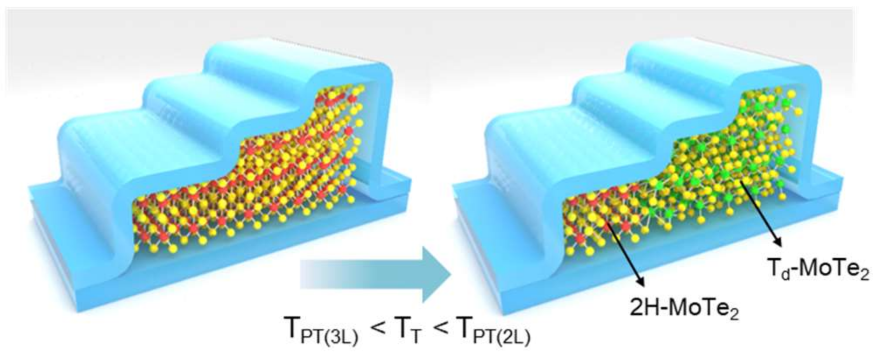

T_{PT} from 2H to T_d decreases as the thickness increases.

H.J. Ryu, …, K.P. Kim, H. Cheong, Y.W. Son, G.H. Lee, **Advanced Functional Materials** (2020)

Formation of Low Resistance Contacts by Phase Transition

Misaligned 2H-T_d heterointerface

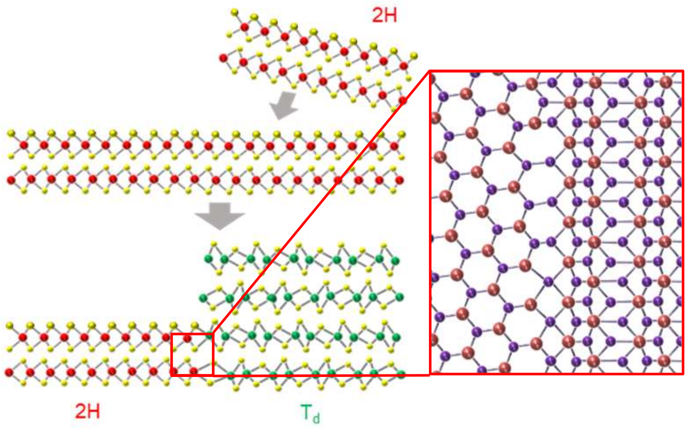

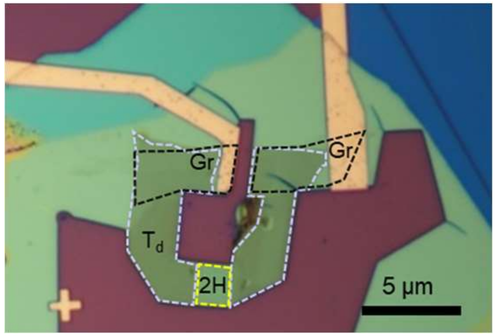

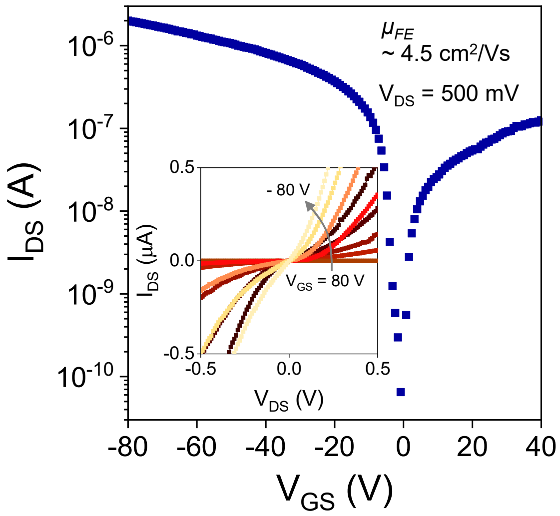

Aligned 2H-T_d heterointerface

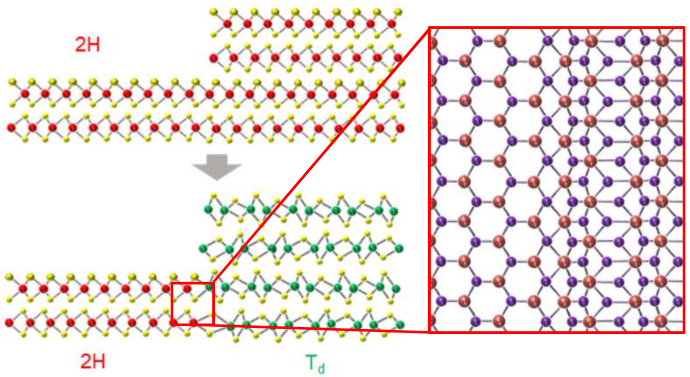

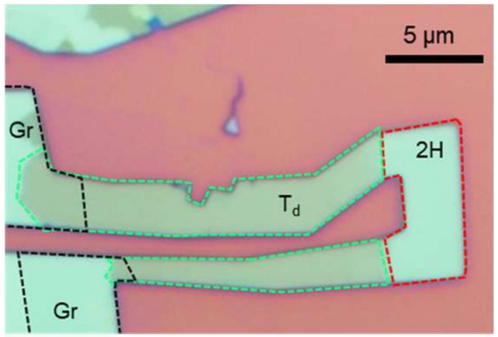

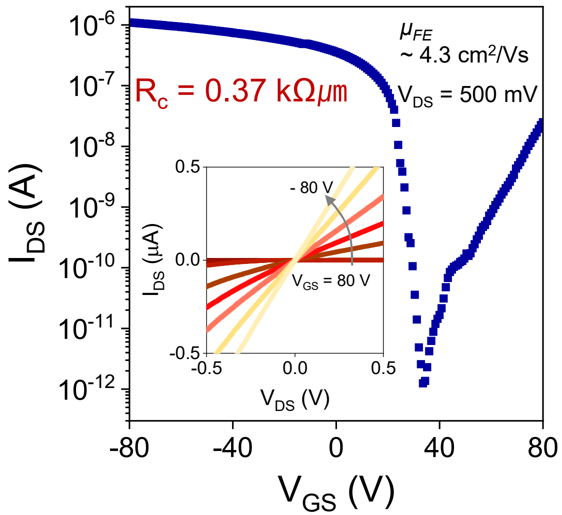

- In-plane 2H-T_d contacts can be fabricated by thickness-controlled PT patterning.
- Low in-plane contact resistance improves device performance of $MoTe_2$ FETs.

H.J. Ryu, …, K.P. Kim, H. Cheong, Y.W. Son, G.H. Lee, **Advanced Functional Materials** (2020)